

C. V. Ward

Departments of Anthropology  
and Pathology and  
Anatomical Sciences,  
107 Swallow Hall,  
University of Missouri,  
Columbia, Missouri 65211,  
U.S.A. E-mail:  
WardCV@missouri.edu

M. G. Leakey

Division of Palaeontology,  
National Museums of Kenya,  
P.O. Box 40658, Nairobi,  
Kenya. E-mail:  
meave@swiftkenya.com

A. Walker

Departments of  
Anthropology and Biology,  
Pennsylvania State  
University, University Park,  
Pennsylvania 16802, U.S.A.  
E-mail: AXW8@psu.edu

Received 6 March 2001

Revision received

25 June 2001 and

accepted 27 June 2001


Keywords: *Australopithecus*  
*anamensis*, Kanapoi,  
Allia Bay, description,  
morphology.

## Morphology of *Australopithecus anamensis* from Kanapoi and Allia Bay, Kenya

The hominid species *Australopithecus anamensis* was originally described in 1995, with new specimens and more secure dates given in 1998. This paper lists all fossils attributed to *A. anamensis*, and provides anatomical descriptions of those not yet described in detail with photographs of all but undiagnostic fragments. We also provide comparative analysis of these specimens. The *A. anamensis* holotype mandible was found at Kanapoi, as were most of the paratypes. The Allia Bay sample is less well represented, and does not preserve many anatomical elements diagnostic of this species. Still, the Allia Bay sample most closely resembles that from Kanapoi, and we suggest that for the time being it be retained as *A. anamensis*. *A. anamensis* most closely resembles *A. afarensis*, but can be distinguished from it in many features. Most of these features are inferred to be primitive for the genus. Based on the limited postcranial evidence available, *A. anamensis* appears to have been habitually bipedal, although it retained some primitive features of its upper limbs. *A. anamensis* differs from *A. afarensis* in having narrower, more parallel jaws with a very slightly more ape-like canine/premolar complex than is found in *A. afarensis*, although not as ape-like as in *Ardipithecus ramidus*. It had slightly larger lower lateral incisors, a unique upper canine morphology, and a different structure of the lateral nasal aperture than *A. afarensis*. *A. anamensis* had at least as great a range of body size, and perhaps slightly greater canine dimorphism, although this is difficult to determine. At present, there appears to be no autapomorphies precluding *A. anamensis* from ancestry of *A. afarensis*.

© 2001 Academic Press

*Journal of Human Evolution* (2001) 41, 255–368  
doi:10.1006/jhev.2001.0507

Available online at <http://www.idealibrary.com> on 

### Introduction

The holotype and paratype series of *Australopithecus anamensis* were found at Kanapoi, Kenya. Other fossils attributed to *A. anamensis* have been found at Allia Bay, Kenya. This species was first described in Leakey *et al.* (1995). Additional specimens and more secure dates were given three years later (Leakey *et al.*, 1998).

All fossils attributed to *A. anamensis* date to between 3.9 and 4.2 Ma. The older of the two sites is the type site of Kanapoi. With the exception of one specimen, a mandible (KNM-KP 29287), all Kanapoi hominins

come from strata dated to between  $4.17 \pm 0.03$  and  $4.07 \pm 0.03$  Ma (Leakey *et al.*, 1998). The mandible KNM-KP 29287 derives from the paleosol developed on the upper tuff, and therefore cannot be much younger.

The Allia Bay fossils are slightly younger than those from Kanapoi. At Allia Bay, most of the hominids were found at the 261-1 site. This site lies just below the Moiti Tuff, dated elsewhere in the region to  $3.94 \pm 0.03$  Ma (Leakey *et al.*, 1995). White *et al.* (1993) report an age of  $3.89 \pm 0.02$  for tuff VT-1 in the Maka area of Ethiopia, a tuff that on chemical grounds is regarded as

**Table 1** Specimens attributed to *Australopithecus anamensis*

Specimen number	Figure	Element
Kanapoi		
KNM-KP 271	13	L distal humerus
KNM-KP 29281	1, 2	Holotype mandible & L temporal fragment
KNM-KP 29282	—	LM <sub>1</sub> or M <sub>2</sub>
KNM-KP 29283	3	Maxilla
KNM-KP 29284	4	R <sub>C</sub> & RP <sub>3</sub> germs
KNM-KP 29285	14, 15	R proximal & distal tibia
KNM-KP 29286	5	Mandible fragments & associated dentition (RI <sub>1</sub> , L & RI <sub>2</sub> -M <sub>3</sub> )
KNM-KP 29287	6	Mandible with teeth
KNM-KP 30498	7	L & R maxillary fragments & associated dentition
KNM-KP 30500	8	Mandibular fragments & associated dentition
KNM-KP 30502	4	Associated mandibular tooth fragments
KNM-KP 30503	16	Proximal manual phalanx
KNM-KP 30505	4	Partial M germ
KNM-KP 30942	—	5 tooth fragments
KNM-KP 31712	9	Associated juvenile mandibular & dental fragments
KNM-KP 31713	10	R mandible with tooth fragments
KNM-KP 31714	4	Ldm <sub>2</sub>
KNM-KP 31715	—	LM <sub>1</sub> or M <sub>2</sub> fragment & two other tooth fragments
KNM-KP 31716	—	P <sup>3</sup> or P <sup>4</sup> fragment & C/ fragments
KNM-KP 31717	4	LM <sup>3</sup> , RM <sub>3</sub> & LM <sub>2</sub> fragments
KNM-KP 31718	—	R Mandibular fragment (M <sub>2-3</sub> )
KNM-KP 31719	—	I <sup>1</sup>
KNM-KP 31720	—	Maxillary M fragment
KNM-KP 31721	—	RM <sup>2</sup> & M <sup>3</sup> partial crowns
KNM-KP 31723	4	RM <sup>3</sup>
KNM-KP 31724	17	L capitate
KNM-KP 31726	4	RP <sup>4</sup>
KNM-KP 31727	—	R <sub>C</sub>
KNM-KP 31728	4	LM <sub>1</sub>
KNM-KP 31729	4	Rdm <sub>2</sub>
KNM-KP 31730	4	LM <sub>2</sub> & RP <sub>3</sub>
KNM-KP 31732	—	Tooth fragments
KNM-KP 34725	11	Associated juvenile dentition and skull fragments
KNM-KP 35838	—	LM <sub>3</sub>
KNM-KP 35839	12	Associated LI <sup>1</sup> , R <sup>C</sup> & LP <sup>3</sup>
KNM-KP 35840	—	LM <sup>3</sup> & maxillary M fragments
KNM-KP 35841	—	M crown
KNM-KP 35842	4	R maxillary M
KNM-KP 35844	—	M fragment
KNM-KP 35845	—	M fragment
KNM-KP 35847	4	LM <sub>2</sub>
KNM-KP 35850	—	Maxillary M fragment
KNM-KP 35851	—	LM <sup>2</sup> or M <sup>3</sup> fragment
KNM-KP 35852	4	L <sup>C</sup>
KNM-KP 37522	—	L mandibular molar
KNM-KP 37523	—	M fragment
KNM-KP 37524	—	Tooth fragments
Allia Bay		
KNM-ER 7727	—	LM <sup>2</sup>
KNM-ER 20419	22	L radius
KNM-ER 20420	—	LM <sup>2</sup>
KNM-ER 20421	—	RM <sup>3</sup>

Table 1 *Continued*

Specimen number	Figure	Element
Allia Bay ( <i>Continued</i> )		
KNM-ER 20422	—	LM <sub>1</sub>
KNM-ER 20423	—	LM <sub>2</sub>
KNM-ER 20427	—	LM <sup>1</sup>
KNM-ER 20428	—	LM <sub>3</sub>
KNM-ER 20432	—	L mandibular fragment (P <sub>3-4</sub> )
KNM-ER 22683	—	LP <sub>4</sub>
KNM-ER 24148	—	Ldm <sup>2</sup>
KNM-ER 30200	18	L maxillary fragment (M <sup>1-2</sup> , partial M <sup>3</sup> )
KNM-ER 30201	19	LM <sub>1</sub>
KNM-ER 30202	19	RI <sup>1</sup>
KNM-ER 30731	19	R <sub>C</sub>
KNM-ER 30744	—	R <sup>C</sup>
KNM-ER 30745	20	L maxillary fragment (partial C, P <sup>3</sup> -M <sup>1</sup> , partial M <sup>2</sup> , M <sup>3</sup> )
KNM-ER 30747	—	LP <sub>4</sub>
KNM-ER 30748	—	L maxillary M fragment
KNM-ER 30749	19	LM <sub>1</sub>
KNM-ER 30750	—	R <sub>C</sub>
KNM-ER 35228	21	RP <sub>4</sub>
KNM-ER 35229	—	L mandibular M fragment
KNM-ER 35230	—	M fragment
KNM-ER 35231	19	RM <sup>1</sup> or M <sup>2</sup>
KNM-ER 35232	19	LM <sub>1</sub>
KNM-ER 35233	19	LM <sub>2</sub>
KNM-ER 25234	—	LP <sub>3</sub>
KNM-ER 35235	19	LM <sup>2</sup>
KNM-ER 35236	19	LM <sup>3</sup>
KNM-ER 35238	19	RM <sup>1</sup>

a correlative of the Moiti Tuff. The age of the bone bed bearing the majority of hominin fossils can be extrapolated to have been  $3.95 \pm 0.05$  Ma (C. S. Feibel, personal communication). KNM-ER 30200, KNM-ER 30201, KNM-ER 30744 were found about 1 km to the east of the 261-1 site in a small drainage channel that cut through the Moiti Tuff. The strata at Sibilot, near site 261-1, yielded a hominin radius attributed on the basis of age to *A. anamensis*, and is estimated to be  $3.9 \pm 0.1$  Ma (Heinrich *et al.*, 1993).

The paleoenvironmental reconstructions for Kanapoi and Allia Bay have been mentioned in Coffing *et al.* (1994), Leakey *et al.* (1995), Ward *et al.* (1999b), and Wynn (2000). As far as can be determined, the habitats sampled at these sites were similar to those described for *A. afarensis* at Hadar,

Ethiopia, and Laetoli, Tanzania; fairly wooded regions that included woodland and bushland, sometimes with edaphic grassland and often well watered (Reed, 1997). They differ from the more closed woodland habitats reconstructed for the earlier *Ardipithecus ramidus* site of Aramis, Ethiopia (Wolde-Gabriel *et al.*, 1994). In one respect, Wynn's (2000) conclusion, based on paleosols and their carbon isotopes, is slightly at variance with the australopithecine habitats interpreted by Reed (1997). The hominin fossils at Kanapoi are associated with soils characteristic of semi-arid vegetational mosaics. Wynn (2000) suggests that this indicates that the hominins thrived in mosaic settings, whereas Reed (1997) concludes that "the environment in which these *Australopithecus* spp. existed was fairly static" and "constrained by minimum and maximum

amounts of rainfall and tree cover.” We cannot be absolutely sure of the specific habitats favored by the Kanapoi hominins, however, because most of the hominin fossils show signs of carnivore damage, and there might be a depositional bias caused by the behavioral proclivities of the predators and/or scavengers, rather than of the hominins.

Preliminary reports of the *A. anamensis* fossils are found in the original publications, and Leakey & Walker (1997) and Ward et al. (1999b). This paper describes the morphology of these fossils in detail, puts the collection in comparative context, and makes some functional and evolutionary interpretations.

### Description of Fossils

Each fossil is described first without specific comparative references to provide an inventory of the preservation and morphology of each. Descriptions are provided by site, separated into craniodental and postcranial sections. Specimens are described in numeric order within these sections. All specimens that have been attributed to *A. anamensis* are listed by anatomical element in Table 1.

Measurements are given in millimeters unless otherwise indicated. Standard metric data are listed in Tables 2, 3 & 4, and other data are included in the text. Dental measurements we previously reported (Leakey et al., 1995; Leakey et al., 1998) were taken following Wood (1991). Dental data published for *A. afarensis*, however, were taken using different techniques (White, 1977) that yield slightly different results. To permit metric comparison with other East African *Australopithecus* specimens, tooth measurements reported (Table 2) in this paper were taken following White (1977). These data should be considered the definitive metric sample for comparative purposes.

Anatomical terminology follows Johanson et al. (1982). Abbreviations used in the text and tables are as follows (most follow Johanson et al., 1982):

AP = anteroposterior/ly  
 ML = mediolateral/ly  
 SI = superoinferior/ly  
 MD = mesiodistal/ly  
 BL = buccolingual/ly  
 LaL = labiolingual/ly  
 PD = proximodistal/ly  
 DP = dorsopalmar/ly  
 Prd = protoconid  
 Med = metaconid  
 Hyd = hypoconid  
 End = entoconid  
 Hld = hypoconulid  
 Pa = paracone  
 Pr = protocone  
 Me = metacone  
 Hy = hypocone  
 Fa = anterior fovea  
 Fc = central fovea  
 Fp = posterior fovea  
 C<sub>6</sub> = tuberculum sextum  
 Mmr = mesial marginal ridge  
 Dmr = distal marginal ridge  
 Mlg = median longitudinal groove  
 Co = crista obliqua  
 IPF = interproximal wear facet  
 L = left  
 R = right

### Kanapoi

At Kanapoi, specimens that were found in close proximity and that appeared to represent a single individual were given one accession number. Many of these have more than one field number. Other specimens that share a field number may represent more than one individual and therefore have different accession numbers. If fragments that make up a specimen cannot be certainly associated, different accession numbers have been assigned. In cases where more than one

Table 2 Dental metrics for *Australopithecus anamensis*

Specimen	Side	I <sup>1</sup>		C		P <sup>3</sup>		P <sup>4</sup>		M <sup>1</sup>		M <sup>2</sup>		M <sup>3</sup>			
		MD	LaL	MD	LaL	MD	BL	MD	BL	MD	BLant	BLpost	MD	BLant	BLpost	MD	BL
Maxillary permanent dentition																	
KNM-ER 7727	L											12.3	14.7	14.3			
KNM-ER 20420	R											16.3					
KNM-ER 20421	R														11.2	13.7	
KNM-ER 20422	L										11.9	10.9					
KNM-ER 20428	L														15.7	13.7	
KNM-ER 30200	R										11.7	11.4	13.2	11.6			
KNM-ER 30202	R	10.5a	9.3														
KNM-ER 30744	L										(9.0)						
KNM-ER 30745	L			(11.0)		9.9	13.0	8.8	13.9		14.1	(13.2)					
KNM-ER 35231	R										12.2						
KNM-ER 35232	L										11.7						
KNM-ER 35235	R										12.9		(12.9)				
KNM-ER 35236	L																
KNM-ER 35238	R										(10.0)						
KNM-KP 29283	L																
KNM-KP 29283	R					(9.3)	12.1	7.5 [7.8]			(12.8)				12.9	14.7	14.7
KNM-KP 30498	L	10.9	8.2					7.9 [8.1]			11.3 [11.9]				13.2	14.8	13.3
KNM-KP 30498	R			(10.6)	10.2	8.7	13.2				11.6						
KNM-KP 31717	L																
KNM-KP 31723	R																
KNM-KP 31726	L							7.2									
KNM-KP 34725	R																
KNM-KP 35839	L	12.4	8.9														
KNM-KP 35839	R																
KNM-KP 35842	R																
KNM-KP 35852	L					(11.0)	(10.1)								11.6	11.1	13.8
															(12.7)	(15.7)	

Table 2 Continued

Specimen	Side	I <sub>1</sub>		I <sub>2</sub>		C		P <sub>3</sub>			P <sub>4</sub>			M <sub>1</sub>		M <sub>2</sub>		M <sub>3</sub>	
		MD	LaL	MD	LaL	MD	LaL	MAX	MIN	MD	BL	MD	BL	MD	BL	MD	BL	MD	BL
Mandibular permanent dentition																			
KNM-ER 20423	L							12.0	8.6	9.7	11.9							12.3	
KNM-ER 20432	L									8.7 [9.2]	10.4								
KNM-ER 22683	L																		
KNM-ER 30201	L																		
KNM-ER 30731	R					8.3	10.6							11.6	10.2				
KNM-ER 30750	R					6.6	9.2												
KNM-ER 35228	R									7.4	9.6								
KNM-ER 35233	L																		
KNM-KP 29281	L	5.9 [6.6]	7.5	6.5 [7.5]	8.6	8.8	9.6	11.7	8.5	7.9 [8.2]	9.8	11.9 [12.7]	11.9	14.8	13.3	13.0	13.4 [13.7]	12.6	14.4
KNM-KP 29281	R	6.1 [6.9]	7.3	6.9 [7.8]	8.6	8.7	9.4	11.5	8.7	7.8 [8.4]	10.3	12.0 [12.6]	12.0	13.5 [13.9]	12.6	14.3	11.9		
KNM-KP 29284	R					9.8	11.4	(11.3)	(8.6)										
KNM-KP 29286	L			7.3 [8.7]	7.8	10.4		12.4	9.4	9.5	11.3	12.3	11.9	13.8	14.3	13.2			
KNM-KP 29286	R				8.0	10.3	11.2	12.3	9.1	9.5	11.7	12.3	11.8	14.5	14.0	14.1	13.4		
KNM-KP 29287	L	6.8		8.6	8.5					9.8	11.4	13.6	12.8						
KNM-KP 29287	R			8.2							10.3			(14.2)	13.1				
KNM-KP 30500	L							13.4	8.9			13.3	13.5	15.8	15.1				
KNM-KP 30500	R											13.8	13.1	15.9	14.7	17.0	13.4		
KNM-KP 31712	L			6.6								12.1	10.5						
KNM-KP 31712	R											11.5	10.5						
KNM-KP 31717	R																		13.7
KNM-KP 31730	L							(10.0)											
KNM-KP 34725	L	7.3	8.5					12.1				13.7	12.2	13.0	14.0				
KNM-KP 35847	L													13.6					

Table 2 Continued

Specimen	Side	dl <sup>2</sup>			
		MD	LaL		
Deciduous maxillary dentition					
KNM-KP 34725	R	(4.5)	(4.0)		
Specimen	Side	dc			
		MD	LaL	MD	BL
Deciduous mandibular dentition					
KNM-KP 31712				10.0	7.9
KNM-KP 31729				(9.7)	7.9
KNM-KP 34725	R	6.8	(5.5)		
KNM-KP 34725	L	(6.7)	5.6	(9.3)	(6.7)

Measurements mainly follow White (1977), except teeth are measured as preserved with corrections for interstitial wear given in [ ], and BL dimensions for M<sup>1</sup> and M<sup>2</sup> given across mesial and distal cusps independently.

All measurements given in mm.

() = value estimated due to damage.

a = tooth measured as preserved despite interstitial wear; estimating original dimension reliably is not possible.

**Table 3** Mandibular metrics for *Australopithecus anamensis*\*

	KNM-KP 29281		KNM-KP 29287		KNM-ER 31713
Minimum breadth between crowns					
P <sub>3</sub>	25.9		—		—
P <sub>4</sub>	28.1		—		—
M <sub>1</sub>	26.4		—		—
M <sub>2</sub>	26.8		—		—
Breadth between crown centers					
P <sub>3</sub>	35.9		—		—
P <sub>4</sub>	37.2		—		—
M <sub>1</sub>	37.6		—		—
M <sub>2</sub>	38.6		—		—
Symphysis dimensions					
SI height	27.0		27.0		27.0
AP length	32.2		38.0		29.0
Maximum length	41.0		42.0		33.8
Minimum breadth	21.0		19.5		17.7
Angle to alveolar margin	141		135		142
	Left	Right	Left	Right	Right
Corpus dimensions at P <sub>4</sub> /M <sub>1</sub> junction					
SI height	34.0	34.0	—	42.3	29.0
ML breadth	19.6	18.5	—	22.5	19.7
Minimum breadth	17.9	17.7	—	19.7	17.8
Height of mental foramen center					
From alveolar margin	18	19	20	23	—
From base of mandible	—	16	—	22	17
Mental foramen SI height	2.2	2.8	2.6	—	—
Mental foramen AP length	4.1	3.3	4.6	—	—

\*Mandibular metrics follow Wood (1991).

individual has been recovered from a site, a note is given at the beginning of the specimen description with possible associations indicated. A map showing the relationship of several of the hominin discoveries found close to the type mandible is given in Wynn (2000, Figure 2).

#### *Craniodental Fossils*

**KNM-KP 29281—Holotype mandible and temporal fragment** (Figures 1 and 2). The two pieces of this specimen were found only a few centimetres apart and are therefore included under one accession number as a single individual.

**A: Holotype mandible (L and R I<sub>1</sub>–M<sub>3</sub>)**

*Preservation.* This adult mandible consists of most of the body with all the permanent teeth, which are complete except for some minor damage. It is missing its rami, angles, and the base posterior to M<sub>1</sub>. The left and right sides of the body are separated by a large crack, and the two halves do not match perfectly. There are several puncture marks on the lateral and medial surfaces of the body, probably carnivore tooth marks. Several cracks are probably weathering damage caused as the mandible dried on a land surface. Minor distortion is caused by cracks that have opened throughout the body. The incisors and canines are hinged anteriorly in their alveoli, particularly on the left side, and matrix has filled in the gaps posterior to



**Table 4 Metrics for new *Australopithecus anamensis* postcranial elements**

Tibia KNM-KP 29285		Phalanx KNM-KP 30503	
Proximal		Maximum fragment length	32.9
Maximum fragment length	103	Midshaft DP depth	7.0
Plateau maximum ML	(70)	Midshaft ML breadth	9.7
Plateau maximum AP	(46)	Distance from flexor ridges from proximal joint surface center	24
Medial condyle AP	(45)	Proximal end DP depth	(9)
Medial condyle ML	(27)	Proximal end ML breadth	12.7
Lateral condyle AP	((37))		
Lateral condyle ML	((26))		
Minimum intercondylar distance	16		
Plateau to distalmost point on tuberosity	31		
Maximum shaft breadth at break	33		
Minimum shaft breadth at break	21		
<i>Semimembranosus m.</i> insertion site SI	15		
<i>Semimembranosus m.</i> insertion site ML	18		
		Capitate KNM-KP 31724	
Distal		PD length	21.8
Maximum fragment length	96	DP depth	(14.8)
AP shaft breadth at break	22	ML width of head	(12.5)
ML shaft breadth at break	22		
Maximum AP depth metaphysis	33		
Maximum ML breadth metaphysis	43		
AP depth of talar facet	24		
ML width of talar facet at center	26		
ML width of talar facet at lateral edge	13		
ML width of talar facet at medial edge	21		
SI length of malleolus	14		
Maximum AP depth of malleolus	13		
SI height of fibular facet	7		
AP depth of fibular facet	(16)		
Width of flexor m. groove	8		

( ) indicates estimate, (( )) more tentative estimate.

them. The left  $I_1$  and  $I_2$  have shifted anteriorly by about 4.3, the right  $I_1$  by a little less, and the right  $I_2$  by only a little. The left incisors have also rotated slightly laterally. The right /C has shifted forward for 2.0, the left /C by 3.9. The true positions can be found by realignment of casts of the teeth using the IPFs as a guide. The labial sides of the incisor and canine alveoli are broken off, as is a piece on the inferior side of the symphysis. In posterior view, it is apparent that the left  $M_3$  is in a piece of the body that has been rotated slightly clockwise a few degrees.

*Lateral aspect.* The tooth rows show a mild heliocoidal occlusal wear plane and a weak

Curve of Spee. The alveolar margin is straight and parallels the occlusal margin where it is preserved. Although the rami are missing, in places a narrow extramolar sulcus is visible. A mild jugum for  $P_4$  and a slightly larger one for the mesiobuccal  $P_3$  root interrupt the body surface. The canine juga are missing, but would have formed rounded anterolateral corners to the mandibular body.

The lateral superior torus is merely the extension of the oblique line for the attachment of the buccinator muscle, and exists only as a rounded eminence that disappears below  $M_1$ . A narrow marginal torus runs anteriorly, passing just inferior to the mental

## KNM-KP 29281A

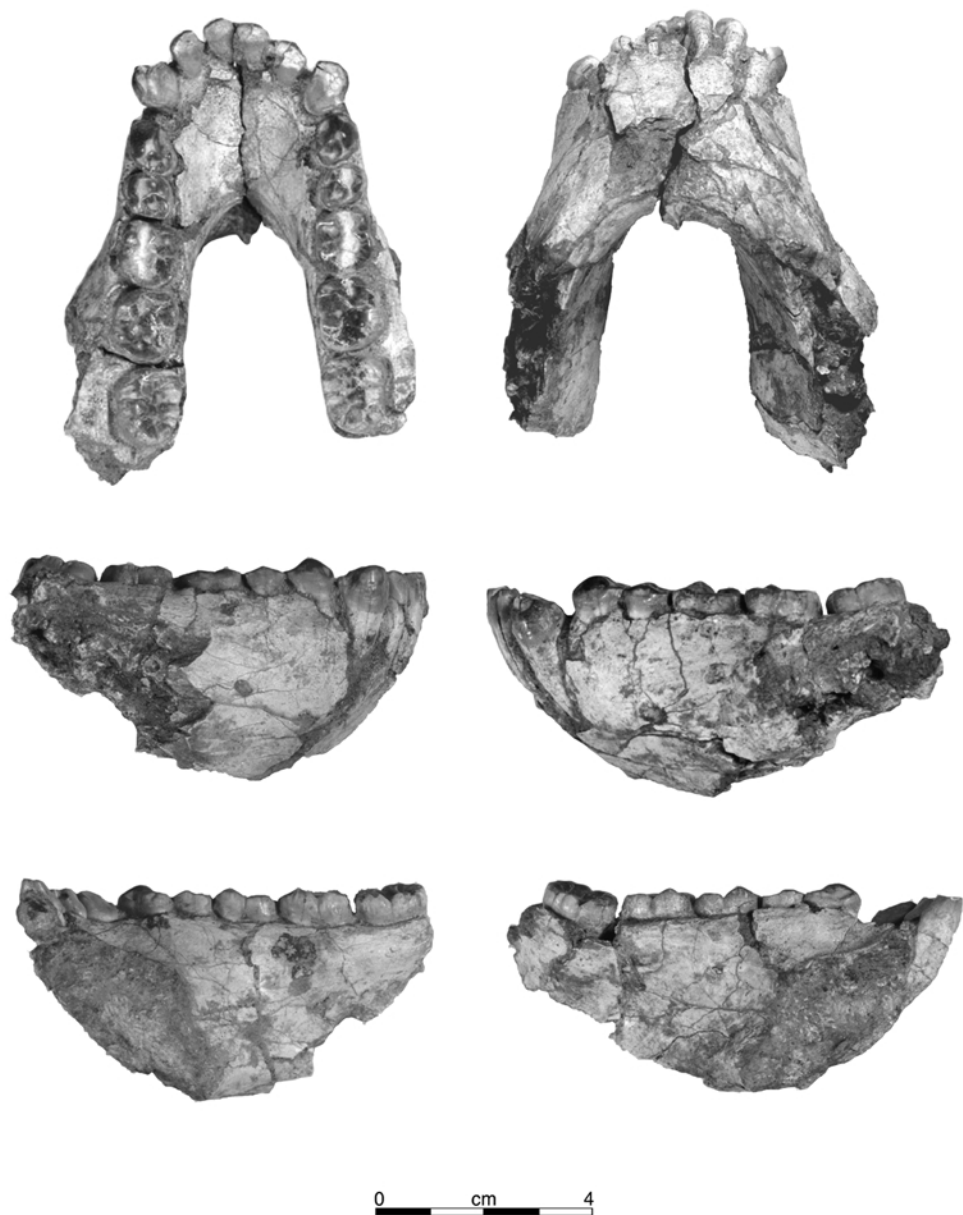


Figure 1. Holotype mandible, KNM-KP 29281A. Top row, occlusal and basal views; middle row, right and left lateral views; bottom row, right and left medial views.

foramen and fades out below  $P_3$ . It is separated from the base by a shallow groove. Anterior to the lateral torus and above the

marginal torus is a broad, shallow intertoral sulcus centered superior and anterior to the mental foramen. There is a single mental

foramen on each side. Each is centered between  $P_4$  and  $M_1$  directly above the base of the symphysis, 17.5 down from the alveolar margin on the left and 19.2 on the right. They open anteriorly. The left one has abraded margins, but the right one measures 3.5 AP by 2.6 SI. The mental surface is strongly but smoothly convex in both directions.

*Posterior aspect.* The postincisive planum is about 24 long, reaching posteriorly as far as the level of the  $P_4$ s and is concave in both directions. It ends in a strong superior transverse torus, which swings laterally from the midline to merge into the medial body wall at the level of the junction between  $M_1$  and  $M_2$ . There is an even stronger inferior transverse torus centered 16 inferiorly and posteriorly from the superior one, and separated from it by a marked genial fossa. The inferior torus reaches as far posteriorly as the mesial edge of the  $M_1$ s at midline, continuing almost directly laterally to merge with the body also level with the  $M_1$ s. There are faint digastric impressions on the underside of the inferior torus on each side, which meet in the midline to form a crest in the center of the torus.

*Medial aspect.* The symphyseal cross-section is strongly inclined, sloping posteriorly with its long axis running  $141^\circ$  to the alveolar margin. The entire external contour is smoothly convex through its rounded inferior margin, with no flattening evident basally. The alveolar margins are straight. The alveolar torus is mild throughout its length except below  $M_3$ , where it becomes more prominent. The alveolar torus is only about 15 SI here, but deepens anteriorly to merge with the superior transverse torus. Inferior to the alveolar torus, the subalveolar fossa is deepest posteriorly becoming shallow anteriorly, where its inferior edge swings up and over the inferior transverse torus allowing it to blend into the genioglossal fossa. No mylohyoid line is evident.

*Basal aspect.* Although much of the base is missing, the preserved contours suggest that it was everted posterolaterally. The preserved basal contour is rounded.

*Occlusal aspect.* The postcanine tooth rows are almost parallel and set close together. The original minimum distance between the canine crowns before distortion can be estimated at about 20. Minimum distances between the lingual sides of the opposite teeth are:  $P_3$ - $P_3$  25.3,  $P_4$ - $P_4$  27.2,  $M_1$ - $M_1$  25.2,  $M_2$ - $M_2$  25.4,  $M_3$ - $M_3$  about 26.5. This last measurement is an estimate because of the slight distortion here.

*Teeth.* Morphological descriptions of the teeth are given for the best preserved side, with any differences between sides noted.

The  $LI_1$  is complete, with two transverse cracks through its root that cause no significant distortion. The  $RI_1$  has alveolar bone adhered to its medial surface. It is missing the inferior labial enamel, and some other small chips. It is split longitudinally, and transverse cracks across its root are expanded causing distortion. The left side is described.

This tooth is worn, exposing an area of dentine across its occlusal plane that is 5.4 MD by 2.5 LaL, with only a thin strip of enamel around its margin. Only 6.9 of labial enamel and 6.5 of lingual enamel remains. The occlusal plane is mildly concave in labial or lingual view and angled slightly distally and lingually. The crown flares out mesially and distally from 4.3 wide mesiolingually at its base to 5.9 at its occlusal edge, and would have been wider before it was worn. Lingual and labial surfaces are transversely convex. The lingual surface is concave SI above its prominent basal bulge. Traces of mesial and distal lingual grooves are left just below the occlusal margin. A tiny area of the IPF remains at the occlusal edge of the mesial surface. Faint traces of transverse hypoplastic lines are visible on the labial face. The root is strongly convex

labially and concave lingually, measuring about 17.5 in length from the labial side of the cervix. It swings mesially just at its apex and there is a distinct mesial groove. At the cervical margin, it measures 4.1 MD by 7.3 LaL.

The right  $I_2$  is broken in a similar way to the right  $I_1$ . It is missing the mesiolingual corner of its crown, so the completely preserved left  $I_2$  is described. This tooth has a longitudinal crack, but has suffered negligible distortion. It has dentine exposed across the entire flattened occlusal surface (5.9 MD by 3.4 LaL) except for a narrow rim of enamel. Only 6.5 of enamel is left SI labially, and 7.4 lingually. Both sides of the crown flare from the cervix increasing MD from 4.8 to 6.6. The occlusal plane appears to slope slightly mesially and lingually, but this impression is mainly due to the higher distolabial corner. Its labial face is uniformly convex in all directions. The lingual face preserves shallow mesial and distal grooves and a mild median ridge above the basal swelling. Interproximal wear has marked the mesial margin of the occlusal face, but no facet is measurable. The root is 4.5 MD near the cervical margin, but mandibular bone and matrix obscures its LaL dimensions. It is 17.4 long and swings distally at its apex.

The left  $/C$  is missing its mesiolabial corner, and other small areas of enamel. The right one is complete, so is described. This crown is a rounded rhombus in occlusal outline. Its occlusal wear plane runs through the high Mmr, and across the crown through the low Dmr located near the cervical margin. The wear plane is angled slightly to slope lingually but is horizontal in a mesiodistal direction, except where it turns to slope sharply inferiorly along the distal margin of the crown. The exposed dentine is hollowed out inside the narrow enamel rim. Although the mesial and distal basal marginal ridges are worn at their highest points, they are intact and confluent as

they swing around the base of the crown lingually. Labially, they are faint, as are the labial grooves. The lingual ridge is asymmetrical, and has a sharp distal margin along a narrow distal lingual fossa, but a flat mesial edge that merges gently with the distal edge of the broad, shallow mesiolingual fossa. The labial surface is tightly convex transversely, and somewhat so SI. Hypoplastic lines are visible on labial and lingual faces, and perikymata are apparent on the labial face. Root dimensions cannot be measured, but on the right side the canine root is exposed for most of its length, and can be seen swinging gently distally.

Both  $P_{3s}$  are well preserved, but the right one shows slightly less wear so the description is based on this. The occlusal outline would be rhomboidal but for the inflated distolingual corner. This tooth has one main cusp near the center. Dentine is exposed in a 1 wide pit on the Prd, and along the distal occlusal ridge. The mesial and distal occlusal ridges and transverse crest are sharp and prominent. The transverse crest has a cusplike representing the Med where it meets the Mmr and Dmr. Lingually the Mmr is narrow and low, arching towards the base of the crown, and bounding a narrow Fa that opens lingually close to the Med. The Dmr is stronger and higher, and bounds a larger Fp. Buccally, there is a pit-like mesiobuccal groove alongside the Mmr. The Mmr swings inferiorly and distally to merge with the basal enamel swelling. There is only a shallow trace of a distobuccal groove. The buccal face slopes strongly toward the cusp apex, and is biconvex. An IPF measuring 4.7 BL has flattened the distal margin of the tooth. Three roots are present. The two distinct buccal roots diverge apically.

The  $P_{4s}$  are also well preserved, but slightly more occlusal enamel remains on the left one on which the description is based. The occlusal outline is asymmetrical. The left  $P_4$  is rhomboidal in outline,

although the right one has a less extensive mesiolingual corner and presumably a smaller Med originally. There are two cusps. The Prd is large and the Med much smaller. The Prd is almost completely worn off, exposing dentine that extends to the mesial and distal margins of the tooth, widening to 2.1 BL at the cusp center and making it lower than the Med. A pinpoint of dentine is visible on the Med. A pit-like remnant of the Fa remains, as does a lower and larger Fp surrounded by a prominent Dmr. The lingual face is straight vertically, and mildly bilobate in occlusal profile, with two faint vertical enamel wrinkles. The labial face is biconvex and slopes towards the buccal cusp. A faint distobuccal groove remains, indenting the occlusal profile of the crown. Interproximal wear has flattened mesial and distal margins of the tooth. The mesial IPF is 4.7 LaL, and the distal one is 6.0 LaL.

Both  $M_1$ s are well preserved, but the left one is missing a small piece of enamel from its mesiobuccal corner. Description is based on the right, even though it is missing a piece of enamel along its distal margin. The occlusal outline is a rounded rectangle. The buccal side is worn more heavily than the lingual side, so that the buccal cusps, Hld and all foveas have been replaced by an elongate, hollowed area of dentine. The lingual cusps have pinpoints of dentine exposed, and on the Med, this area of dentine extends halfway down towards the Fc. Wear has obscured details of relative cusp sizes but the Med is the highest, and is larger in area than the End. The Mmr is almost worn through by interproximal wear. The Dmr is intact on the unbroken left side. The mesiobuccal groove is set slightly mesial to the lingual one. It continues across the vertically convex buccal face where it becomes doubled, and forms a strongly bilobate occlusal profile as it continues to the cervix. The lingual groove is more pronounced occlusally, and is sharp as it cuts the occlusal margin and passes along the

vertical, bilobate lingual face to the cervical line. Interproximal wear has left a broad concavity in the mesial occlusal profile, and has flattened the distal profile of the unbroken left side. On the right, the mesial IPF measures 6.1.

Although both  $M_2$ s are completely preserved, the right one is described because it is slightly less worn. This tooth is a rounded rectangle with bilobate sides with a barely concave mesial margin caused by interproximal wear. The buccal cusps are much larger than the lingual ones, and together with the Hld comprise more than half the crown. The lingual ones are higher as preserved, with the Med the tallest. The entire surface is worn, but dentine is exposed in a 1.7 MD slit on the right Prd. The slit-like Fa is located to the lingual side of the MD axis, as are the Fc and Fp. Only a trace of the Fp remains. The lingual and mesiobuccal grooves are continuous across the crown. The lingual groove sharply incisives the occlusal margin, and continues to the cervix. Faint vertical enamel wrinkles mark the vertical lingual face. The mesiobuccal groove splits just before it passes the occlusal margin, and has a mesial branch that terminates occlusally at a large protostylid, and a distal branch that continues to the cervix along the distal margin of the protostylid. Immediately posterior to this branch are three small, vertical enamel grooves extending along the superior half of the sloping buccal crown face. The distobuccal groove is largely obliterated by occlusal wear, and is faint along the side of the crown. The mesial IPF indents the mesial occlusal profile and measures about 5.0 BL. A distal IPF is obscure, although one is visible on the left  $M_2$ .

The  $M_3$ s are both missing pieces of enamel from their distobuccal corners, but the right one is missing more. The left one has a crack through the mesial cusps and the tip of its Med damaged. Description is based on the left. This tooth is an elongate

Figure 2. Holotype temporal, KNM-KP 29281B in lateral and inferior views.

rectangle in occlusal outline. The occlusal surface is worn with polishing on all cusps and flattening of the buccal cusps and Hld, but no dentine is exposed. The Med is higher than the others, but the Prd is largest in area. There is a large Hyd and a smaller End. Each is divided into mesial and distal parts by grooves. A C<sub>6</sub> is present and larger than the Hld. A deep, transversely wide Fa runs from the MD axis of the crown to the lingual margin, bounded by the Mmr mesially and a transverse ridge connecting the mesial cusps distally. There is no Fp. The lingual and mesiobuccal grooves are deep and continuous, meandering across the crown, incising the occlusal margins strongly and continuing to the cervical margins. Vertical enamel grooves are visible on the buccal, lingual and distal faces, some of which incise the occlusal margin. No protostylid is visible on the left M<sub>3</sub>, although a distinct one is seen on the right one. The M<sub>3</sub> roots incline strongly buccally and mildly distally, as seen on the damaged right side.

**B: Left temporal fragment**—This piece of left temporal bone consists of a maximum

of about 52 AP. About 25 SI of the squamous portion remains, as does much of the temporomandibular joint and the tympanic with the external acoustic porus. Laterally, the zygomatic process is broken off at its base from the prearticular area posteriorly, cutting through the mandibular fossa and postglenoid process. Several large air cells are exposed here. The lateral margin of the external acoustic porus is preserved at its inferior edge, but the rest of the margin is broken away. The inferior surface of the fragment extends posteriorly from the sphenosquamosal suture. It preserves much of the articular surface, part of the prearticular area and inferior surface of the tympanic. The sphenotemporal suture is preserved about 25 anteriorly from the tympanic. The medial surface of the fragment shows a mixture of broken bone pieces and matrix.

The small remaining piece of the squame has fine ridges running superoposteriorly, especially on its posterior part, that follow the course of the temporalis muscle fibers. There is a small tubercle about 4.5 anterior to the most anterior portion of the zygomatic root, in the position to have been

associated with a septum that divided the temporalis muscle. It lies at the anterior end of a faint linear ridge that, like the striations further posteriorly, runs superoposteriorly across the squame. The external auditory porus is small and elliptical in outline. Its long axis is oriented  $90^\circ$  to the superior surface of the zygomatic origin. The porus measures a maximum of 8.9 by 5.7 as preserved.

The articular tubercle is flat, with only a mild convexity demarcating it from the inferior temporal surface. The tympanic plate makes a large angle with the articular surface of the temporomandibular joint, so that the whole of this medial part of the temporomandibular joint is just one shallow, cup-like cavity. It is not possible to estimate how much of the articular surface extended laterally past the squame, but about 20 is preserved medially. The squamotympanic fissure is represented by a 6.4 long slit in the middle of the cavity. The postglenoid process is fused to the tympanic, and would have continued laterally to it. As preserved, the tympanic plate measures 11.6 AP from the squamotympanic fissure to the broken edge of the stylomastoid foramen and 26.3 perpendicular to this to the edge of the acoustic porus. The sheath of the styloid process is partly preserved on the posterior aspect of the tympanic.

On the medial surface, some remaining pieces of bone appear to be endocranial bone and one has a trace of a meningeal vessel groove on it, but on the whole this fractured surface is uninformative.

**KNM-KP 29282: LM<sub>1</sub> or M<sub>2</sub>** (not figured). This is a broken molar, either M<sub>1</sub> or M<sub>2</sub>, preserving a worn crown and partial roots. It was discovered during screening, just washing into the sandy stream channel at the base of the slope from which the type specimen, KNM-KP 29281, and the worn premolar and molar, KNM-KP 31730 were found (Wynn, 2000, Figure 2). It is possible that

this specimen is the same individual as KNM-KP 31730, but separate accession numbers have been allocated because of the large distance, from the base to the top of the slope (approximately 10 m), separating the two specimens.

The molar is the most heavily worn mandibular molar in the sample, with dentine exposed over the entire occlusal surface. The roots are nearly complete buccally, but are largely missing lingually. Mandibular bone is preserved between the roots, but only the buccal cortex remains. The occlusal outline is rectangular. The buccal side is broken, and enamel is missing from the mesiobuccal corner, and distal side of the crown. The smaller area of lingual dentine is set at higher plane than the much larger buccal portion, which is strongly hollowed out transversely. On the buccal face, the mild mesiobuccal groove extends to the cervical margin. Wear and damage obscures any potential evidence of a proto-stylid. A tiny portion of the mesial IPF is visible and contacts the occlusal margin. Distally no IPF is preserved. The remaining mesiobuccal root is at least 14.5 long and less distally inclined than is the remaining 11.5 long distobuccal one.

**KNM-KP 29283: Maxilla** (Figure 3). This maxilla was a surface discovery, but the I<sup>1</sup> and both lateral incisors were recovered separately through excavation.

*Preservation.* This is a weathered adult maxilla with all teeth except the left I<sup>1</sup> and right M<sup>3</sup>. The maxilla is preserved in two halves. Both preserve the intermaxillary suture anterior to the nasal aperture. Posterior to this, the left side preserves the suture inferiorly along the palatine process. The right side, however, is broken 3 laterally from the midline on the palatine process. Therefore, the two halves can be articulated only anterior to the incisive foramen and nasal aperture. The superior portion of the clivus is missing on both sides of the midline

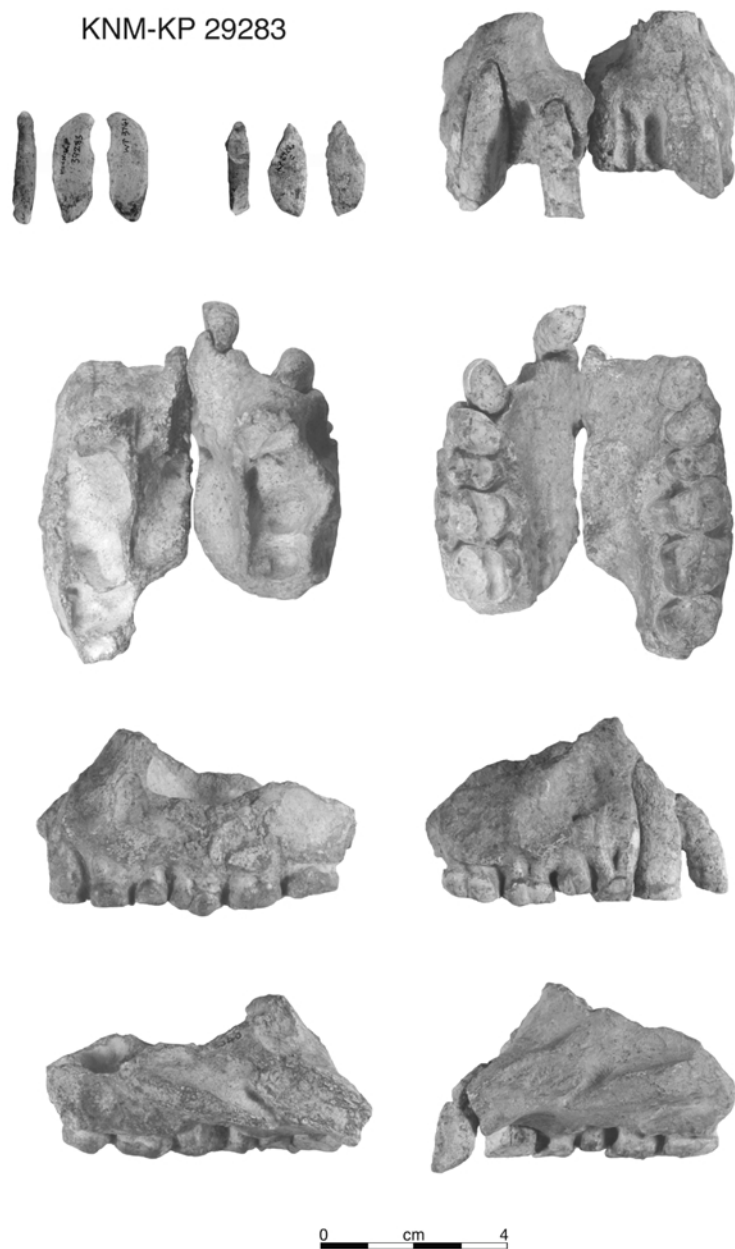


Figure 3. KNM-KP 29283 maxilla with associated  $I^2$ s.  $LI^2$  in lingual, distal and mesial views;  $RI^2$ , in lingual, distal and mesial views; maxilla in facial view at top, second row, superior and palatal views; third row, left and right lateral views; bottom row, left and right medial views.



within the nasal aperture. The incisor alveoli are partially preserved, with their labial portions broken away. The labial and buccal margins of the canine alveoli are broken away over the entire length of the canine root on the right, and for much of it on the left. On the right side, the P<sup>3</sup> buccal roots are exposed and much of the P<sup>4</sup> roots, but it is impossible to tell how much of the root exposure is due to damage and not resorption. The right I<sup>1</sup>, both I<sup>2</sup>s and the RC/ were fossilized separately. On the left side, the maxillary tuberosity is eroded, exposing cancellous bone. Only about 10 of bone is preserved above the alveolar margins. There is lateral exposure of the distal M<sup>1</sup> root, probably due to abrasion.

*Facial aspect.* The anterior margin of the maxilla is slightly convex transversely where preserved. There is a mild, vertical depression laterally where the bone flares around the canine jugum on each side. The I<sup>2</sup> alveoli are set lateral to the nasal cavity. The inflated canine juga and the anterior P<sup>3</sup> juga form large rounded anterolateral corners to the profile of the bone. The nasal aperture is smoothly continuous with the external surface of the bone. No ridges or crests delimit the preserved portion laterally or inferiorly. The lateral walls of the aperture extend 12.5 superior to the floor on the right and about half that on the left. The nasal aperture is 22.3 wide. A depression about 8 wide just inside the lower lateral margin of the nasal aperture is delimited posteriorly by a rounded ridge that runs posteriorly and superiorly from the posterior edge of the clivus.

*Lateral aspect.* The lateral contour of the alveolar process is gently convex. The canine fossae are asymmetrical and quite irregular. On the right side, the canine fossa is deep and measures just over 11 × 11. There may be some pathology, also suggested by an irregular and convoluted floor of the maxillary sinus on this side compared with that of the left. On the right side, the

alveolar bone along P<sup>3</sup> to M<sup>1</sup> is resorbed, exposing the bases of the roots. Just postero-inferior to the canine fossa, right above the tips of the distobuccal P<sup>3</sup> and single buccal P<sup>4</sup> roots, there is a circular depression measuring 5 in diameter of obscure origin. The root of the zygomatic is preserved as a raised area of abraded bone. Inferior to it is a shallow depression, bounded posteriorly by the rounded jugum for the distobuccal M<sup>1</sup> root. The jugum for the distobuccal root of M<sup>2</sup> is pronounced. These juga give the lateral margin of the alveolar process a mildly undulating profile. Similar contours are seen on the more abraded left side. On the left, however, the canine fossa appears to have been smaller, although it is broken superiorly. There is also less root exposure.

*Inferior aspect.* The postcanine tooth rows are almost parallel to each other, and are slightly concave lingually. Minimum breadths of the palate between teeth are: C/ 34, P<sup>3</sup> 38, P<sup>4</sup> 38.5, M<sup>1</sup> 38, and M<sup>2</sup> 35.5. The palatine processes rise gradually posteriorly, so that the palatal depth increases steadily. As measured from tooth cervices, palatal depth is 6 at P<sup>3</sup>, 8 at P<sup>4</sup>, 10.5 at M<sup>1</sup>, and 12.5 at M<sup>2</sup>. The length of the tooth row from the mesial side of C/ to distal M<sup>3</sup> is 63.3. The incisive foramen is about 5 in transverse diameter and is centered 17 from the alveolar margin, between the P<sup>3</sup>s. The greater palatine foramen is not present, but the vascular groove is, lying at the inflection between the alveolar and palatine processes. On the left side, a severe alveolar resorption pit measuring 15 AP has exposed up to 9.0 of the M<sup>1</sup> roots and 4.0 of the P<sup>4</sup> root. On the right side, resorption is less extreme, but is present in roughly the same location.

*Superior aspect.* The nasal cavity is narrowest at a point just posterior to the internal ridge, where it is about 21.5 wide, broadening posteriorly to about 27 above the level of the M<sup>1</sup>. On the left, the maxillary sinus as it is exposed is 46 AP, running from a point

level with P<sup>4</sup> to the posterior break. It is up to 15 ML, with its widest point above M<sup>1</sup>. It is divided into a large anterior cavity, a small middle cavity superior to M<sup>3</sup>, and an even smaller one posterior to that. There is a faint division of the larger cavity separating the roots of M<sup>1</sup> and M<sup>2</sup>. The right maxillary sinus reveals a more complex set of irregular loculi than the left, with a deep anterolateral pocket reaching down towards the canine fossa, and two smaller pockets preserved superior to the canine root. The sinus is preserved for 37 AP, running from the level of P<sup>3</sup> only to M<sup>2</sup>. It is up to 17 ML at the M<sup>1</sup> level.

*Medial aspect.* Subnasal anatomy is exposed on the midline break. The incisive canal is 3.2 wide in the sagittal plane near the foramen and expands posteriorly to about 6 near the nasal cavity. The long axis of the canal runs superiorly and posteriorly at an angle of about 25° to the inferior surface of the palatine process. The naso-alveolar clivus is a maximum of 11.4 thick. From the anterior margin of the nasal aperture, the floor of the nasal aperture passes backwards about 13 before dropping inferiorly about 12 to the palatine processes. The left palatine process, which preserves the midline suture, expands in thickness posteriorly from a thin apex at the incisive canal to 6 at the level of M<sup>2</sup> at midline. The opening of the incisive canal is just over 12 across, and it opens posteriorly and laterally to the widest portion of the nasal cavity.

*Teeth.* The teeth are heavily worn, especially anteriorly. The right ones are less heavily worn, so these are described where both sides are preserved. Little detailed occlusal morphology remains. There is a clear helicoidal wear pattern along each tooth row.

The right I<sup>2</sup> consists of the root and the labial portion of the crown. The labial enamel is only preserved for an arc 3.2 mesially and 2.2 distally. The lingual side is worn well below the original cervical

margin, so that the occlusal plane was oriented superolingually and slightly distally. The root is broken superiorly, but can be replaced into the preserved portion of its alveolus. The root is 22 long. It is triangular in outline near the cervix and becomes rounder apically. The root is convex in outline on its labial side and concave on the alveolar side. A mesial groove is present.

The I<sup>2</sup>s are morphologically similar, so the more complete left one is described. Only 2.4 of enamel remains labially on the left, although 3.8 remains on the right. The root is worn down below the original cervical margin lingually, so that the occlusal wear surface is strongly angled labially. It is also angled to slope lingually and distally. A narrow band of enamel remains mesially, but almost none distally. The root is 22 long from the labial enamel line. It is strongly compressed MD, measuring 4.6 MD by 8.2 LaL near the cervix, and is hooked labially at its tip. The preserved labial and lingual margins of the root are mildly convex, so that it widens to a maximum of 9.0 LaL. The root has mild mesial and distal grooves.

The canine has only 3.5 of the labial enamel and a thin ribbon of distal enamel remaining. Its occlusal surface is planar and slopes lingually. Almost the entire root is exposed. It is fairly straight but convex labially, 28.6 long. It is oval in section, measuring 9.0 MD by 11.5 LaL near the cervix. The root has a mesial groove. It is nearly vertical, with its long axis oriented at over 85° to the cervical margins of the postcanine teeth in lateral view.

All that remains on the P<sup>3</sup> crown is a very thin rim of enamel. It had about 6 of buccal enamel remaining, but most of the buccal enamel has been broken away. The dentine exposure is hollowed out. Mesial and buccal labial grooves extend about 2 superiorly from the occlusal plane, and there is a pronounced basal enamel bulge. It has three distinct roots. On the right, the roots are

exposed for 13.0 mesially and 12.7 distally, which is most of their length. The mesio-buccal and distobuccal roots diverge at about 30°.

The right P<sup>4</sup> is displaced superiorly. It has enamel chips missing from its buccal and lingual surfaces. The left P<sup>4</sup> has lost enamel from the mesiolingual corner. Some occlusal enamel remains between the cusps and in the Fp. A 3.2 wide area of dentine is exposed lingually, but the buccal exposure cannot be measured owing to damage. Extensive contact facets are evident, altering the mesial and distal faces of the crown.

The left M<sup>1</sup> is missing enamel on most of the mesial half of the tooth, and the right one is missing a small piece from the distolingual corner. In occlusal outline the M<sup>1</sup> tapers distally. The lingual half of the crown is a heavily excavated dentine basin surrounded by a 2 high thin rim of enamel. Wear has flattened the buccal cusps. Dentine exposure is difficult to assess due to weathering, but there is a clear 1.3 wide dentine pit on the Pa. The two buccal cusps are mostly preserved, with the Me the larger. A pit-like Fp remains bounded by a Dmr. The buccal groove is pronounced, and continues to the cervical margins making the buccal face strongly bilobate. Interproximal wear has removed much of the mesial enamel.

The occlusal outline of the M<sup>2</sup> also tapers distally. The preserved buccal cusps are roughly the same size and flattened by wear. Dentine is exposed as a continuous excavated strip along the two lingual cusps. There is also a 1 wide dentine pit on the Pa. The shallow remains of a Fp are present. Both lingual and buccal faces are bilobate, with lingual and buccal grooves extending to the cervical margin. A weathered distal IPF is visible but cannot be measured.

The M<sup>3</sup> has a strongly tapered occlusal profile, with a rounded distal margin. The mesial cusps are substantially larger than the distal ones, occupying most of the

crown. The Pa is higher than the distal cusps. The occlusal surface is flattened by wear and there are two mesial dentine exposures, 1.9 BL on the Pa and nearly 5 and deeply excavated on the Pr. The lingual and buccal grooves are mild, and extend all the way up the crown faces.

**KNM-KP 29284: R/C and RP<sub>3</sub> germs (Figure 4).** This specimen was found *in situ* in an excavation to recover further parts of the adult maxilla, KNM-KP 29283. Because these two teeth are germs they are clearly from a different individual.

**A: R/C.** This is the nearly complete crown or a /C germ that is slightly weathered and cracked around its cervical half. There is no trace of any root formation. It is strongly asymmetrical. In occlusal outline, it is almost a quadrilateral with corners mesiolabially, mesiolingually, distolabially and the most prominent one distolingually. Its lingual face is marked by pronounced mesial and distal lingual fossae and a sharp lingual ridge, all of which are concave distally. The mesial edge of the lingual ridge is rounded, but its distal edge is sharp. The high Mmr is faint as it passes the mesial edge. The incisive and cervical halves of the sharp mesial margin are set at about 30° to one another in lingual view. The cervical portion almost parallels the distal margin of the crown and the incisive portion angles distally towards the apex. The sharp distal margin of the crown is concave, swinging out inferiorly to meet a strong distal basal tubercle 10.0 from the crown tip and 3.3 from the preserved base. This tubercle exists as the pinnacle of the Dmr, which inclines inferiorly both lingually and labially, but more steeply labially. Lingually, it meets the base of the lingual ridge. Nested just above the distal tubercle there is a smaller tubercle. Labially, there is a broad distolabial groove with a sharp distal edge and a gentler mesial edge that blends into the labial face. The labial face is tightly convex transversely, but

## Kanapoi Isolated Teeth

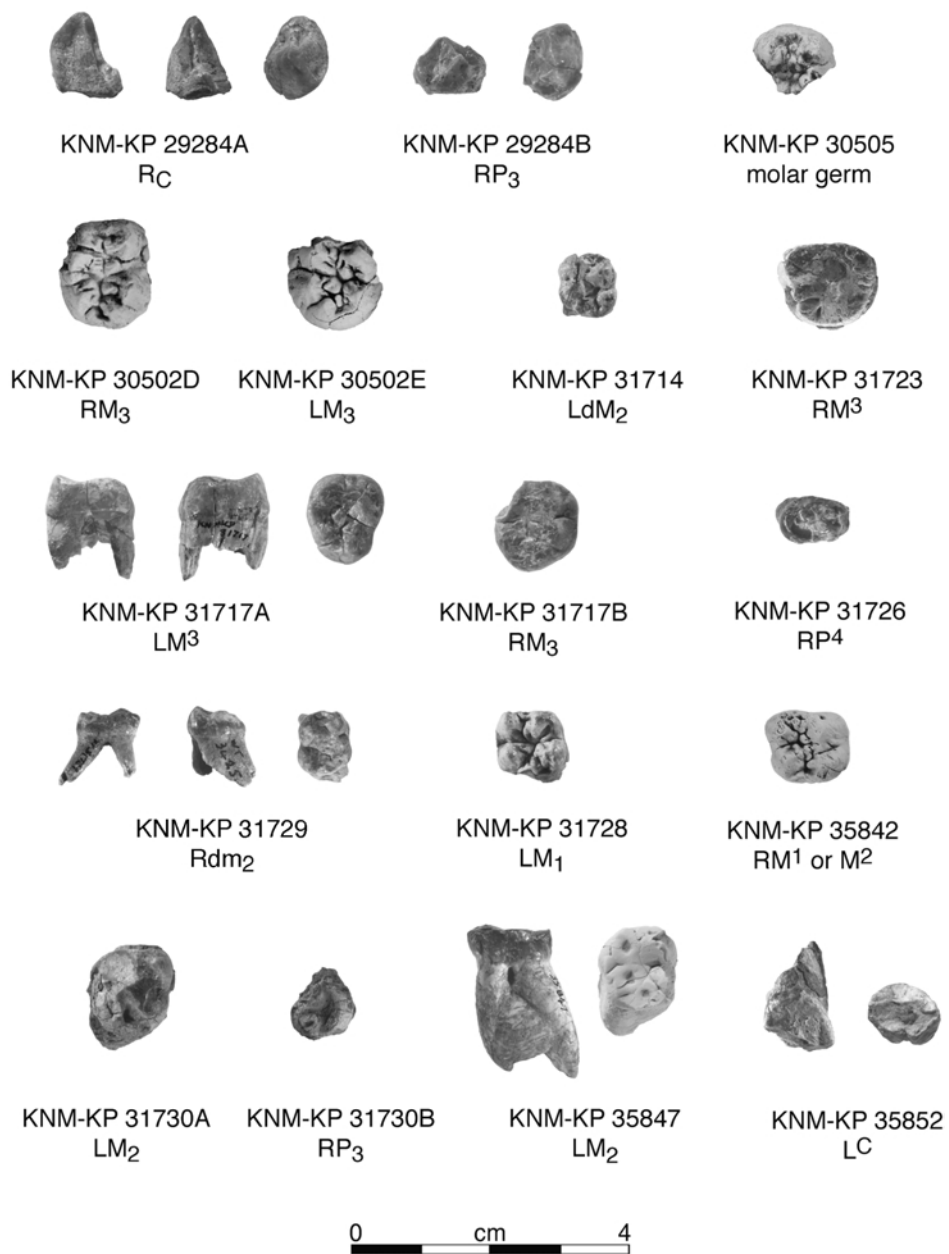


Figure 4. Dental specimens from Kanapoi not associated with jaw fragments. KNM-KP 29284A in lingual, distal and occlusal views, KNM-KP 29284B in lingual and occlusal views, KNM-KP 30505 in occlusal view, KNM-KP 30502D, KNM-KP 30502E, KNM-KP 31714, KNM-KP 31723 in occlusal view, KNM-KP 31717A in mesial, distal and occlusal views, KNM-KP 31717B and KNM-KP 31726 in occlusal view, KNM-KP 31729 in buccal, distal and occlusal views, KNM-KP 31728, KNM-KP 35842, KNM-KP 31730A and KNM-KP 31730B in occlusal view, KNM-KP 35847 in buccal and occlusal view, and KNM-KP 35852 in mesial and occlusal views.

is almost straight SI. There is almost no mesiolabial groove, only a sharp, straight edge inferior to the Mmr. Hypoplastic lines are evident on the lower half of the labial face, with a particularly strong one 2·4 above the inferior margin. Perikymata are also visible.

**B: RP<sub>3</sub>.** The crown of this germ is almost complete with no trace of root development. It is split in two by a vertical crack passing mesiodistally through its middle, but it is not distorted. Lingual enamel is broken away from the sides adjacent to the basins, although more extensively so around the Fp. Enamel is also missing from the inferior edge of the distal margin of the crown. The crown has an ovoid occlusal margin, with the long axis running mesiobuccally to distolingually. The large Prd is located in the center of the tooth. The mesial and buccal occlusal ridges and transverse crest are sharp. The transverse crest meets a tiny Med. The mesial ridge is continuous with the sharp Mmr. The distal ridge meets the Dmr at a distal tubercle. The Fa is BL narrow, and the Fp is broader with its sides marked by radial wrinkles. The buccal surface of the tooth is convex transversely. It is mildly convex SI, inclining strongly toward the Prd. Mesial and distal labial grooves are bounded by sharp marginal ridges. Faint vertical enamel ridges are visible on the buccal face.

**KNM-KP 29286: Mandible fragments with associated mandibular dentition (I<sub>1</sub>, L & R I<sub>2</sub>-M<sub>3</sub>) (Figure 5).** Apart from the fragments that make up KNM-KP 29286A, this specimen was recovered through screening and comprises a complete set of lightly worn associated teeth. Several have their roots embedded in expanded and cracked mandibular bone and matrix. Several tooth fragments that do not appear to belong to this specimen were also recovered but given a separate accession number, KNM-KP 31732.

**A: R mandibular fragments (I<sub>2</sub>-P<sub>3</sub>).** This piece of mandible is badly broken. The only remaining cortex is about 1 along its inferior edge below I<sub>2</sub> and much of the area below P<sub>3</sub>, although here it is weathered. The alveolar margin between I<sub>2</sub> and /C is mildly abraded but close to preserving its original contour. Most of the rest of the bone is badly splintered, distorted and intermingled with matrix. The mesial wall of the P<sub>4</sub> alveolus is exposed at the posterior break.

The tip of the I<sub>2</sub> crown is broken off, with enamel preserved only 3·9 labially and 5·7 lingually. The break exposes the pulp cavity. The root is complete although the tip is separated from the rest of the tooth by a 3 wide transverse crack. The superior half is displaced slightly labially relative to the apical end, which appears to be in its original position. Most of the tip is obscured by matrix. The I<sub>2</sub> lingual face preserves a mild basal tubercle, above which it is gently concave SI and flat transversely. The gently convex labial face has faint vertical enamel wrinkles and perikymata visible. The root measures 5·1 MD by 8·0 LaL near the cervical margin. The exposed side of the root has a mesial groove.

The canine crown is complete except for a small area of enamel at its distolabial cervical margin. The distal half of its root is complete, but the mesial half is missing about 11 from the mesial cervical margin, exposing the pulp cavity throughout its length. The canine crown measures 14·3 high labially as preserved, and was probably about 15 before wear. It is highly asymmetrical. The tip of the cusp is worn transversely, preserving a tiny spot of dentine, and polishing extends most of the way along the distal crown margin. The mesial margin is sharp, making a 30° bend at the Mmr in lingual view at midcrown. The Mmr swings distally and cervically, terminating inferior to the wide and deep mesiolingual fossa. In lingual view, the distal margin of the crown becomes concave towards the distal basal

## KNM-KP 29286

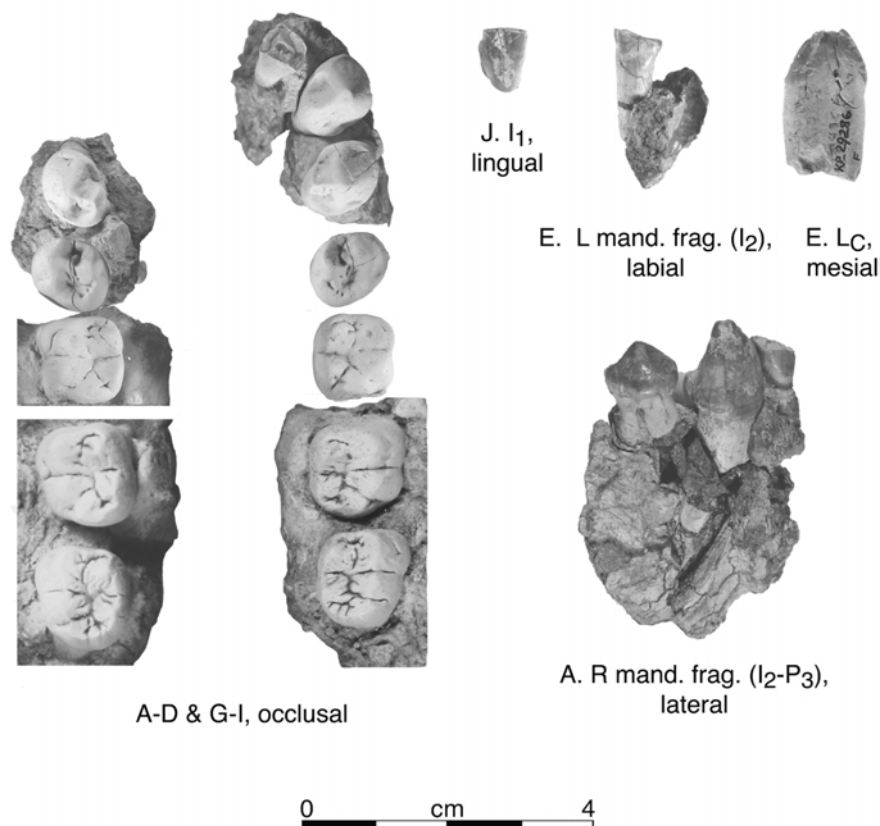


Figure 5. KNM-KP 29286 associated mandible fragments and mandibular dentition. On left, (A), (B), (C), (D), (G), (H), and (I) in occlusal view; (J) in lingual view; (E) in two pieces, mandible fragment with I<sub>2</sub> in labial view, and L<sub>C</sub> in mesial view; bottom right, (A) in lateral view.

tubercle. The Dmr is faint, extending from this tubercle mesially. The lingual ridge is sharp at its top, but widens inferiorly. The distal lingual fossa is a narrow slit. The labial face is transversely convex and mildly so. There is almost no mesial labial groove, but a wide, shallow distal labial groove. There is little basal swelling of the crown on any side. Hypoplastic lines mark the labial surface. The root measures 8.0 MD by 11.7 BL near the cervical line. It has a pronounced mesial groove. The canine alveolus measures about 30 deep. The pulp cavity is about 5.5 wide LaL.

The P<sub>3</sub> crown is complete, with some hairline cracks through it that cause no distortion. Most of the middle portion of its mesiobuccal root is missing. This lightly worn P<sub>3</sub> has a large Prd occupying the center of the tooth. The mesial and distal occlusal ridges and transverse crest are sharp, as are the marginal ridges. All show some polishing from occlusal wear. There is an incipient Med. The Fa opens lingually, because the Mmr dips almost to the cervical line. The Fp is larger and opens superiorly, as the Dmr is more pronounced and higher than the Mmr. Buccally, the Mmr and Dmr

merge with a horizontal basal enamel swelling. Above it, the strongly sloping buccal face is convex transversely and straight SI. The labial grooves are moderate.

**B: RP<sub>4</sub>.** This is the crown with up to 4·3 of the root. Cracks run through the crown but cause no distortion. The occlusal outline is a broad oval that is slightly broader lingually. It is lightly worn. This tooth is bicuspid. A large Prd occupies about half the crown, its apex about one third of the way from the buccal margin in occlusal view. The Med is smaller but almost as high. Mesial and distal occlusal ridges are rounded. The transverse crest is notched in mesial or distal view. The shallow Fa is smaller and higher than the Fp, but both are marked with enamel wrinkles. The Mmr is narrow and meets the base of the Med. The stronger Dmr meets the Med nearer its apex and close to a pit that is separate from the Fp. The buccal face is convex transversely. It is nearly straight vertically, sloping strongly towards the apex, with a gentle basal swelling that connects the mesial and distal labial grooves. The distal labial groove is more pronounced than the mesial one, and delineates a small cuspule at the occlusal margin. An obliquely set mesial IPF measures 2·8 BL by 1·4 SI. Another oblique, lingually placed distal IPF measures 4·1 by 2·1. The preserved top of the root has grooves mesially, mesiolingually and distally.

**C: RM<sub>1</sub>.** This crown is complete and preserves up to 2 of the root. The crown is almost square but slightly elongate MD. From largest to smallest the cusp areas are: Prd, Med, Hyd, End, Hld. All show wear; the lingual cusps are faceted and the buccal flattened with small areas of dentine exposed. A protostylid is present, delineated from the Prd by a narrow slit along its mesiobuccal corner. The Fa exists as a slit running up the Med nearly to its apex from the Mlg. Distal to it is a less extensive groove, bounded posteriorly by a ridge

connecting the two mesial cusps. The Fp is a cleft connecting the End and Hld. It is traversed by the distal lingual groove, which disappears about halfway down the distolingual crown face. The sharp lingual groove deeply incises the occlusal margin but disappears halfway down the vertical lingual face. The mesiobuccal groove is deep near the occlusal margin, but is only a broad and shallow depression towards the cervix. The buccal face is strongly bilobate, and the lingual face is straighter. The distobuccal groove terminates near the occlusal margin. A mesial IPF measures 4·7 BL by 2·3 SI and does not meet the occlusal plane. A faint distal IPF measures about 3 BL by 2 SI.

**D: R mandibular fragment (M<sub>2-3</sub>).** This is a piece of badly splintered mandibular bone that preserves no morphology. The complete M<sub>2</sub> and M<sub>3</sub> crowns are present, with roots partially encased in extensively cracked bone.

The M<sub>2</sub> tapers distally with a rounded distal margin. From largest to smallest, the cusp areas are: Prd, Med, End, Hyd and Hld. The tooth is lightly worn; the lingual cusps are faceted and the buccal flattened but without dentine exposure. Its foveas resemble those of the M<sub>1</sub>. The mesiobuccal groove passes the protostylid to fade out toward the cervical margin. The lingual groove incises the occlusal margin strongly but is faint on the lingual face. The distobuccal groove is shallow on the side of the crown and disappears just past the occlusal margin. The protostylid is found only on the buccal face of the Prd and is most pronounced at the mesiobuccal groove. The buccal and lingual faces are like those of M<sub>1</sub>. Vertical enamel wrinkles mark the buccal face. The mesial IPF is weathered and cannot be reliably measured. The distal IPF is a sliver 3·2 BL along the occlusal margin.

The M<sub>3</sub> is lightly worn on all cusps. It is mesiodistally elongate with a receding, rounded distobuccal corner. Relative cusp sizes and shapes are the same as for M<sub>2</sub>,

except that the Hld is smaller and there is a small  $C_6$  adjacent to its pit-like distal fovea. The occlusal surface enamel is crenulated. The Fa is a broad single slit marked by vertical enamel wrinkles. The deep mesiobuccal groove continues to a point near the cervix, just distal to a distinct protostylid that flanks the entire buccal face of the Prd. The lingual and distobuccal grooves both disappear midcrown. The mesial and buccal sides resemble those of the other molars. Faint vertical enamel wrinkles mark all sides of the crown.

**E: L mandibular fragment ( $I_2$ -/C).** This fragment of mandible is badly splintered. Part of the distal wall of the  $I_2$  alveolus and mesial wall of the /C alveolus remain. The  $I_2$  has its crown broken diagonally so that the exposed face is angled distally. The pulp cavity is exposed. Up to 7.4 of enamel is preserved lingually and 6.5 labially along the mesial edge. A chip of enamel is missing at the mesiolabial corner. A 1 wide transverse crack divides the root just below the crown lingually and 4.4 below it labially. The apical end of the root is missing past about 7 from the crown. The /C is missing the distobuccal corner and superior half of its crown. The root is preserved for up to 13.3 of its length. The morphology of these teeth is like those of the right side.

**F: L mandibular fragment ( $P_3$ , roots  $P_4$ ).** Small amounts of cortex remain on this fragment, but no morphology is preserved. The  $P_3$  is complete. Two broken roots of  $P_4$  are visible. The  $P_3$  is like the right one, but is more compressed MD, with a slightly lower crown and lower Dmr.

**G: LP $_4$ .** This is the crown with up to 4.5 of its root. It cannot be joined to fragment F described above. The crown is split by a thin mesiodistal crack, but has suffered negligible distortion. An obliquely set mesial IPF measures about 2 BL by 1 SI. A more distinct, oblique, lingually placed distal IPF measures 2.9 by 1.8. In all other aspects it resembles the RP $_4$ .

**H: L mandibular fragment ( $M_1$ ).** This is the crown and partial roots of the tooth encased in badly splintered mandibular bone that preserves no morphology. A small piece of the lateral surface of the body about 9 long is visible, but not in its original position. The  $M_1$  crown is nearly the mirror image of the right one, except that a distinct transverse pit is located along the distobuccal groove incising the edges of the Hyd and Hld. The protostylid is more extensive extending almost to the mesiobuccal groove. Vertical enamel wrinkles are visible on the buccal and lingual faces.

**I: L mandibular fragment ( $M_{2-3}$ ).** These complete  $M_2$  and  $M_3$  crowns have part of their roots preserved, encased in a badly fragmented piece of mandibular bone. The only original bone that remains in position is the alveolar margin around  $M_2$ . Details of the occlusal groove pattern differ between sides, and the left ones are less worn, but these teeth are essentially mirror images of the right ones. The  $M_3$  has a larger Hld and a double  $C_6$ , contributing to its more rectangular occlusal outline compared to the right.

**J: I $_1$ .** This is most of the crown weathered in patches. The long IPF on one side suggests that it may be a right, as listed in Leakey *et al.* (1995), but because the other side of the crown is too weathered to assess, this tooth cannot be attributed to a side with certainty. The top of the root is visible mesially and distally, but the crown does not reach the cervical line labially or lingually. The tooth is worn, exposing a strip of dentine. The lingual side has gentle, broad mesial and distal lingual fossae. The labial side is straight and flat. The IPF measures 5.2 SI by 1.6 LaL, and occupies most of the right side of the crown in lingual view.

**KNM-KP 29287: Mandible with teeth (Figure 6).** This specimen was largely recovered through screening. The initial



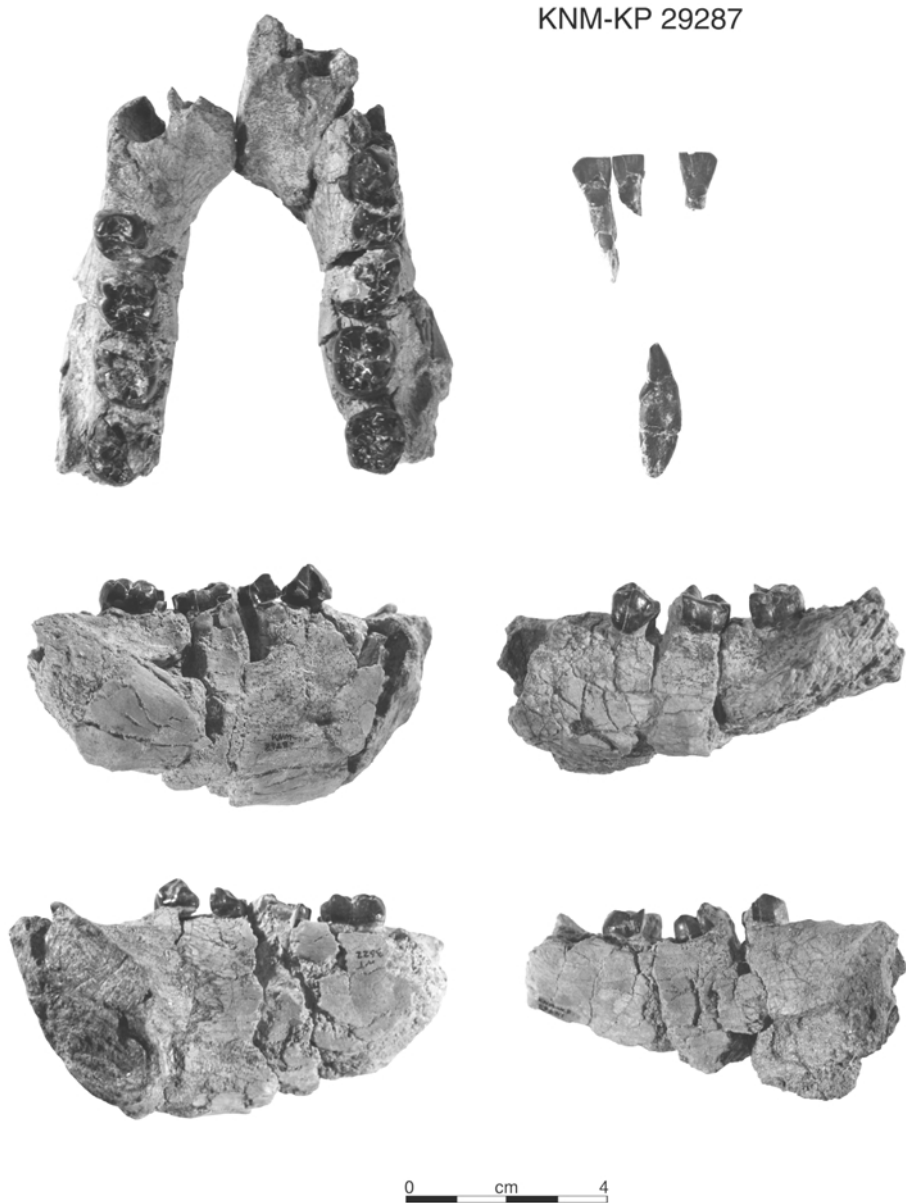


Figure 6. KNM-KP 29287. Top row left, occlusal view of mandible KNM-KP 29287 A and B, and right, incisors KNM-KP 29287 C, H, D from right to left in lingual view, and below KNM-KP 29287 C in medial view. Middle row, mandible KNM-KP 29287 A and B in left lateral views. Bottom row, mandible in right and left medial views.

discovery, two fragments of left and right edentulous mandible, were found close to the to the origin of a small stream channel. Subsequent screening for about 50 m along

this channel led to the recovery of numerous bone and tooth fragments that were reconstructed to make up this almost complete mandibular body.

**A: L mandible (alveoli I<sub>2</sub>-/C, partial crowns P<sub>4</sub>-M<sub>2</sub>, roots P<sub>3</sub>, partial roots M<sub>3</sub>).** *Preservation.* This is a mandible of an adult. The left body is more poorly preserved than the right, so mandibular morphology is described for the right side (B). The left portion of the mandible is preserved anteriorly from a point just lateral to the symphysis internally and about 14 anterior to the mental foramen externally, and extends to the third molar distal roots posteriorly. The left body is damaged anteriorly, with a break passing transversely through the alveolus of the I<sub>2</sub> and /C. The base is missing, with cortex preserved for a maximum of 28 inferiorly from the alveolar margin on the lingual face. The alveolar margin is intact only along the lingual side of M<sub>2</sub>, and it is abraded everywhere else. The preserved cortex is cracked throughout and weathered in places, but distortion appears minimal. A carnivore tooth mark is visible anterosuperior to the mental foramen.

*Morphology.* The mandibular canal is exposed along the broken inferior surface from the posterior break to a point inferior to the M<sub>1</sub>-M<sub>2</sub> junction, and is about 5.6 in diameter. At the posterior break, there appears to be a crypt situated just lingual to the mandibular canal for a supernumerary molar or a Stafne's or other type of developmental cyst. The canal is at least 7.6 in diameter and immediately lateral to the distal root of M<sub>3</sub>, which itself is seen in longitudinal section at the posterior break.

The single mental foramen is oval in section. Its posteroinferior margin is abraded, but it appears to have opened slightly superiorly.

The I<sub>2</sub> alveolus is vertically oriented, with a MD width of about 5 and an estimated minimum depth for the I<sub>2</sub> root of 14.6. The extremely large left canine alveolus measures about 10.5 in maximum diameter transversely, in an axis running diagonally from the middle of the I<sub>2</sub> alveolus to just buccal to the P<sub>3</sub> root. Although a small

triangle of bone is missing from its lateral margin, the alveolus is apparently not distorted, because a CT image of the preserved right canine root and alveolus reveals comparable dimensions (F. R. Spoor, personal communication). The LP<sub>3</sub> has no crown. A single mesial root is visible running behind the canine alveolus. A separate distal, plate-like root appears in the broken cross-section of the alveolar margin, but this root bifurcates deeper in the mandible, as suggested on the right side and visible on a CT image (F. R. Spoor, personal communication).

The LP<sub>4</sub> is almost complete, missing enamel only along its distolingual corner. Its occlusal outline is a rounded rhombus. The Prd is the larger of the two cusps and is set directly buccal to the Med. The only apparent occlusal wear is a flattened light facet on the Prd that has exposed a small, circular area of dentine about 0.4 across. The faceting runs from the tip of the Prd slightly onto the transverse crest, and more so mesially onto the Mmr although it does not contact the mesial IPF. The Med and all ridges and crests are polished. The Fa is smaller and situated higher than the Fp. The transverse crest is split, so that there is a small Fc between them. The Dmr is stronger and wider than is the mesial Mmr, and it merges buccally with the buccal marginal ridge. The oval mesial IPF is 3.3 BL by 2 high. It contributes to the flat occlusal outline of the mesial side of the crown. There is a single slight lingual groove, distal to the lingual cusp. On the buccal face, there is a distinct distobuccal groove but only a trace of a mesiobuccal groove.

The LM<sub>1</sub> is missing enamel along its entire mesial margin to the center of the two mesial cusps, so the Mmr and Fa cannot be seen. The crown is a rounded rectangle in occlusal outline with mildly bilobate sides. The tooth has two relatively high faceted lingual cusps, two worn and flattened relatively low buccal ones, a flattened Hld and a small polished C<sub>6</sub>. The Med is the dominant

cusps but the relative cusp areas cannot be determined due to the missing mesial portion of the tooth. The buccal cusps are set mesial to the lingual ones. Wear facets are seen on all cusps, with wear striae running predominantly BL. Small, circular areas of dentine are exposed on the two buccal cusps, with the Prd exposure bigger than that on the Hyd, measuring about 0.5 in diameter. The strong lingual groove traverses the tooth surface to continue as the mesiobuccal groove, but it becomes faint across an isthmus joining the two buccal cusps. There are cingular remnants extending from the mesiobuccal groove, and another extending mesially from the distobuccal groove. The buccal and lingual enamel lines are fairly straight where preserved.

The LM<sub>2</sub> crown is broken through the mesial cusp tips and is missing its mesial portion. Its morphology is similar to that described for the right M<sub>2</sub>. A small, single distal IPF is visible.

**B: R mandible (alveoli I<sub>2</sub>, broken roots I<sub>1</sub>, /C-P<sub>3</sub>, partial crowns P<sub>4</sub>-M<sub>2</sub>).**

*Preservation.* The right body is nearly complete from the symphysis to the mesial part of the M<sub>3</sub> alveolus. It has many weathering cracks and fragments of bone missing. The alveolar margin is complete only on the lingual side of M<sub>2</sub> and between M<sub>1</sub> and M<sub>2</sub>. A large SI crack runs through the canine alveolus across the entire bone, separating anterior and posterior portions that have been joined together. Cracking and abrasion along the margins of the two pieces disrupt the contours of the bone, especially medially, but this region does not otherwise appear distorted.

*Lateral aspect.* What is preserved of the extramolar sulcus opens anteroinferiorly adjacent to M<sub>2</sub>. A strong lateral torus marks the root of the ramus, and is located about halfway down the body from the alveolar margin. There is a faint concavity just below the torus. The oblique line is obscured by

damage to the cortex, but on the left side can be seen to be short, extending anteriorly to where it terminates just below the mesial edge of M<sub>1</sub>. There appears to be a slight hollowing of the bone posterosuperior to the mental foramen. The single mental foramen is large with abraded margins, but probably would have been about 4 in diameter. The direction it opened cannot be determined. It is situated beneath the distal root of P<sub>3</sub> just below the SI midpoint of the corpus. Anterosuperior to this, the contours of the bone flare out slightly toward what would have been a fairly prominent canine jugum, although the bone overlying the canine root is largely missing. Only a weak marginal torus is apparent where the base is broken posteriorly. The corpus does not appear to deepen posteriorly, although much of the inferior margin is lost. At the symphyseal midline the height is estimated at 43, posterior to I<sub>2</sub> it is 42, /C 44, P<sub>3</sub> 43, and P<sub>4</sub> 42.3.

*Posterior aspect.* The postincisive planum is hollowed ML and almost straight AP, until it curves into the superior torus at about the level of the P<sub>3</sub> roots. The superior torus is strong and high, located almost halfway toward the base from the alveolar rim. It is separated from the strong inferior torus by a shallow and rounded genioglossal pit. The inferior torus is as posteriorly extensive as the superior one. The area of the sublingual fossa is obscured by a large crack.

*Medial aspect.* The symphysis is long and low, sloping posteriorly with its long axis running 135° to the alveolar margin. Its external contour is uniformly convex, arching smoothly around its inferior margin. The mylohyoid line is partly obscured by cracks and spalling, but appears as a rounded ridge running anteroinferiorly from the posterior break. The alveolar prominence is fairly flat inferior to P<sub>4</sub>, gently curving into a shallow, anterior subalveolar fossa that appears to run parallel to the base.

*Basal aspect.* At the short section of the basal contour below the mandibular tori is a

pronounced concavity leading to a strong digastric tubercle situated about 5 from the midline. Because bone is missing here, any crest along the mandibular base is obscured. The mandibular body is noticeably everted between  $M_2$  and  $M_3$ . The small preserved portion of the mandibular base is smooth, forming a rounded ridge along its inferior-most extent. There is a small, longitudinal ridge that begins near the anterior-most preserved portion of the base.

*Occlusal aspect.* Corpus thickness can be estimated at  $P_3$  (22), at  $P_4$  (20), at  $M_1$  (21), and at  $M_2$  (23), but these estimates are rough due to spalling and weathering.

*Teeth.* On the right no canine crown remains, but pieces of the right canine root are present for most of its length, especially lingually. The actual length of the R/C root is 24.4. Apart from the Dmr and distal face of the  $P_4$  that are almost completely preserved, the  $P_4$  and  $M_1$  look like their antimeres.

The  $M_2$  has 4 main cusps, of which the Med is the dominant, a small Hld, and a  $C_6$  made up of 2 cuspules. From largest to smallest the cusp areas are: Med, Prd, Hyd, End, Hld,  $C_6$ . There are wear facets and polish on all cusps, and the buccal cusps are slightly flattened but with no dentine exposure. The Mlg runs from the shallow and poorly delimited Fa to the crenulated Fc, where it disappears. Two secondary fissures run mesially from the tip of the Med towards the Fa and the Mlg, and others run posteriorly from close to the tip of the Med to the Fc and lingual groove. Secondary fissures also run similarly down the distal cusps into the Fc, the lingual groove and the Fp. The lingual and mesiobuccal grooves are continuous across the crown. The lingual groove extends onto the lingual face and terminates near the cervix. The mesiobuccal groove deeply incises the buccal face, and terminates at a prostyloid that continues mesially around the Prd and distally as a cingulum around the Hyd as far

as a break on the MD corner. A small part of the mesial IPF is visible, but most is missing because of the broken chip of tooth. On the distal margin of the tooth an irregularly shaped distal IPF has two distinct parts. Both  $M_3$ s were evidently erupted and in contact with the  $M_2$ s.

**C: LI<sub>2</sub>.** This  $I_2$  is complete except for chips of enamel lost along the edges of a break running across the crown, and some bone along a crack across the root. The tooth is lightly worn, exposing a ribbon of dentine about 5 long and 0.5 wide on the mesial incisive edge. The lateral two-fifths of the edge slopes downwards, away from the incisive wear plane at about 45°. There is polishing in the proximity of the occlusal edge on both the lingual and labial faces. The mesial margin of the tooth is fairly straight, and the tooth expands slightly in width mesially from the cervix. The distal margin flares out more substantially to make this tooth 8.5 MD. The labial surface of the  $I_2$  is concave, with a hint of a distolabial groove. The mesial surface has a reciprocal facet for the central incisor. The lingual surface is concave in both major directions. The basal tubercle is present but not accentuated. The distal IPF is visible but not clearly demarcated. It is about 2.9 by 2. The root is strongly compressed MD with longitudinal grooves on both mesial and distal faces. It is 16 long measured on the mesial surface from the incisal angle to the root tip.

**D: RI<sub>2</sub>.** This specimen preserves the lingual half of the crown; most of the labial surface is broken away. In its preserved parts, this tooth is the mirror of the left one.

**E: RP<sub>3</sub>.** This partial crown is missing a wedge from the buccal face extending from the cervical margin most of the way to the apex, and another piece from the distal margin. Enamel is preserved to the cervical margin only on the distolingual corner. There is no dentine exposure, but the ridges and crests show polishing. The surface of the tooth shows perikymata which are worn

away apically, most likely as the result of antemortem wear. The tooth is oval in occlusal outline with a more tightly convex distolingual portion. It has one central cusp. The mesial occlusal ridge joins a short Mmr that encloses a small Fa. The transverse crest runs lingually for about 5 before it bifurcates and sends a mesial branch to the cervix and a distal branch to join a Dmr. The distal occlusal ridge runs distally to join a short Dmr that encloses a larger Fp. A portion of the distal IPF can be seen on the Dmr adjacent to the break of the missing fragment. No trace of the canine contact facet is apparent, although that area of tooth is preserved.

**F: RM<sub>3</sub>.** This crown has lost the enamel around the entire cervical margin; slightly so lingually, about halfway up mesially and buccally, and all the way to the occlusal surface distally. No root is preserved. The occlusal outline is a rounded rectangle, with what would have been a convex posterior margin. It has four main cusps, of which the Prd is the largest and the others are subequal in area. All cusps are traversed by secondary fissures, and accessory cuspules are visible in the Fc. As on the M<sub>2</sub>, the mesiobuccal groove is continuous across the central basin with the lingual groove. The Mmr extends partially around the Med. There are three developmental pits around the Med and wear facets on both mesial cusps and on the Hyd. The facet on the Hyd exposes dentine, and is associated with a large chip of enamel that was broken from the buccal side of this cusp during life. This happened in life, rather than post mortem, because this is the only cusp with dentine exposure in a facet, its antimeric cusp has almost the full thickness of enamel left and the edges of the broken enamel defect are smoothed over. If this had occurred by post mortem rolling it would also have abraded the edges of the wear facets, but these are still sharp. As for the M<sub>2</sub>, the Mlg terminates at the Fc after meeting the continuous lingual and mesiobuccal grooves. The lingual groove

extends to the break close to the cervix. The V-shaped mesiobuccal groove deeply incises the buccal face.

**G: LM<sub>3</sub>.** This is the buccal and distal portion of the left M<sub>3</sub> crown. It is similar to its antimeric. The buccal surface of the tooth retains almost the entire extent of its enamel, and has a less pronounced mesiobuccal groove than its antimeric. It shows a proto-stylid that extends mesially from the mesiobuccal groove. Distally, a cingulum borders the Hyd. Many cuspule-like vertical striations indent the buccal and distal faces. Both preserved cusps show wear, extending from the Hyd into the central basin.

**H: LI<sub>1</sub> crown.** This crown is missing the cervical half of the lingual surface. A tiny portion of root is preserved on the mesiolabial corner. The crown is worn, exposing a ribbon of dentine about 0.5 wide. The facet for the other I<sub>1</sub> is an elongated oval, measuring about 4.0 long SI by 1.4 LaL, with weakly defined edges. The I<sub>2</sub> facet is clearer and roughly circular, measuring about 2 in diameter. The labial surface is smoothly convex, with well-marked perikymata on the cervical half, but these have been worn off the incisive half. The lingual surface is almost flat to slightly concave, with light undulating ridges running from the wear plane towards the marginal tubercle. There are roughly symmetrical mesial and distal grooves separating similarly sized mesial and distal ridges. The mesial and distal margins are subparallel, so the tooth has a roughly rectangular outline in lingual view, and does not splay out markedly from the cervix.

**I: 7 crown fragments** (not figured). These fragments include parts of two incisors, a canine, and three molars or premolars. One is indeterminate.

**KNM-KP 30498—L and R maxillary fragments and associated maxillary dentition** (Figure 7: G–L not figured).

This specimen was discovered washing down the southern slope of a small hillock

## KNM-KP 30498

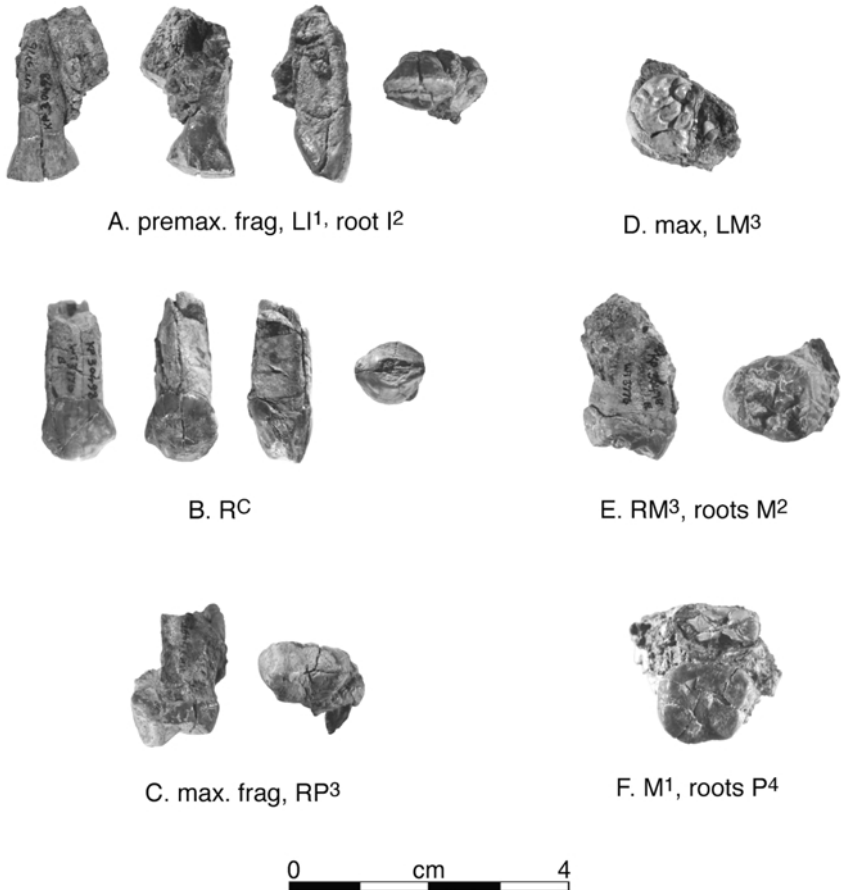


Figure 7. KNM-KP 30498 associated maxillary dentition. (A) in labial, lingual, mesial and occlusal views, (B) in labial, lingual, mesial and occlusal views, (C) in distal and occlusal views, (D) in occlusal view, (E) in mesial and occlusal views, and (F) in occlusal view.

65 m from the site of discovery of the type mandible, KNM-KP 29281 (Wynn, 2000, Figure 2). Apart from the initial isolated teeth, the majority of these teeth were recovered through screening. Specimens KNM-KP 30505, which includes a molar germ, and KNM-KP 30942, tooth fragments, were also recovered in the screening.

**A: L premaxillary fragment (I<sup>1</sup>, root I<sup>2</sup>).** This is a complete I<sup>1</sup> crown and root, along with maxillary bone lateral to it housing just over half of the I<sup>2</sup> root. The I<sup>1</sup> crown

is cracked and weathered, but the morphology is preserved. On the labial and mesial faces, cracks run through the crown vertically from the root widening to about 0.2 at the occlusal surface. The crown is heavily worn almost to the basal tubercle. Dentine exposure is 2.5 at its maximum LaL by 9.3 MD. Both the mesial and distal margins of the crown flare out strongly from the cervix almost symmetrically, but the distal margin slightly more so. The basal tubercle is swollen, and the Mmr and Dmr

fade into it. There are traces of three lingual grooves running into the tubercle from the wear facet. Both IPFs are indistinct due to weathering, but the distal one can be seen set distolingually on the Dmr. Mesial and distal enamel lines are strongly concave towards the occlusal surface. The lingual enamel line is mildly convex, but the labial one is damaged. The root measures 17 long from the cervical margin labially. The root is 7.7 LaL and 6.8 MD at the cervix.

Only 12.5 of the I<sup>2</sup> root is preserved from its apex, and its original length is estimated to have been 18. It is oval at its broken section, with only a faint distal groove traversing its distal side. It measures about 5.3 MD by 7.7 LaL at its break. Its apex is blunt, and the root appears to converge upon the I<sub>1</sub> root apically.

**B: RC/.** This tooth is missing only the apex of its root, and the enamel at its distal edge obscuring any Dmr. The crown is weathered, and has a 0.2 wide crack running LaL through its center. It flares out mesially and distally from the root, below its arched cervical margins. The crown is worn across the tip, exposing a tear-dropped area of dentine measuring 5.2 MD by 2.8 LaL that slopes distally and lingually. The crown is asymmetrical, with the Mmr separated from the main cusp by a shallow marginal groove. This pronounced marginal ridge and marginal groove continue across the occlusal surface and faintly onto the labial surface, respectively, in the occlusal outline in labial and lingual views. The labial surface is uniformly convex, with perikymata exposed near its cervical margin. The lingual surface has a swollen cervical tubercle that is continuous with the shallow mesial and distal marginal grooves, and with the pronounced, rounded median lingual ridge that is located towards the mesial edge of the tooth immediately adjacent to the mesial marginal groove. Distal to the median lingual ridge, and inferior to the cervical swelling the

lingual face of the tooth is flat. There is no discernible facet for the I<sub>2</sub>. The root is 9.1 MD by 7.5 LaL at the cervix. The premolar facet cannot be seen on the canine because of the missing enamel in this area.

**C: R maxillary fragment (P<sup>3</sup>).** This is a completely preserved crown, with partial roots surrounded by some maxillary bone. Part of the canine alveolus is preserved mesially, indicating the position of this premolar in the maxilla. Much of the specimen is weathered, obscuring the occlusal morphology. The crown has two tiny expansion cracks running across its partially worn occlusal surface that would affect measurements minimally. It is a bicuspid tooth with a tall, conical Pa that occupies more than half of the occlusal area, and a low rounded Pr. There are indistinct mesial and distal grooves adjacent to the rounded Mmr and Dmr respectively. Wear has flattened both cusps and there is a tiny area of dentine exposure on the tip of the Pa, but none on the Pr. Ridges and crests are polished by wear. Both buccal and lingual faces slope inwards towards their tips, but the buccal one slopes more strongly. The lingual surface is smoothly convex all around, but the buccal face has slight mesial and distal grooves and ridges. There is a strong mesio-cervical enamel extension of the buccal face. The crown flares out mesially and distally from its root about equally, and bulges just below the cervical margin labially and lingually. The mesial IPF is set midway on the mesial border; it is small but indistinct due to weathering. The P<sup>3</sup> has two roots, with distinct buccal and lingual roots. The lingual one is missing only its apex, and measures 14.2 long as preserved, which is almost all of its original length. It angles lingually from the crown and somewhat distally. Only about 2.2 of the buccal root is left. Part of the alveolus for P<sup>4</sup> is visible, and about 5 of the P<sup>4</sup> root near its apex is adhered to the bone surrounding the P<sup>3</sup> roots.

**D: L maxillary fragment (M<sup>3</sup>).** This is a fragment of maxilla with no preserved cortex, and the lingual two-thirds of a M<sup>3</sup> crown with its roots embedded in the maxillary bone. The surface of the tooth is quite weathered. Enough of the crown is preserved to show that it is an almost symmetrical mirror copy of the other one (E), although the details of the cuspules are not identical.

**E: R maxillary fragment (M<sup>3</sup>, root M<sup>2</sup>).** This is a complete M<sup>3</sup>, except for fragments of the enamel broken from the cervical margin lingually and distally. It has a single root that is encased in maxillary bone on all but its distal sides. A sliver of the distolingual root of M<sup>2</sup> is preserved mesially. The occlusal outline of the M<sup>3</sup> is a rounded triangle, with the blunt apices mesiolingually, mesiobuccally and distally, so it is formed by the two mesial cusps and an irregular set of distal cuspules. The occlusal surface is lightly worn with flattening and polishing of mesial cusps and ridges. The Pa is the larger of the two mesial cusps. There is a small Fa 7.2 wide cut into by the only wear facet that is across the mesial part of the tooth. No dentine is exposed. Cuspules are arranged in a series of bead-like structures centered on a Fc. The lingual face of the crown is corrugated by four distinct vertical ridges and adjacent grooves. The M<sup>3</sup> root is in the shape of an irregular cone that is about 11 long. The mesial IPF is oval, and measures 3.3 BL by 1.9 high.

**F: L maxillary fragment (M<sup>1</sup>, roots P<sup>4</sup>).** This specimen consists of a complete worn and cracked M<sup>1</sup> crown, its broken roots, most of the P<sup>4</sup> roots and intervening maxillary bone. The M<sup>1</sup> crown is complete. Its occlusal outline is a rounded rhombus, with the buccal cusps set mesial to the lingual ones. From largest to smallest the cusp areas are Pr, Pa, Me, Hy. Wear has flattened all cusps. Dentine is exposed on all cusps except the Me. The Pa dentine pit is circular and measures 0.7, the Pr one is

tear-dropped measuring 1.9 by 2.3, and the Hy one is a tiny circular one of 0.2. The crown has a strongly sloping lingual side and more vertical buccal side. The buccal groove is obscured on the buccal surface by a crack running through the crown. A lingual groove sets off the Hy. Not much remains of the groove system except for the trace of the buccal groove extending along the occlusal surface almost to the center of the crown. There is no trace of a Fa, and the Fp is present as a small V-shaped depression set about 4 mesially from the distal margin. The mesial IPF is about 6 wide but obscured by adhering matrix that retains the impression of the distal P<sup>4</sup> enamel.

**G: RP<sup>2</sup>.** The root of this tooth is almost complete, but the badly cracked and weathered crown preserves only a sliver of enamel on the distobuccal corner and the lingual portion near the cervical margin. The latter has a swollen basal portion, and there is a trace of the Dmr before the break. The root is weathered and cracked with small pieces missing. It measures 7.7 LaL by 4.8 MD at the cervix, and it is 15 long. The LaL widest point on the root is near its midpoint, where it measures about 9.3 by 4.5.

**H: M fragment.** This is a fragment of a molar, possibly the mesial side and adjacent occlusal surface. It is worn nearly flat, with a groove separating two partial cusps. The beginnings of a root flare strongly away from the crown. At the edge of the preserved occlusal margin, the enamel measures a maximum of 1 thick.

**I: RP<sup>4</sup>.** This is the buccal half of a cracked crown with a short fragment of root, measuring a maximum of 5 from the cervix. Weathering has obscured details of the crown, but it appears that the buccal face had distinct mesial and distal grooves. The buccal face is also weathered and cracked, but appears to have had mesial and distal grooves running towards its occlusal margin. What appears to be the buccal half of the



mesial IPF is visible. The distal IPF is large, and although only half is preserved, is a broad band 2.1 high across the distal surface of the tooth. No dentine is exposed.

**J: LP<sup>3</sup>.** This is most of the distal half of the LP<sup>3</sup> crown. Morphology is like the right P<sup>3</sup>.

**K: LC/.** This is an 18 long, badly cracked and weathered root with neither the cervical margin nor apex preserved. Its dimensions are obscured by damage.

**L: Molar root.** This is a badly cracked, weathered and spalled molar root with neither end preserved, measuring 14.9 long as preserved.

**KNM-KP 30500: Mandibular fragments and associated mandibular dentition** (Figure 8; H–L not figured). This specimen was recovered as a surface find and additional pieces were found through screening. There are no associated specimens.

**A: L mandibular fragment (M<sub>1</sub> and M<sub>2</sub>).** This specimen consists of part of a mandibular body extending to a point just inferior to the tips of the molar roots, along with M<sub>1</sub> and M<sub>2</sub> crowns. The cortex of the body is badly weathered. Laterally it swells below M<sub>2</sub> to the lateral torus at the point where it extends posterosuperiorly to meet the ramus. The internal margin of the body is mildly concave AP.

The LM<sub>1</sub> is complete except for small pieces of enamel missing from the edges of cracks running through the surface. Its surface is weathered, but most morphology is preserved. In occlusal outline it is a rounded square with an expanded distolingual corner. The Med is the highest and largest, and the central basin is large. From largest to smallest the cusp areas are: Med, End, Prd, Hyd, Hld. The tooth is worn on all cusps, with flattening of the buccal cusps and the Hld which all have small dentine pits measuring less than 1 in diameter. The Fa is represented only by small,



Figure 8. KNM-KP 30500 partial mandibular dentition with associated mandibular bone, in occlusal view.

irregular pits, and the Fp by a 2.4 long cleft delineating the Dmr. The lingual surface of the tooth is quite vertical, but the buccal one slopes considerably. A distinct protostylid borders the Prd. The lingual groove runs across the central basin, and is largely continuous with the mesiobuccal groove, which ends in a distinct pit at the protostylid. A short distobuccal groove indents the buccal face distally. A distinct distal IPF is about 4.8 wide BL.

The LM<sub>2</sub> is also slightly weathered, and has cracks crossing it diagonally in both directions. Its occlusal outline is a rounded rectangle. Polishing indicates light wear but no dentine is exposed. From largest to smallest the cusp areas are: Med, End, Prd, Hyd, Hld. Like the M<sub>1</sub>, the central basin is

large and mildly crenulated, and is divided by the continuous lingual and mesiobuccal grooves. These grooves are more evident than on the  $M_1$  because this tooth is less worn. A distinct shelf-like protostylid, bordered distally by the mesiobuccal groove, delimits the Prd. The distobuccal groove incises the buccal face distally, terminating at a V-shaped notch. The cingular remnants along the buccal face are stronger than on the  $M_1$ . The Fa is again a series of 4 pits, set behind the Mmr, and the Fp is a short cleft delineating the Dmr. The mesial IPF is about 4.8 wide BL. Weathering obscures any traces of a distal IPF.

**B: LM<sub>3</sub>.** This tooth is complete except for enamel missing from the distal and lingual surfaces, and it has cracks running through it. It is morphologically similar to the RM<sub>3</sub> (E), which is more complete.

**C: R mandibular fragment (M<sub>1</sub>).** This specimen preserves a badly weathered, small section of the lateral surface of the mandibular body around the  $M_1$  roots. The fragment measures up to about 17 AP and 12 SI. The  $M_1$  crown is missing its mesiolingual corner, and is cracked. The root apices are broken away. Wear has flattened the two buccal cusps and exposed small islands of dentine on the Hld. The roots are broad and plate-like narrowing apically and distally inclined. A marked furrow indents the mesial face of the mesial root. The rest of the morphology resembles the LM<sub>1</sub> (A).

**D: RM<sub>2</sub>.** This tooth is cracked and weathered but the crown is complete. The roots are preserved, and surround some mandibular bone. They are broad and plate-like, and bifurcate at the tips. The roots incline distally. Crown morphology resembles the LM<sub>2</sub> (A).

**E: RM<sub>3</sub>.** This tooth is complete except for enamel missing from its distalmost surface. Cracks run through its weathered crown. The occlusal outline is more triangular than that of the other molars, resembling an elongate rectangle mesially, that tapers to a

distal apex. There are 5 main cusps, the largest and most salient of which is the Med. From largest to smallest the cusp areas are Med, Prd, Hyd, End, Hld. Although there is no dentine exposure there appears to be polishing on all cusps and some flattening of the buccal cusps. A small protostylid borders the Prd, terminating distally at the distinct mesiobuccal groove. The Fa comprises a series of distinct pits, as for the  $M_1$  and  $M_2$ , but in this case the pits are joined by a meandering furrow. The Fc is extensively crenulated, and comprised of a series of fissures and inflated ridges that radiate from the cusp tips to the basin. The Hld is cracked and weathered, but it appears to be partly separated from the other cusps. The lingual surface of the crown is steep, and the buccal surface sloping. The mesial roots are broad and plate-like. The single distal root is roughly triangular in section, following the contour of the posterior margin of the crown, with longitudinal furrows on either side, particularly the buccal one. The apices of the roots are broken.

**F: LP<sub>3</sub>.** This crown is almost complete, but is missing its cervical enamel along its distal margin up to the Dmr. Parts of the roots are present, extending about 3–4 from the cervix inferiorly on most sides, but to only about 1.5 lingually. Large cracks traverse the crown, with the largest missing a chip of enamel at the tip of the main cusp. The occlusal outline is a triangle with apices mesially, distolingually and distobuccally. The tooth is weathered, but does not appear to have been worn although slight polishing is apparent on the Prd. There is a single cusp. The transverse crest bifurcates into a mesial branch that runs mesially to join the Mmr and encloses the Fa. The distal branch joins the Dmr to enclose a larger, deeper Fp. The Fp has several small furrows emanating from the center, but the Fa is relatively smooth. There was a single mesial root and a plate-like distal root that already shows

two separate pulp cavities indicating that it probably divided lower down the root. The enamel is weathered, obscuring any possible canine facet. The missing distal enamel obscures any potential distal IPF. A weathered hypoplastic groove traverses the base of the crown along its buccal side.

**G: LP<sub>4</sub>.** This crown is complete except for part of the lingual face that is broken and has enamel missing along the distal surface. A 1 wide piece of root is preserved mesially. This is a bicuspid tooth, with the Prd larger than the Med. The occlusal surface is weathered, and only slight wear is apparent in some flattening of the Med and light polishing of ridges. The smaller, smooth Fa is set higher than the larger Fp, which has small fissures and ridges running into its center from the two cusps. The mesial IPF is oval, and about 3·5 BL by 2·1 high. The buccal face shows two indistinct mesial and distal ridges.

**H: I root.** This is a piece of incisor root that is compressed MD. It is 17·5 long as preserved. No crown is preserved, and the root tips are missing. Near its center it is 8·7 LaL by 4·1 MD.

**I: R/C.** This is a fragment of a right canine, preserving the distolingual corner of the crown with some root attached. The tip of the crown is broken off. The tooth is weathered. Little can be said about its morphology, although on the lingual face, a distinct distal marginal groove is bordered by a Dmr.

**J: C root.** This is a fragment of canine root split longitudinally. It is cracked and weathered, and preserves little morphology but shows the pulp cavity.

**K: L/C.** This specimen is a broken canine, preserving the distobuccal corner of the crown and about 7·5 of the adjacent root. The entire specimen is traversed by a large, longitudinal crack and is weathered. The root appears to have a slight transverse bulge, but this is greatly enhanced due to postdepositional taphonomic processes.

Although broken away, the shape of the remaining crown indicates that there was a distal cuspule or strong ridge. The occlusal outline takes a sharp turn between buccal and distal faces. A distal IPF is apparent.

**L: 7 mandible and root fragments.** These are small fragments of mandibular bone and tooth root that cannot be reliably assigned to particular teeth.

**KNM-KP 30502: Associated mandibular tooth fragments** (Figure 4; A–C, E, J and K not figured). Apart from the initial fragment, these tooth fragments were recovered through screening.

**A: LP<sub>4</sub>.** This is the lingual part of a P<sub>4</sub> crown with partial basins preserved. There is a small Med separated from the broken Prd by a notch in the transverse crest. The Fa is higher and smaller than the Fp. The Fp has small ridges extending into it from each cusp. The lingual surface of the crown is evenly convex SI.

**B: RM<sub>1</sub>.** This is the mesiobuccal corner of a RM<sub>1</sub> crown, preserved not quite down to its cervical margin. The entire Prd is preserved, along with the mesial and buccal parts of the Med and part of the central basin. The Med was the higher of the two preserved cusps. There is dentine exposure on the Prd, which is circular and 0·8 in diameter. The Med has a groove running from its tip into the Fa, which is bounded by a mild Mmr. There is a trace of a small protostylid on the mesiobuccal corner and posteriorly as a distinct but short shelf originating at the base of the buccal notch. The mesiobuccal groove extends from the buccal notch into the Fc. The buccal side of the tooth slopes strongly toward the occlusal surface. There is a tear-drop shaped mesial IPF 5 wide by 1·6 high placed centrally on the mesial surface of the crown.

**C: RM<sub>2</sub>.** This is a wedge-shaped piece of an M<sub>2</sub> crown preserving the buccal side into the central basin, but not all the way to the cervical margin. Half of the Prd, all of the

Hyd, and most of the Hld remain. Faint wear facets are visible on the Hyd. It has a strongly sloping buccal side, which is cracked and slightly weathered. The deep mesiobuccal groove extends from the buccal notch where there is a cingular remnant to Fc. Secondary fissures that pass into the Fc form radial ridges emanating from the cusps.

**D: RM<sub>3</sub>.** This crown of a germ preserves almost the entire unworn occlusal surface, except for the mesiolingual slope of the Med, and it is missing its cervical enamel. A large transverse crack divides the mesial portion of the crown. The tooth is a rounded rectangle in occlusal view, with five main cusps. Numerous secondary fissures form inflated ridges, and smaller cuspules that fill the basins. The mesiobuccal groove is continuous across to the crown with the lingual groove, terminating buccally at a proto-stylid. The deep Fa is 3.8 wide and demarcated by a Mmr. A Mlg runs from it to the deep, sinuous Fp that is about 3 wide. The buccal side of the tooth slopes strongly.

**E: LM<sub>3</sub>.** This is most of the unworn crown of a germ, missing the mesial edge and mesiolingual corner, as well as some enamel along the cervix. Although details of the central basin cuspules also differ slightly, this tooth is morphologically similar to the right one. Unlike the right M<sub>3</sub>, the Fp is broad and shallow, but has two small cuspules bounding it mesially.

**KNM-KP 30505: Partial molar germ (Figure 4).** This specimen was discovered in the screening for the adult isolated teeth, KNM-KP 30498. The tooth is clearly from another juvenile individual. Several additional tooth fragments, KNM-KP 30942, that do not appear to belong to either of these specimens, were also recovered.

This is a partial mandibular molar germ with the remains of 2 half cusps. It is probably the mesial half of the crown because the fovea is so clearly delineated. It is probably a

left, because the slope of the buccal portion is stronger than the small slope of the lingual face. There are numerous secondary fissures and accessory cuspules on the occlusal surface. This germ is associated with a small piece of deciduous molar root.

**KNM-KP 30942: Five molar fragments (not figured).** These fragments were discovered in the screening for KNM-KP 30498. As they cannot be associated with any certainty to this specimen or the tooth germ, KNM-KP 30505, also recovered in the screening, they are given a separate accession number.

These are five molar fragments. Each has part of the crown. The largest appears to be most of the mesial or distal face of a molar. Little informative morphology is preserved. The dentoenamel junction is clear on several, but because none preserve unworn cusp tips standard enamel thickness measurements are not possible.

**KNM-KP 31712: Associated juvenile mandibular and dental fragments (Figure 9; B, C, J and K not figured).** Apart from the initial mandibular fragment, this specimen was recovered through extensive screening of a steep slope and gully. No additional specimens were recovered in the screening. KNM-KP 31714, 31728 and 35842 were recovered from the vicinity of this site, but are not considered to represent this individual.

**A: R mandibular fragments (dm<sub>1</sub>, roots dm<sub>2</sub>, P<sub>3</sub> & P<sub>4</sub> in crypts).** This specimen includes the medial cortex of a right mandible measuring 16.2 SI by 23 AP, a partial crown of the Rdm<sub>1</sub>, roots of dm<sub>2</sub>, and the crowns of P<sub>3</sub> and P<sub>4</sub> in their crypts. The mesial margin of the M<sub>1</sub> alveolus is visible on the posterior side of this specimen and part of the canine alveolus just below the P<sub>3</sub> germ. The lingual alveolar margin is missing, leaving a straight contour that is a minimum of 2.1 lingually from the tooth

KNM-KP 31712

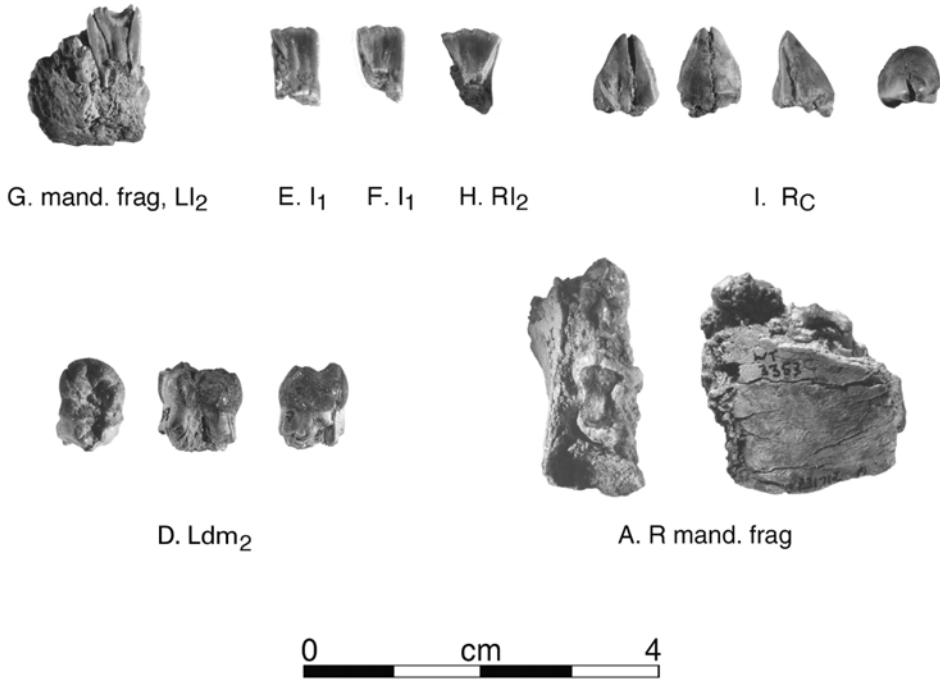


Figure 9. KNM-KP 31712 associated juvenile dentition. (G), (E), (F) and (H) in lingual views, (I) in lingual, labial, distal and occlusal views, (D) in occlusal, lingual and distal views, (A) in occlusal and medial views.

roots. In occlusal view, the anterior end of the mandibular bone curves medially toward the symphysis along its inferior edge, but the superior edge is almost straight. The preserved part of the alveolar eminence is smooth, with a slight bulge adjacent to the developing  $P_4$ . Laterally, the buccal sides of the deciduous molar roots are exposed. The inferior margins of the developing  $P_3$  and  $P_4$  crowns are visible tucked within the roots of the  $dm_1$  and  $dm_2$  respectively. Just inferior to the  $P_3$  crown, the medial wall of what is probably the  $/C$  crypt is preserved for 5 AP by 4.3 SI.

The  $dm_1$  crown is broken. Most of the enamel is broken or spalled off, but some remains on the mesial, distal, lingual and occlusal faces. A matrix-filled crack, 0.5

wide, runs transversely BL through the mesial cusps. The occlusal outline is a narrow, elongate ovoid oriented MD with a fairly straight lingual side and rounded mesial margin. Some of a high, pointed Med is preserved just mesial to the MD midpoint of the lingual occlusal margin. Also preserved is the lingual side of the Hyd, which was worn to expose a pinpoint of dentine. The floor of the Fa is lingual to the MD axis and terminates distally in a Dmr that is smooth from wear. A basal bulge of the crown is evident on the mesial and lingual sides. Both roots of this tooth run almost straight inferiorly, but the distal one angles slightly distally toward its apex.

The  $dm_2$  crown is completely broken away, but it would have been larger in all

dimensions and relatively broader BL than the  $dm_1$  crown. Its mesial root runs inferiorly, hooking distally at its apex and the distal root angles distally.

**B: R mandibular fragment.** This is the lateral surface of mandibular bone, which almost fits on A, but cannot be joined directly. It comprises two pieces joined at a large, uneven crack running vertically past the posterior edge of the well preserved mental foramen, and is up to 1 wide. The fragment measures 18.8 SI and 37.6 AP. Posteriorly, the beginning of the extramolar sulcus appears medial to a gently rounded lateral torus that becomes sharper as it begins to form the base of the ramus at its posterior extent. Little or no oblique line is evident. The alveolar margin is broken, but adjacent to the  $dm_1$  and  $dm_2$  it appears to be close to its original contours, as the internal contours of this fragment match the contours of the deciduous molar roots of A. An apparent crypt is present mesially, possibly for the permanent canine. The anterior break of this fragment slopes anteriorly and inferiorly and the posterior break posteriorly and inferiorly. The anterior portion of the fragment is flat SI but begins to curve medially at its superior edge and laterally along its inferior edge. The posterior part is vertically convex. There is a shallow depression immediately superior to the mental foramen. The mental foramen measures 3.1 by 2.0, its long axis running posteroinferiorly to anterosuperiorly.

**C: RI<sub>1</sub> or I<sub>2</sub>.** This is a crown and root, with mandibular bone adhering to the distal portion of the root. The distal part of the crown is broken and largely missing, and the broken face is vertically concave. Enamel is completely missing from the lingual face, apart from a thin strip along the mesial edge. The root is largely complete but hidden apically by mandibular bone adhering to it. A flattened surface at the inferior and mesial corner of this adhering bone may be the wall of a permanent incisor crypt. The crown is

slightly worn across the occlusal surface. The labial face is vertically convex, and marked by faint vertical grooves. It exhibits no basal swelling. A small mesial IPF is visible mesially, running 1 down from the occlusal edge. The root measures 4.4 LaL by 3.3 MD near the cervical margin.

**D: Ldm<sub>2</sub>.** This is the crown with up to about 4 of the root all around. Enamel is missing from the mesiobuccal and mesiolingual corners up to the cusp tips and across the mesial face except for a narrow, vertical isthmus, but the floor of the Fa is preserved. A crack runs up the lingual side of the End to its tip. The occlusal outline is a rounded rectangle. The size of the broken Prd cannot be assessed but from largest to smallest the areas of the remaining cusps are: Med, Hyd, End, Hld. The two lingual cusps are taller and slightly more distally placed than the buccal ones. All show some wear, with the buccal cusps slightly flattened and a pinpoint of dentine is exposed on the Hyd. A large Fa is bounded by a large but broken Mmr, and separated from the mildly crenulated Fc by a sharp crest connecting the two mesial cusps. This crest is notched by the broad Mlg. A small Fp sits between End and Hld, inside a Dmr. The lingual groove is distal to the mesiobuccal one and notches the occlusal margin as it continues to the cervical margin. The mesiobuccal groove is pronounced and terminates in a deep notch close to the superior margin of the buccal face, but inferior to this the two lobes of this face continue to be divided by a shallow furrow. The distobuccal groove ends in a small pit. The lingual and buccal faces are both bilobate, but the buccal one is more sloping towards the occlusal surface than are the lingual and distal sides. A mesial IPF is just visible on the isthmus of enamel preserved. None is present distally.

**E: I<sub>1</sub>.** This is a partial unerupted crown missing its left edge in lingual view. It is too incomplete to attribute to the right or left side. Three mammelons mark the occlusal

margin, which are the continuations of faint lingual ridges. The lingual side is vertically concave and only mildly so transversely. The labial surface is smoothly convex, and marked by faint vertical furrows and ridges. Perikymata are apparent on this surface.

**F: I<sub>1</sub>.** This fragment is also too incomplete to attribute further. It was recovered in two pieces that have subsequently been joined along a vertical crack that divides the central portion from the left side in lingual view. Its morphology resembles E.

**G: Mandibular fragment (LI<sub>2</sub> in crypt).** This fragment consists of the external cortex just lateral to the symphysis, about 13.3 SI and 14.9 ML. The I<sub>2</sub> is in its crypt, and the anterior wall of the /C crypt is visible. The preserved anterior cortex is smooth and flat, flaring slightly laterally just at its inferior edge.

The I<sub>2</sub> crown is incomplete. Vertical cracks that run up the right and left sides from the crown base diverge towards the mesial and distal margins at the occlusal surface. Most of the mesial half of the occlusal margin is broken away, except at the mesial corner. On the preserved distal portion, two small mammelons are present. The distal corner of the occlusal surface is rounded, while the mesial one is sharp. Vertically elongate mesial and distal lingual fossae are visible. The lingual face is concave vertically, except for a ridge along the occlusal surface, but horizontally is only slightly so. The labial face is convex horizontally and vertically and perikymata are visible. The superior half of the labial crown surface is marked by small vertical grooves leading towards the mammelons on the preserved part. An area 6.8 SI by 6.0 ML of the crypt for the L/C is visible at the medial edge of the posterior side of this fragment.

**H: RI<sub>2</sub>.** This triangular shaped fragment of the unerupted RI<sub>2</sub> preserves the unworn occlusal margin, but both mesial and distal sides are missing. The mesial and distal

breaks, as on the other incisors, are slightly curved, widening from the base towards the occlusal margin. The occlusal margin curves gently down towards its distal margin. Four mammelons make up the occlusal margin, with faint vertical ridges running inferiorly from them on the labial side. The labial surface is convex SI and MD, and the lingual surface is concave in the same dimensions except for a ridge of enamel at its occlusal edge. As on the other incisors, perikymata are visible on the labial face.

**I: R/C.** This is most of an unerupted crown. A 0.4 wide crack at the apex splits the crown into mesial and distal halves. The occlusal outline is strongly convex labially, and flat lingually. The crown is asymmetrical, with the apex situated slightly distal to the LaL axis. The labial surface is smooth and tightly convex transversely, except for a vertical flattening toward the apex. The mesial and distal labial grooves are weakly developed. The distal margin of the labial surface is longer than the mesial one. The mesial margin terminates in a sharp Mmr, 5.4 from the crown apex that continues onto the lingual face, angling inferiorly and distally to the break, standing well out from the tooth surface. No distal basal tubercle is preserved, as this crown is incompletely formed. In lingual aspect the prominent, sharp, lingual ridge is eccentrically placed close to and parallel with the distal margin, so that most of the lingual face is flat, measuring a maximum of 6.0 MD. The distal lingual groove is deep, narrow and V-shaped, and extends from the base of the crown almost to its apex.

**J: RM<sub>1</sub>.** This is the unerupted crown with only a 1 long piece of root preserved on the mesial side. It has a crack running obliquely from the mesiolingual corner of the tooth through the tip of the Prd. Its outline is an elongated, rounded trapezoid with long axis running mesiolingually to distobuccally, with an inflated mesiobuccal corner and bilobate lingual and buccal sides. The Med

is slightly taller than the other cusps. From largest to smallest the cusp areas are: Med, Prd, Hyd, End, Hld. The tooth was not in wear. The occlusal surface is extensively crenulated by secondary fissures that form enamel ridges and cuspules. The ovoid buccal portion of the Fa is bounded by the Mmr, which is incised by two shallow furrows but barely separated from the Fc. It continues lingually as a slit anterior to the Med. The Fp is a narrow pit, which incises the edges of the End and Hld. It is bounded by the Dmr, which has a pit-like slit along its distal side. The Mlg extends the length of the crown. The mesiobuccal groove is deeper and more mesially placed than the lingual one. It terminates in a pit bounded by a cingular remnant less than halfway down the crown, which is confluent anteriorly with a ridge-like protostylid. This protostylid, in turn, traverses the Prd to eventually meet the Mmr. The distobuccal groove ends in a more restricted cingular remnant in the form of a small cuspule less than halfway down the crown. The lingual groove extends to the cervical margin. All sides of the crown are convex, but the buccal one is the most sloping.

**K: LM<sub>1</sub>.** This is the unerupted crown, with 1–3 of root preserved mesially. There is a crack running through the Fa from mesial to buccal that has a sliver of enamel up to 1.3 wide missing from it along its mesial face. A second crack runs transversely through the distal cusps and is widest lingually, a maximum of 0.3 across. This tooth is a mirror copy of J, except for some details of the groove system that differ.

**L: Mandibular fragments.** These are several additional fragments of mandible that were recovered with this specimen but are too fragmentary to be diagnostic.

**KNM-KP 31713: R mandible with tooth fragments** (Figure 10; B and C not figured). This was a surface find and subsequent screening led to the recovery of the

two partial teeth. No additional specimens were recovered.

**A: Mandible—Preservation.** This mandible is preserved from the left I<sub>2</sub> alveolus through an area close to the distal M<sub>2</sub> medially and adjacent to the M<sub>2</sub>/M<sub>3</sub> junction laterally. Its surface is weathered and traversed by many cracks, the most significant of which runs horizontally along the inferolateral side of the body and is about 1 wide. Bone is missing from the anterior and lateral surface of the alveolar region from the level of the mental foramen anteriorly, exposing all four incisor alveoli and the broken canine root. A small amount of the alveolar margin remains mesial to the canine, but along the mesial sides of the incisor alveoli the bone is abraded, and the alveolar margins are broken off along both sides of the premolars and molars. The tooth crowns are almost all broken away, and the remaining parts of the teeth are cracked and split. Only the lingual half of the canine root remains for most of its preserved length, exposing the pulp cavity, but the root is complete near its apex. The buccal P<sub>3</sub> root is broken away. The buccal surface of the P<sub>4</sub> root is exposed where the bone is missing. The posterior break exposes the mesial wall of the alveolus for the distal M<sub>2</sub> root.

*Anterior aspect.* There is a mild basal incisura. The I<sub>1</sub> alveoli are about 11.3 deep. Their inferior margins diverge at their deepest point.

*Lateral aspect.* The extramolar sulcus begins next to M<sub>1</sub>. Anterior to it, the rounded ramal contour continues as the oblique line, which arcs inferiorly and fades below M<sub>1</sub>. The lateral torus is broad and blends smoothly with the base. The surface becomes slightly concave along its anterior break, just posterior to the mental foramen. The mental foramen is located at the junction between P<sub>3</sub> and P<sub>4</sub>, a minimum of 17 from the base. Only its posteroinferior margin is visible, but this is quite sharp



## KNM-KP 31713



Figure 10. KNM-KP 31713 edentulous mandible. Top row, occlusal, basal and anterior views; bottom row, lateral and medial views.

so it must have opened anteriorly and/or superiorly.

*Posterior aspect.* The weak superior transverse torus is difficult to discern because the bone is largely broken here, but it appears to reach posteriorly only to  $P_3$ . The post-icisive planum is short and mildly hollowed. A broad and shallow genioglossal fossa has a small supraspinous foramen in it. The inferior transverse torus is stronger than the superior one, extending to the level of the junction between  $P_4$  and  $M_1$ , and is sharply convex superior to the mandibular base. The edge of a genial tubercle is preserved next to the break.

*Medial aspect.* Although this mandible is broken to the left of the midline, symphyseal contours can be appreciated. The symphysis

is inclined sharply inferiorly and posteriorly, its long axis can be estimated to have been set  $142^\circ$  to the postcanine alveolar margins. It is vertically convex except for a mild depression inferior to the incisor alveoli. The mylohyoid line is barely visible as a roughened line running posterosuperiorly from the symphysis to the posterior extent of the bone. The alveolar prominence is broad and evenly rounded, and is continuous with the weak superior transverse torus. A distinct, continuous subalveolar fossa is present, tapering anteriorly below the mylohyoid line.

*Basal aspect.* The basal contour is not everted. It is rounded in the symphyseal region, becoming slightly sharper inferior to the canine jugum. A digastric fossa is

evident, bounded anterolaterally by a small, sharp ridge, but its posterior margin is unclear.

*Occlusal aspect.* The canines and incisors form a smooth arc anteriorly. Although the bone is missing here, preserved tooth roots indicate that the canine jugum would have extended as far or further laterally than did the P<sub>3</sub> jugum, so that the lateral alveolar contour would have swung medially anterior to the /C jugum.

**B: R/C.** This is a partial canine crown that cannot be joined to its root in the mandible. Most of the mesial side of the crown is broken away. Enamel remains only on the labial and distal surfaces, but does not extend to the occlusal margin at any point, and is missing along its distolingual corner of the crown to within about 3 of the cervical line. Many vertical cracks traverse the tooth.

The amount of wear cannot be determined although dentine exposed by wear is visible superior to the broken distal tubercle. The labial surface is smooth. About 4 of the root remains on the labial side, and can be estimated to be about 10.3 by 7.5 near the cervical margin.

**C: RM fragment.** This is a badly weathered fragment, probably the distolingual corner of a mandibular right molar. The End can be seen, with parts of the Med and distal marginal ridge present, along with the depth of the Fc. The crown is not preserved to its cervical margin. Wear is difficult to assess due to weathering, but little had taken place because the distolingual cusp is still fairly pointed. There is no dentine exposure on the occlusal surface.

**KNM-KP 31714: Ldm<sub>2</sub>** (Figure 4). This specimen was recovered in the vicinity of, but some distance from, the juvenile specimen, KNM-KP 31712. No additional fragments were found in the screening, but KNM-KP 31728 and 35842 were recovered from higher on the slope. This specimen

could conceivably be associated with one or other of these specimens.

This is a weathered partially worn crown that has almost the entire occlusal surface preserved and up to 5.6 of the distal root. The mesial face is missing, as is the enamel along the cervical margin of much of the other sides. An oblique crack runs through the apex of the Prd and just mesial to the Hyd tip. The crack is widest (0.4) at the Prd. The distal cusp has its apex chipped off and the margins weathered. The occlusal outline is a rounded rectangle with a convex distal margin. Small dentine pits are exposed on all five cusps. From largest to smallest the cusp areas are: Med, Prd, Hyd, End, Hld. The lingual cusps are higher and more pointed, and set distal to the buccal ones. The four main cusps all have small dentine pits exposed. The broken Fa is a broad ovoid with crenulated sides and floor. The Fc is large, and positioned distal to the MD midpoint and lingual to the BL midpoint of the crown. The Fp is a pit-like depression between the End and Hld, bounded distally by a high Dmr. The lingual face of the tooth is also less sloping than the buccal one. On the buccal face, the mesiobuccal groove disappears at a small but deep pit midcrown, but on the lingual face, the lingual one continues to the broken edge of the fragment.

**KNM-KP 31715: LM<sub>1</sub> or M<sub>2</sub> fragment and two other tooth fragments** (not figured). These two fragments were found 1.5 m distant from each other. Extensive screening did not produce any additional pieces.

**A: LM<sub>1</sub> or M<sub>2</sub>.** This is a LM<sub>1</sub> or M<sub>2</sub>, preserving the buccal portion of the crown with parts of the Prd, Hyd and End, and the buccal sides of 4.5 of the mesial root, and most of the distal root. It is worn to just expose islands of dentine on both buccal cusps. The mesiobuccal groove is mild and disappears halfway down the buccal face.

The buccal face is sloping, gently bilobate in occlusal view and convex in distal view. The demarcation between dentine and enamel is apparent on the broken surface, as is the root canal. The edge of an IPF is just visible on the lingual side of the broken distal surface.

**B: M fragment.** This is a partial lingual fragment of a mandibular molar, preserving the lingual groove occlusally and the central portion of the lingual face to the cervix.

**C: Tooth fragment.** This tooth fragment preserves a portion of the mesial or distal face of a molar with a partial IPF.

**KNM-KP 31716: P<sup>3</sup> or P<sup>4</sup> fragment and C/ fragments** (not figured). This specimen was found on the surface of the base of the slope below the excavation for the juvenile, KNM-KP 34725 (Wynn, 2000, Figure 2), the worn M<sub>2</sub>, KNM-KP 35847, and the adult associated teeth, KNM-KP 35839. It does not appear to belong with any of these individuals, and was at least 10 metres distant from the majority of these fragments.

**A: P<sup>3</sup> or P<sup>4</sup>.** This is the distal portion of the crown and about 8 of the root. Both partially preserved cusps are worn to the same height, almost down to the level of the base of the Fp and for the Pr to the dentine. A distal IPF measuring 3.7 BL by 2.1 SI sits just to the lingual side of center, and is widest in its lingual half. The root flares slightly distally and buccally towards its apex. Enamel weathering has exposed perikymata on the distal face.

**B: C/.** This is a small fragment of C/ preserving only a limited area of enamel on the lingual face, with part of the basal tubercle. Inferior to this, the lingual face is nearly flat. A faint distal labial groove is visible, as are perikymata.

**KNM-KP 31717: Associated molars** (Figure 4). This specimen was found washing down a slope about 10 m to the west of the type mandible KNM-KP 29281.

After screening, a trench was excavated (Wynn, 2000, Figure 2) but no additional fragments were recovered *in situ*.

**A: LM<sup>3</sup>.** This is a crown with partial roots. The Pa and adjacent root are separated from the rest of the tooth by thin cracks. The occlusal outline is a rounded triangle with a convex distobuccal side. The mesial edge shows a slight concavity at the IPF, which measures 4.8 BL and 2.8 SI, but may have been larger as it is slightly obscured by weathering. There is slight wear of the occlusal surface that has flattened and polished the cusps and ridges and has made cusp sizes difficult to determine and obscured details of basin morphology. No dentine is exposed. There appears to be a slit-like Fa, but the Fp does not appear to have been distinct from the Fc. The Fc shows some crenulations. The double lingual groove disappears half-way up the lingual face. There is a small cusplule bounded by vertical incisions near the occlusal margin of the Pr. There is another small pit on the mesial aspect of the cusp adjacent to the occlusal plane. Faint vertical enamel ridges ring the sides of the crown, especially occlusally. The roots appear to have angled distally. They measure 13.3 BL by a maximum of 9.6 MD near the cervix.

**B: RM<sub>3</sub>.** This is the crown, missing its mesiolingual corner, and preserving about 3 of the root at the distobuccal corner. Wear has flattened the buccal cusps but dentine is exposed only barely on the Prd apex. Secondary fissures run into the central basin. The small Fa is slit-like, and the Fp is obscured by wear. Faint traces of fissures suggest that a large, possibly double C<sub>6</sub> was present. The distal margin of the tooth tapers to a rounded point in occlusal view. The mesiobuccal groove is deep, forming a pit-like depression close to the buccal occlusal margin and continuing about half-way down the buccal face. This depression is bounded mesially by a protostylid made of two cusplules, a smaller distal and larger

mesial one. There is another small pit mesial to the protostylid. There is also a distinct distobuccal groove that terminates a short way down the crown. The lingual groove is distinct near the lingual margin of the occlusal surface, but fades half-way down the lingual face. Faint vertical enamel ridges ring all sides of the crown. An IPF is present along the mesial edge, producing a visible mild concavity in occlusal view, but cannot be measured.

**C: RM<sup>2</sup>.** This is the mesiolingual quarter of a crown, missing a triangular wedge of enamel from the mesiolingual corner with about 4 of the root preserved mesially. The crown is worn, largely obliterating occlusal morphology, although there is no dentine exposure. A rounded lingual groove divides the lingual surface, making it bilobate. Division between enamel and dentine is apparent on the broken surfaces, and enamel is preserved up to 1.6 thick along the mesial occlusal margin and 1.5 along the labial margin.

**KNM-KP 31718: R mandibular fragment (M<sub>2-3</sub>)** (not figured). This was a surface recovery with no associated pieces.

This is a heavily cracked piece of mandible with M<sub>2-3</sub>. The cracks are up to 1.5 wide and run throughout the crown, root and bone, splitting them into small fragments and obscuring nearly all the morphology. The incomplete M<sub>2</sub> is also badly cracked and split. Only the distal portion of the crown is preserved, with one piece consisting of the End and sides of the tooth separated by a 1.6 split from a distal portion preserving the H1d and a sliver of the Hyd. Some facetting of the H1d and Hyd indicates slight occlusal wear, but there is no obvious dentine exposure. A faint distal IPF measures 2.2 SI by 2.4 BL.

The M<sub>3</sub> crown is complete but severely damaged by cracking obscuring details of surface morphology and occlusal wear. The mesial portion of the crown was wider than

the distal part, and the buccal surface more SI convex and sloping than the lingual one. The lingual cusps are higher than the buccal ones. There is a small C<sub>6</sub>.

**KNM-KP 31719: I<sup>1</sup>** (not figured). This was a surface discovery in the vicinity of KNM-KP 29286. The tooth is badly weathered and broken. Only a thin strip of enamel remains at the lingual margin and along one side at the enamel line. A faint basal enamel bulge is evident. About 12 of the weathered root is preserved. It is triangular in cross-section.

**KNM-KP 31720: Maxillary M fragment** (not figured). This was a surface discovery in the vicinity of KNM-KP 34725 and close to KNM-KP 35850, 35851 and 35852. It is a badly weathered molar fragment that preserves a complete lingual root and adjacent portion of a heavily worn crown. Overall weathering and cracking through the crown obscure its morphology. The root is about 16.5 long.

**KNM-KP 31721: RM<sup>2</sup> & M<sup>3</sup> partial crowns** (not figured). This was a surface discovery about 20 m to the west of KNM-KP 30498 and 40 m to the east of the type mandible, KNM-KP 29281 (Wynn, 2000, Figure 2). Screening of this area revealed additional specimens including KNM-KP 31723 and 31724. None of these can be certainly associated.

**A: RM<sup>2</sup>.** This large mesial portion of the crown is broken diagonally through the Pa and Hy. There is matrix and some damage to the enamel on the mesial half of the Pr. Wear has flattened the cusp apices, particularly the Pr but no dentine is exposed. Striations are visible passing BL across the Pr. A small Fa is preserved bounded by the Mmr. A tiny enamel pit is visible on the mesial side of the Pr. The lingual groove disappears about half-way up the side of the crown. The lingual face of the tooth is

strongly sloping, convex in distal view, and mildly bilobate in occlusal view. Faint vertical enamel ridges are visible on the lingual side, and faint perikymata are apparent near the cervical margin. The mesial IPF is 5.9 BL by 2.9 SI, and reaches to the occlusal surface.

**B: RM<sup>3</sup>.** This is a strip of lightly worn molar crown, about 5.6 wide. It is probably the distobuccal portion of an RM<sup>3</sup>. It preserves the distal part of the Pa and three other smaller cusps. The two occlusal grooves defining the Me disappear just over the occlusal margin. The central basin is smooth and lacks crenulations. Faint vertical enamel wrinkles mark the distobuccal face of the tooth.

**KNM-KP 31723: RM<sup>3</sup>** (Figure 4). This was a surface discovery about 20 m to the west of KNM-KP 30498 and 45 m to the east of the type mandible, KNM-KP 29281 (Wynn, 2000, Figure 2). Screening of this area led to the recovery of additional specimens including KNM-KP 31721 and 31724. None of these can be certainly associated.

This complete worn crown preserves about 3 of the root along the lingual and distal sides. The surface is weathered, and there is a crack through the Pa running diagonally towards the Hy. Enamel is missing along the cervical margin of the mesial half of the tooth. The occlusal outline is trapezoidal, tapering distally. The tooth is worn nearly flat, obscuring most details of occlusal morphology although there is no dentine exposed. The buccal cusps are higher and less worn than the lingual ones. The two buccal grooves define a cuspule between the large Pa and small Me, and both grooves disappear about halfway up the buccal face. Faint vertical enamel wrinkles are visible on the sides of the crown, and the remains of a mesial IPF are visible, though not measurable, despite the weathered enamel.

**KNM-KP 31726: RP<sup>4</sup>** (Figure 4). This specimen was found in the screening for KNM-KP 31727 but is considered to represent a second individual.

This is a worn P<sup>4</sup> with most of the crown and 7.5 of the lingual root preserved. The enamel is missing from the buccal and most of the distal sides. As preserved, the occlusal outline is a rounded rectangle with its long axis running BL. The Pr is worn to expose a hollowed-out area of dentine 3.3 BL by 4.4 MD and preserves only a narrow band of enamel around its margins. The higher Pa is also worn, exposing an area of dentine 2.6 MD that continues to the broken edge of the tooth. A concave mesial IPF measures 5 BL by 1.7 SI and extends to the occlusal margin. The lingual side of the crown bulges out from the base, and is tightly convex in distal view. There were two distinct roots that diverged just above the crown. The preserved lingual root diverges strongly lingually from the crown. It measures 5.9 BL by 4.9 MD near the cervix.

**KNM-KP 31727: R/C** (not figured). This specimen was a surface find. A second specimen, KNM-KP 31726, which is considered to represent a second individual, was found in the subsequent screening.

This /C lacks its entire mesial portion, and much of the crown. The distobuccal portion of the remaining crown is lost, so that whereas 7 of the crown is preserved lingually, only 5 remains buccally. Enamel is worn away from the enamel line, but its probable original extent is discernable. A distinct distal basal tubercle is preserved with a distinct and deep distal lingual groove adjacent to it, and a sharp median lingual ridge bounding the groove mesially. Mesial to this, a small, flat area of the lingual face remains. The root extends to a point 22.8 from the cervix just below the distinct basal tubercle. It measures a maximum of 9.7 near the cervix, roughly BL, broadening to a maximum of 10.5 about one third of the way

down its length, after this it tapers towards its apex.

**KNM-KP 31728: LM<sub>1</sub>** (Figure 4). This specimen was found in the vicinity of the juvenile mandible KNM-KP 31712, and higher on the slope than the worn dm<sub>2</sub>, KNM-KP 31714 and the unworn molar KNM-KP 35842. It is possible that this specimen could be associated with one or other of the latter.

This is an unworn crown, possibly a germ. None of the root is present. Enamel is almost completely missing from the mesial and distal sides, and towards the base of the buccal and lingual sides. None of the cervical margin remains. The Hld is partially preserved. The mesial half of the Mmr is broken away. The occlusal outline is a rounded rhomboid. The four main cusps are subequal in area, but the lingual ones are slightly taller. The occlusal surface is traversed by secondary fissures. The cusps are high and pointed, and demarcated by distinct grooves. A small and slit-like groove is separated from the Fc by a ridge connecting the mesial cusps. This groove is incised by the Mlg. Two tiny remnants of the Fa are visible anterior to this. The lingual and mesiobuccal grooves are nearly continuous. The fissure between the End and Hld terminates distally in a tiny V-shaped pit representing the Fp. The mesiobuccal groove deeply incises the buccal face, making it strongly bilobate. The lingual groove is less pronounced on the lingual face, disappearing about 2 from the occlusal margin. The buccal side is more sloping than the lingual.

**KNM-KP 31729: Rdm<sub>2</sub>** (Figure 4). This was a surface recovery from the western bank of the small drainage channel close to the type mandible, KNM-KP 29281. No further specimens were found in the screening.

This tooth consists of the crown and up to 8.0 of the distal and 6.5 of the lingual root.

Enamel is missing from the mesial face. The occlusal outline is a rounded, elongate trapezoid with convex mesial and distal sides widening distally. Wear has exposed dentine islands, each about 1 in diameter, on the buccal cusps, but the lingual cusps have only pinpoints of dentine exposed, with polishing extending from the Med apex towards the central longitudinal groove. From largest to smallest the cusp areas are: Med, Hyd, Prd, End and Hld. The taller lingual cusps are set distal to the buccal ones. The Fa is deep but small, and bounded by a thin Mmr that is crenulated at its occlusal edge. The Fa is bordered distally by a sharp crest running buccally from the Med. The Fp exists only as a distal extension of the Fc. The occlusal grooves are deep and incise the occlusal margins, but the lingual groove is deeper than the mesiobuccal one. The lingual, buccal and distobuccal grooves form a distinct Y-pattern. The mesiobuccal groove terminates in a small cleft bounded by a 2 long ridge-like protostylid, and is mesial to the lingual one. The buccal side of the crown is more sloping and vertically convex than the lingual one. The distal IPF is 2.1 SI by 3.1 BL, and located lingually, not quite reaching the occlusal rim. The roots diverge strongly, with the mesial one projecting almost directly inferiorly, but the distal one inclining distally. They measure a minimum of 8.3 MD near the cervix, where they are both 6.8 BL. Both have longitudinal grooves, but the distal one is faint.

**KNM-KP 31730: LM<sub>2</sub> & RP<sub>3</sub>** (Figure 4). These two teeth were found on the same slope above the type specimen, KNM-KP 29281, and above the isolated worn molar KNM-KP 29282. It is possible that KNM-KP 29282 represents the same individual but the distance separating these specimens was too large to make this likely. KNM-KP 31730A was a surface discovery whereas KNM-KP 31730B was discovered *in situ* in an excavation extending from this

spot to the southern side of the slope, where the juvenile, KNM-KP 34725 was recovered.

**A: LM<sub>2</sub>.** This is a very worn, weathered and broken tooth. The mesial root has its buccal half broken away and much of the rest of the roots are encased in matrix, except along the distolingual and mesiobuccal faces. Most of the enamel is broken away from the sides of the crown. Only an 8·7 MD by up to 5·5 BL portion of enamel remains on the occlusal surface between the lingual cusps. This portion is flattened and polished from wear, obscuring any meaningful morphology. A worn area of dentine remains buccal to this enamel island, and in the position of the Pr this is a deeply incised pit. The roots are inclined distally and buccally from the crown, and are roughly parallel.

**B: RP<sub>3</sub>.** This weathered tooth is worn, and preserves 8·5 of its single root buccally by only 2·5 lingually. Enamel is missing from the distal and lingual sides. Dentine is exposed over most of the flattened occlusal surface. Enamel remains at the depth of each basin. The buccal face was strongly sloping towards the occlusal surface, and a trace of the mesiobuccal groove and Mmr are apparent. The enamel bulged from the root on all sides.

**KNM-KP 31732: Tooth fragments** (not figured). These tooth fragments were recovered in the screening for the isolated lower dentition, KNM-KP 29286. Because none of them obviously appears to belong to this individual they were given a separate accession number. However, these eight fragments may not be associated and could well represent more than one individual.

**A: L/C.** This is approximately the distal one-third of a crown, which has been broken transversely through its tip and vertically through the buccal and lingual faces. It preserves most of the distal margin which is polished. The Dmr forms a small tubercle at

the cusp's distal margin, visible in lingual and labial views. This ridge, which has a small IPF for P<sub>3</sub> just lingual to the tubercle, sweeps along the cervical margin of the crown, fading toward the crown center. A gentle distal lingual fossa is visible, but otherwise the lingual face is transversely flat and SI concave. The labial face is convex transversely and flatter vertically. Hypoplastic lines are visible across the labial face and perikymata can be seen along the polished distal ridge.

**B: Tooth fragments.** These are seven small fragments of molars and premolars.

**KNM-KP 34725: Associated juvenile dentition and skull fragments** (Figure 11; F, J, K, N, O, Q and V not figured). This specimen was largely recovered *in situ*. Through screening, a number of skull fragments were found washing down a slope after eroding from a bed close to the top of a small hillock (Wynn, 2000, Figure 2). Excavation led to the recovery of the isolated teeth associated with this specimen as well as dental parts of additional specimens. These include KNM-KP 35839, 35840, 35847, 37522 and 37523.

**A: Rdi<sup>2</sup>.** This is the lightly worn crown and 10·3 of its root, with a piece of maxillary bone adhering to the mesial surface of the root. The tooth is weathered over its entire surface and enamel is lost from the mesial and distal faces. The occlusal surface slopes from the superior mesial corner inferiorly and distally, from 2·9 to 0·75 below the mesial enamel line. A narrow strip of dentine is exposed over the entire occlusal surface. The Mmr and Dmr are faint, running from the basal tubercle to the occlusal margin along the vertically concave lingual face. The labial side is convex, and marked by fine vertical furrows. The crown flares out from its root mildly, and only on the mesial side. The enamel line arches higher mesially than distally. The root is straight, and measures 3·3 MD by 4·1 LaL.

## KNM-KP 34725

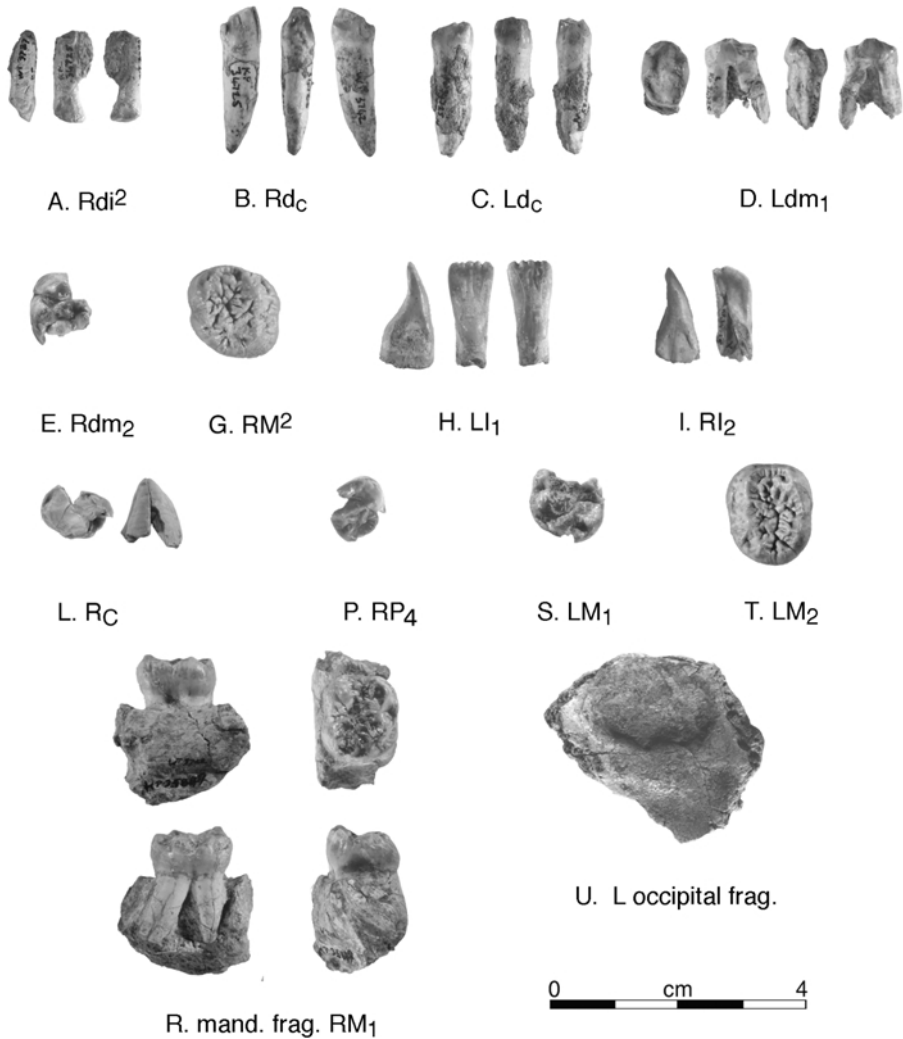


Figure 11. KNM-KP 34725, associated juvenile partial dentition and cranial fragments, (A) in lateral, labial and lingual views, (B) in lingual, distal and labial views, (C) in lingual, labial and mesial views, (D) in occlusal, buccal, distal and lingual views, (E) and (G) in occlusal view, (H) in mesial, lingual and labial views, (I) in distal and lingual views, (L) in occlusal and labial views, (P), (S) and (T) in occlusal view. (R) upper row in lingual and occlusal views, lower row in buccal and distal views, (U) in internal view.

The slit-like pulp cavity is visible on the superior break and measures just over 1 LaL. The root projects directly superiorly from the crown.

**B: Rd<sub>c</sub>.** This is the crown and complete root. It is the mirror version of the left d/c

(C), but less worn. The crown is worn to within 4.4 of the base distally, almost to the distal basal tubercle, and 5.6 mesially. A 3.2 wide vertical strip of enamel has spalled off the labial surface, and another up to 1.4 wide off the distolingual corner. Even if



there had been no missing enamel, the tooth is narrower LaL than MD. A sharply distinct distal basal tubercle and a less distinct mesial basal tubercle are present, the latter leading to a short lingual marginal ridge. The mesiolingual fossa is broad and shallow, about 3·7 wide at the worn occlusal margin. The distal lingual groove is deep and narrow, only 1·3 wide at the occlusal margin, because the median lingual ridge closely approximates the distal margin of the crown. The root measures 18·2 long, and 6·0 LaL by 5·25 MD at the cervix. Its apex curves distally.

**C: Ld<sub>c</sub>.** This specimen preserves the crown and root. It is worn to within 3 of the base of the crown lingually and 5 labially, with a hollowed 4·0 MD by 3·4 LaL area of dentine exposed on the distally angled occlusal surface. A basal tubercle is present at the distal corner of the crown. The lingual surface is vertically straight below the basal bulge, and this surface slopes labially toward the crown. The rounded labial surface is more vertical and smooth, with distinct distal and faint mesial grooves. It is the more worn antimer of the right one (B).

**D: Ldm<sub>1</sub>.** This tooth consists of a crown and two roots, the mesial one measuring 7·9 and the distal one 11·2 long. The roots are missing their apices. Enamel is missing from the mesiobuccal corner and much of the lingual face. The crown is ovoid in occlusal view, almost twice as long MD as it is BL, and wider mesially than distally. It is heavily worn so that dentine is exposed on most of the occlusal surface. Wear is oblique, sloping inferiorly and buccally, and the lingual cusps are higher than the buccal. The mesial cusps occupy about two-thirds of the crown surface, with their apices near the MD midpoint of the tooth, although the lingual one is slightly distal to the buccal one. There appears to have been an extensive Mmr with the remains of an incipient mesial accessory cuspule. Both buccal and lingual faces of the crown are roughly vertical in mesial view,

initially bulging out slightly from the root, and then sloping slightly towards each other. The lingual groove notches the lingual occlusal margin and barely continues onto the lingual face. Just below the cervix, the roots measure a total of 8·9 MD, and both are 5 wide BL. The mesial root angles slightly mesially toward its apex, while the distal one diverges distally. Both incline slightly buccally away from the crown.

**E: Rdm<sub>2</sub>.** This is the mesiolingual corner of the worn crown, preserving the Med. The Fa and part of the Fc are preserved. Dentine is exposed on the Prd continuing distally to the break. The Med has a small dentine pit at its tip and an elongated exposure running down its buccal side reaching almost to the dentine exposure on the Prd. There are two tiny tubercles on the side of the Med. The top of the root is also preserved adjacent to this cusp. The lingual face was bilobate, divided by a distinct lingual groove.

**F: RI<sup>2</sup>.** This is the distal third of the crown of the I<sup>2</sup> germ. The distal margin is concave in labial or lingual view, with its most widely flaring point about midcrown. The lingual face has a sharp edge, which extends superiorly from the Dmr. The Dmr demarcates a distinct distal lingual fossa that extends about 3 from the basal break, about half way towards the occlusal surface. Mesially the crown is broken through the distal shoulder of a well-developed median lingual ridge. Superior to this point, the lingual surface is flat in all dimensions. The labial surface is smooth and horizontally convex, except for a gentle but wide distal labial groove. It is straight in mesial view except at the basal bulge and adjacent to the apex where it becomes convex.

**G: RM<sup>2</sup>.** This germ consists of a complete crown with its root just beginning to form. It is a rounded rhomboid in occlusal view, with bilobate labial and lingual margins, and convex mesial and distal ones. It is heavily crenulated, obscuring the divisions between

cusps and foveas. A small Fa can be seen, but the broad Fp is merged with the Fc. The lingual side of the Hy is damaged, obscuring enamel relief. The Mmr and Dmr are marked by vertical wrinkles. A distinct cingulum with vertical wrinkles traverses the lingual side of the tooth from the mesial side of the Pr, and continues as a cingular remnant to a point parallel with the Hy. The lingual groove is complex, and terminates at this feature. The buccal groove is not visible on occlusal surface, but exists as a gentle furrow on the buccal side forming the bilobate contour. The buccal, lingual and distal sides of the crown are vertically convex. The mesial side is straighter and angles mesially from the enamel line. The buccal side is more sloping than the lingual one. Vertical enamel wrinkles ring the crown. Perikymata are visible on all sides near the enamel line, and a possible hypoplastic line is apparent 4·6 below the cervix on the distal side of the crown.

**H: LI<sub>1</sub>.** This is a complete unworn unerupted crown with 3·4 of its root, as measured on the lingual side. The crown measures 13·3 SI lingually. The occlusal surface inclines slightly distally and inferiorly. Five distinct mammelons disrupt the occlusal edge, with corresponding vertical grooves on labial and lingual surfaces of the tooth extending almost halfway toward the root. The lingual face is distally dished, flaring sharply towards the cervix. The labial face is only slightly convex. Curved hairline cracks diverging superiorly are visible on both labial and lingual faces separating the central portion from the mesial and distal. The mesial and distal margins of the tooth flare out from the base gently, so that the MD diameter of the tooth increases from 5·6 at the base to 7·3 at the occlusal edge. Horizontal perikymata are visible on the inferior half of the labial and lingual surfaces, and fine vertical grooves on the inferior half of the labial side. The enamel line arches superiorly about 5 at the

incisal angle of either side of the tooth. The root measures 8·9 LaL by 4·6 MD.

**I: RI<sub>2</sub>.** This is the distal two thirds of a germ made up of two pieces joined together at a hairline crack with no distortion. The crown is formed down to the labial cervical margin. Several mammelons are present, one on either side of the crack dividing the two fragments, and some more minor ones laterally along the occlusal edge. The distal margin of the occlusal surface curves inferiorly to the vertical distal side of the tooth. The lingual fossa extends over most of the lingual surface. The labial surface is convex except for the shallow distal labial fossa that runs along the upper half of the crown. Perikymata are clearly visible on the distal and labial surfaces. The distal enamel line is strongly arched.

**J: LI<sub>2</sub>.** This is a small fragment of the occlusal half of the distal portion of I<sub>2</sub>, measuring only 8 SI by 4 MD. It is similar to the I<sub>2</sub> of the right side (I).

**K: Mandibular I fragments.** These are five incisor crown fragments that are too small to attribute to a specific tooth. Two have basal tubercles and the left side of the crown in lingual view. One is the central portion of the occlusal surface, and a narrower section of the middle of the crown. Another is a broken distolabial portion of the crown, with enamel missing from its distal surface. The last fragment is the left side of a crown when viewed lingually. None of these pieces can be joined with each other or other incisor fragments from this specimen. There is no reason to presume that any belong to another individual, however. Mammelons are present on the two preserving some occlusal margin, and perikymata are visible on all.

**L: R/C.** This is an unerupted R/C crown missing most of its lingual face. It is split down the buccal face with a thin crack superiorly but half-way down, the enamel is missing in a wedge shaped piece about 2·6 wide at the base of the preserved crown. Part

of the lingual face remains mesially and distally. The crown is 13·4 high as preserved, pointed and unworn at the tip. It is similar to that of KNM-KP 29286 in size and morphology, but is unworn. The labial face is smooth and tightly convex in occlusal view, with strong perikymata running horizontally across it. There is a distinct distal labial groove that deepens cervically, whereas the mesial labial groove is indistinct and terminates at a Mmr. On the lingual face, the deep distal lingual groove is clearly demarcated by sharp parallel vertical ridges, comprising the distal margin and central lingual ridge, which run either side of it. A mesial lingual groove is visible just mesial to the broken section. The preserved distal portion of the lingual face is flat, with a sharp distal border. At the distal break, the base of a sharp distal cingular ridge is visible. The mesial margin of the crown is convex in labial or lingual view, with the Mmr and another, cuspule-like feature further apically along it. The distal border of the crown is also sharp, and is concave in labial and lingual view.

**N: L/C.** This is a 10 SI by 7 MD piece of the superior labial surface of the left canine preserving much of the distal lingual groove and bordering the central lingual ridge and distal margin. It is a good mirror of the right one (L).

**O: LP<sub>3</sub>.** This is all but the mesiolingual corner and distal margin of the crown of the P<sub>3</sub> germ. The Prd is centrally placed, and the Med exists only as a tubercle on the median lingual ridge. The mesial and distal ridges and transverse crest are sharp. There is a mildly crenulated, deep Fp. The buccal surface of the crown is convex in occlusal and mesial views. It is bounded mesially and distally by sharp, vertical marginal ridges. Perikymata traverse the buccal face, as do faint vertical enamel wrinkles.

**P: RP<sub>4</sub>.** This is the broken unworn crown of a P<sub>4</sub> germ comprising two pieces with an insubstantial join. The mesiolingual corner

is missing, as is the distal margin and distobuccal corner. The crown would have had an oval occlusal outline. On the occlusal face, the deep Fa is delimited mesially by a distinct Mmr, and distally by a sharp transverse crest. The Fp is deep, set lower than the Fa, and crenulated around its distal margin. Two distinct inflated ridges descend from both cusps to its base. There is a distinct but small End on the lingual end of the sharp Dmr. Mesial and distal buccal grooves are visible on the buccal face and there are horizontal perikymata near the base.

**Q: LP<sub>4</sub>.** This is the distobuccal fragment of an LP<sub>4</sub> preserving the distal part of the Prd, Dmr, and part of the Fp. The Fp is wrinkled and deep. A distal labial groove fades out just at the inferior edge of the fragment. Faint vertical enamel ridges and perikymata are visible on its face.

**R: Mandibular fragment (RM<sub>1</sub>).** This M<sub>1</sub> is complete. It sits in a piece of mandible that is 23 long, and extends 16·8 inferior to the alveolar border. The lateral surface of the mandible is missing so that both roots are exposed buccally. Part of the distal side of the P<sub>4</sub> alveolus and proximal wall of the M<sub>2</sub> crypt are preserved. Medially, there is a deep subalveolar fossa inferior to a pronounced alveolar swelling. The anterior edge of the subalveolar fossa curves medially adjacent to the anterior break. The molar crown is a rounded rectangle in occlusal view with a convex distal margin. The four major cusps are subequal in area and the Hld is slightly smaller, although it is almost as large as the Hyd. The mesial cusps are placed next to each other, but the End sits slightly distal to the Hyd. All cusps and the Fc show occlusal wear, and small islands of dentine are exposed on the buccal cusps. The Med is only lightly worn and remains high and pointed, and both lingual cusps remain higher than the buccal ones. The Fa is an elongate slit just distal to a thin Mmr, it is continuous with a larger pit between the

two mesial cusps. A faint ridge connecting these cusps barely divides the Fa from the Fc. The Fp is small, and lingual in position. The crenulated enamel of this tooth makes divisions among foveas difficult to discern. The mesiobuccal groove terminates in a pit bordered by the distinct cingulum that extends mesially along the buccal surface of the tooth to become a protostylid ridge. This ridge is in turn continuous with the Mmr, so that the tooth is ringed mesially and lingually with a nearly continuous cingulum-like structure that extends distally nearly to the Dmr. The lingual groove is mild and disappears by mid-crown on the lingual surface. Faint vertical enamel ridges ring the sides of the crown. A distinct mesial IPF measures 5.0 BL and 1.7 high. It is confluent with the occlusal margin, and cuts into the crown margin in occlusal view. There is no distal IPF. The enamel line is straight on all sides. The roots adjacent to the enamel line measure 10.8 MD by 10.8 BL. The mesial root is 11.2 long and the distal one 12.0 long. Both curve distally near their apices. The mesial one extends almost directly inferiorly, while the distal one angles distally. Above the point where the root is hidden by the investing mandibular bone, the mesial root can be seen to have a longitudinal groove separating its mesial and buccal portions.

**S: LM<sub>1</sub>.** This is a partial crown, preserving the distolingual corner and most of the buccal side. The mesial cusps are missing, and enamel is lost from most of the distal face and the distobuccal corner. It is a mirror of the R side.

**T: LM<sub>2</sub>.** This germ consists of a crown with its roots just beginning to form. Its occlusal outline is a rounded rectangle with convex distal margin. The occlusal surface is highly crenulated by numerous secondary fissures and inflated enamel ridges and cusps. The mesial cusps are larger than the distal ones, of which the Med is largest. A wrinkled, BL elongate Fa is evident. The Med is higher than the others. There is a

small C<sub>6</sub> present between the Hld and End, in place of a Dmr. A Mmr is present, as is a vertically wrinkled cingulum along the entire buccal surface. This cingular ridge is strongest where the mesiobuccal and distobuccal grooves terminate in it. Its most prominent section occupies the region usually attributed to a protostylid. The lingual surface is divided halfway down by a lingual groove. Perikymata ring the crown towards the enamel line, and a possible hypoplastic line is apparent 4.6 from the crown, measured at the center of the distal edge.

**U: Occipital fragment.** This is a piece of left lateral occipital squame, preserved from almost the midline to asterion, and missing its superior portion. It measures up to 33.1 ML by 29.2 SI. The lambdoid suture is preserved for only about 15 medial to asterion, and the occipitomastoid suture for about 11 inferiorly. The sutural surfaces are weathered. The external surface is also weathered and preserves little morphology, but a faint, rounded superior nuchal line is discernable. Above it, the bone is convex SI, and below it almost flat. Endocranially, the lateral margin of the groove for the superior sagittal sinus can be seen. A distinct groove for the transverse venous sinus extends across the middle of the fragment. Superior to it, the internal surface of the bone is concave in all dimensions. Inferior to the sinus there is also a concavity that extends to the break. The cranial vault bone is thicker superior than inferior to the transverse sinus groove, perhaps suggesting a relatively posteriorly-positioned cerebellar fossa. No part of any other sinus groove remains.

**V: Cranial vault fragments.** These are more than 15 fragments of cranial vault associated with this specimen, some of which can be joined. None can be attributed to a specific bone.

**KNM-KP 35838: LM<sub>3</sub>** (not figured). This specimen was a surface recovery. No other specimens are associated with it.

The specimen is a broken and worn crown and complete roots. The crown lacks the mesial and lingual margins. The roots are cracked and weathered. The Hyd and Hld are preserved, along with parts of the End. Wear has flattened the occlusal surface and obscured much of the morphology. A large area of dentine 2.6 in diameter is exposed on the Prd at the break, and a tiny, pinpoint of dentine is exposed on the Hyd. A faint Mlg is visible, with traces of the worn mesial and distal lingual grooves visible lingual to it. Part of a  $C_6$  is visible at the broken distal edge of the tooth. The mesiobuccal groove incises the occlusal rim. It extends onto the buccal face where it becomes a shallow furrow halfway down the side of the crown contributing to the bilobate contour of this side of the tooth. Fainter grooves delineating the Hld are visible, and continue a short way down the sides of the tooth. The mesial roots extend almost straight inferiorly, and are too poorly preserved to measure accurately, but their lengths can be estimated at about 13 linguallly and 11.5 buccally. The distal root bends distally towards its apex and its broad side is angled slightly buccally. It is 13.2 long, and about 9.0 BL near the cervix.

**KNM KP 35839: associated LI<sup>1</sup>, RC' & LP<sup>3</sup>** (Figure 12). A and B of this specimen were found on the surface close to the excavation of KNM-KP 34725 (Wynn, 2000, Figure 2). KNM-KP 35839C was found *in situ* about 20 cm below the level of the lowest fragment of KNM-KP 34725. Additional specimens found either in screening or excavation were KNM-KP 35840, 35847, 37522, and 37523.

**A: LI<sup>1</sup>.** This is a complete crown and up to 11.8 of root. Light wear has just flattened the occlusal margin but has not exposed dentine. There is a developmental defect, such that the crown is bent distally near its cervical margin. A large groove running 8.7 from the occlusal edge circles the base of the

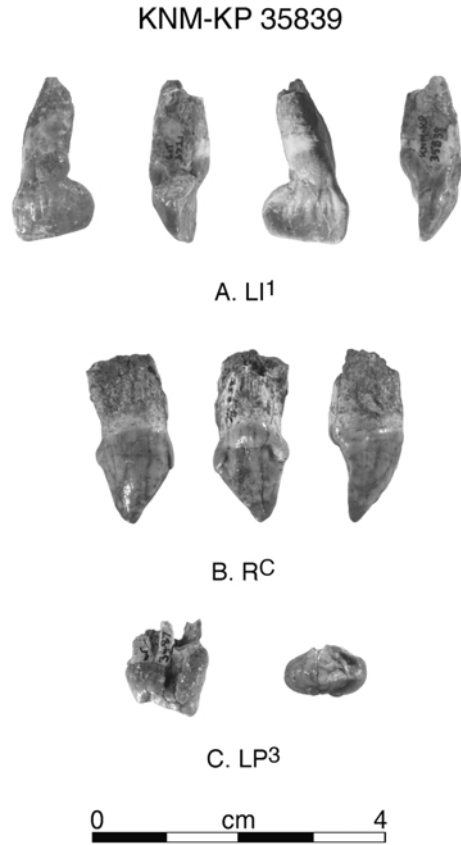


Figure 12. KNM-KP 35839 associated maxillary teeth. (A) in labial, distal, lingual and mesial views, (B) in labial, lingual and distal views, and (C) in mesial and occlusal views.

crown, and marks the inflection point of the bend in the crown. The enamel is pitted on the distal side inside the defect concavity. A 3.9 SI by 1.8 LaL IPF is present on the lower half of the mesial surface. If this facet is placed vertically as if at the LaL axis, the root angles strongly laterally in labial view. The vertically crenulated lingual face is concave SI and MD, with a distinct gingival eminence. The mesial and distal lingual fossae are bounded by marginal ridges. The median lingual ridge is better developed in the SI center of the crown, because between this point and the cervix the defect has distorted the morphology. The labial surface

is convex MD, and almost straight SI except towards the cervix, where the defect also has distorted the surface. A vertically elongated pit measuring 2.7 SI by 0.8 MD is visible on the mesial portion of the crown near the cervix, which has almost no bulge from the root. Perikymata are also visible near the cervical margin. Incremental lines are visible on the root running perpendicular to the long axis.

**B: RC/.** This is an unworn complete crown, about 14.6 high, with up to about 12 of a weathered root. A vertical crack traverses the lingual surface but obscures no morphology. The surface of the root is weathered and cracked. The crown is ovoid in occlusal view with the long axis running mesiolabially to distolingually. It is diamond shaped in lingual view and unworn, although some polishing is visible at the cusp apex, distal margin and distal tubercle. Distinct basal tubercles are present. Sharply delineated marginal ridges extend lingually to the basal bulge of the crown, bounding the superior edges of the mesial and distal lingual fossae, and merging at a swollen basal tubercle. Labially, marginal ridges extend for 5.6 distally from the mesial basal tubercle and 3.1 mesially from the distal tubercle. The median lingual ridge is rounded, and set just 4.2 from the mesial margin, so that the distal lingual fossa is much larger than the mesial one. The distal margin of the crown is predominantly straight but convex near the apex and concave towards the basal tubercle. The straight mesial margin is more vertical than the distal margin, giving the crown an asymmetrical lingual profile. The labial surface is convex MD marked by faint vertical enamel ridges, and traversed by uneven perikymata and possible hypoplastic lines. The root measures a maximum of 10.9 by a minimum of 9.0 adjacent to the crown. It is inclined distally away from the crown.

**C: LP<sup>3</sup>.** This is the crown and up to 4.6 of its root in places. It is missing enamel on its

distal surface. It also exhibits enamel defects in the form of a pit on the distal half of the buccal face, and a deep indentation in the mesial face along the cervical line, just above a malformed Mmr. This defect has affected the occlusal outline mesially. The Pa is about twice as tall as the Pr, which is little more than a tubercle at the lingual end of a sharp transverse crest. Little or no wear is evident. The Fa exists only as a small slit due to the pathological shape of the crown. The Fp is deeper, and is extensive and indented by transverse fissures. The Dmr is broken. Aside from the defect, the buccal face of the tooth is strongly sloping and straight, beginning at the basal bulge. The lingual side is less sloping, but also bulges near the root. The buccal face tapers rootward and the enamel line is strongly convex with a mesiocervical rootward enamel extension. Perikymata are visible on the buccal face. The root is MD compressed, and appears to have been affected by the pathology of the mesial crown, so that its mesial side appears pushed inward. It measures 10.2 BL by 6.2 MD as preserved near the cervix.

**KNM-KP 35840: LM<sup>3</sup> & M fragments** (not figured). This specimen was found on the surface close to the excavation of KNM-KP 34725 and 35839 (Wynn, 2000, Figure 2). Additional specimens found either in screening or excavation of this site include KNM-KP 35847, 37522, and 37523. It is possible that this is the same individual as KNM-KP 35839 although it shows no signs of the pathology so evident on the incisor and premolar of this specimen.

**A: LM<sup>3</sup>.** This is a LM<sup>3</sup> preserving 5.8 of the buccal root and 9 of the lingual one. The occlusal surface is lightly worn with only slight polishing. The crown is missing a triangular chip on the mesiolingual corner and a larger piece is lost distobuccally. Its occlusal outline is a triangle with straight

mesial side, slightly rounded lingual side and convex distobuccal side. It is broader BL than MD. The Pa is largest and tallest, and both mesial cusps are larger in area than the distal ones. Slight wear is apparent on the cusps. The occlusal surface is distinctly crenulated, and the Fc is indented by secondary fissures and inflated enamel ridges. The Fa is a shallow, narrow slit near the mesial edge of the crown, and separated from the Fc by a pronounced, broad, incised ridge connecting the mesial cusps. No Fp is preserved. The lingual groove is distinct, incising the occlusal margin to terminate half-way up the crown in a wrinkled, shelf-like cingular remnant. The buccal groove is fainter, but still incises the occlusal margin and disappears half-way up the buccal face. The lingual side of the tooth is more sloping than the buccal, and has more of a basal swelling. A mesial IPF is present, and although weathering obscures its dimensions was at least 2.5 MD by 1.5 SI. It did not meet the occlusal surface. The roots were widely divergent, and adjacent to the crown can be estimated to be 14.1 BL by 9.4 MD.

**B: L maxillary M fragment.** This is a small maxillary left molar fragment comprising part of the root and adjacent buccal face of the crown as well as a triangular wedge of worn occlusal surface, including the Fc and partial Pr. The latter has a small area of dentine exposed.

**C and D: M fragments.** These are two small, indeterminate molar fragments.

**KNM-KP 35841: M crown** (not figured). This was a surface recovery in the vicinity of KNM-KP 34725 but at the base of the slope to the east.

The specimen is a fragment of molar crown, consisting of the side of a tooth and a sliver of worn occlusal surface, measuring 7.1 transversely by 5.8 high, and 3.1 of adjacent root. It is too fragmentary to attribute to a specific tooth.

**KNM-KP 35842: R maxillary M** (Figure 4). This specimen was found in vicinity of KNM-KP 31712, 31714 and 31728. Some of these specimens could represent one individual, but they were widely dispersed and there are no obvious associations.

This is a right M<sup>1</sup> or M<sup>2</sup> crown lacking roots. It is unworn and slightly weathered. Most of the enamel is missing from around its cervical margin, except along most the mesial and labial faces and the cusp apices and several cuspsules are chipped. It is rectangular in occlusal outline, with an inflated mesiolingual corner and bilobate buccal edge. The buccal cusps are set mesial to the slightly taller lingual ones. From largest to smallest the cusps are; Pr, Pa, Me and Hy. Secondary fissures form small cuspsules and inflated ridges of enamel over the occlusal surface. The Fa comprises two small but deep pits, bounded by the Mmr, and a sharp ridge connecting the mesial cusps bounding it distally. These ridges appear to be cuspidate, but the cuspsules or tubercles along them are weathered. The Co is clearly defined and transected by a Mlg connecting the deep Fc and equally deep Fp. The Fp is slit-like, bounded distally by a strong Dmr. The lingual groove is truncated on the occlusal surface but on the lingual face terminates in a distinct V-shaped notch half-way up the crown. The more mesially placed buccal groove is distinct on the occlusal surface but only faintly visible on the buccal face, continuing as a shallow furrow to the break. There is an enamel pit on the mesial side of the Pr.

**KNM-KP 35844: M fragment** (not figured). This is a small fragment of worn molar crown lacking roots.

**KNM-KP 35845: M fragment** (not figured). This specimen was found in the screening of a site approximately 20 m distant from KNM-KP 31712. It is a small fragment of worn molar or premolar crown.

**KNM-KP 35847: LM<sub>2</sub>** (Figure 4). This specimen was found *in situ* in the excavation for KNM-KP 34725 and 35839 (Wynn, 2000, Figure 2). Because it is worn it cannot represent the same individual as either of these specimens. Other specimens recovered either in the screening or excavation at this site are KNM-KP 35840, 37522, 37523.

This is a worn crown and complete roots. The roots surround some mandibular bone. The lingual side of the crown is broken away. However, it can be seen that the occlusal outline of the crown was a rounded, MD elongate rectangle with a mildly bilobate buccal face. The Med appears to have been the most extensive. Dentine exposures on the Prd, Hyd and Hld are 1.5, 1.4 and 1.1 in diameter, respectively. There are small exposures of dentine on the remaining portions of the two lingual cusps, but most of these cusps are missing. Wear has flattened the buccal cusps and obscured the foveas and grooves, although a Y-pattern is apparent. Traces of a large shelf-like protostylid are visible along most of the buccal side of the Prd. The faint mesiobuccal and distobuccal grooves disappear just over the occlusal edge on the buccal face. The buccal face has a basal bulge, and then slopes occlusally. A crack divides the mesial face and the large, obliquely oriented IPF. This facet measures 5.2 BL and 2.3 SI and runs obliquely toward the crown, meeting the occlusal surface only in its buccal half. The distal IPF is 4.2 BL by 2.2 SI, and extends to the occlusal margin. The deeply grooved mesial root is 18.3 long and angles distally towards its bifid apex. Near the cervix, it measures 12.6 MD, and is 12.4 wide bulging to 13.3 midway down its length. The tips swing buccally and slightly distally. The distal root is 18.9 long. It is more angled distally and buccally, with only a faint longitudinal groove merging to a single tip that is mainly formed by its buccal portion. Near its cervix it is 11.3 wide bulging to 12.4 near its midpoint.

**KNM-KP 35850: maxillary M fragment** (not figured). This was a surface recovery in the vicinity of KNM-KP 34725, and close to KNM-KP 31720, 35851 and 35852. It is an extremely rolled and weathered fragment of worn maxillary molar crown with no details of occlusal morphology remaining.

**KNM-KP 35851: LM<sup>2</sup> or M<sup>3</sup> fragment** (not figured). This was a surface recovery in the vicinity of KNM-KP 34725, and close to KNM-KP 31720, 35850 and 35852. It is an unworn distobuccal portion of a maxillary molar crown. It is too incomplete to assign with certainty to a particular tooth, but is probably M<sup>2</sup> or M<sup>3</sup>. It preserves the Me and Dmr. The bases of the Hy, Pr and Pa are preserved with much of the Fc. The Dmr delineates a narrow Fp, and is largely occupied by a distal conule traversed by two light grooves. This distal conule is separated from the Hy by a continuation of the deep Mlg that traverses the fragment and terminates half-way up the distolingual crown face. The buccal groove continues from the Fc, notching the occlusal margin to run down the length of the preserved buccal face. Faint vertical fissures mark the preserved sides of this crown and all of the cusps.

**KNM-KP 35852: LC/** (Figure 4). This was a surface recovery in the vicinity of KNM-KP 34725 and close to KNM-KP 31720, 35850 and 35851. It is the weathered, worn crown and up to about 9.5 of the root. A 1.8-wide crack divides the labial surface of the whole tooth, where most of the surface enamel is missing. The root is broken at an angle, exposing an oval-shaped oblique section of root canal. The crown is worn to the level of the mesial and distal basal tubercles, but slightly more so distally, with a mildly sinusoidal wear plane. Dentine exposure measures 9.8 MD by 4.1 LaL. The pulp cavity is exposed in a small circle



at the center of the occlusal surface. The undamaged distal portion of the lingual surface is worn smooth, but there is a hint of a distal basal bulge present connecting Mmr and Dmr. A vertically concave mesial lingual groove notches the occlusal surface. A distal IPF meets the occlusal margin, and measures 3·7 LaL and a maximum of 1·8 high. Near the cervix, the root measures 8·2 LaL by 10·0 MD. Its surface is weathered. At the distal break the pulp cavity is difficult to measure accurately because it is broken obliquely, but is estimated at about 2 in diameter.

**KNM-KP 37522: L mandibular molar** (not figured). This specimen was recovered *in situ* in the excavation for KNM-KP 34725 and 35839. The occlusal wear indicates that it is unlikely to belong to either to one of these and it cannot be associated with any certainty to any of the other specimens recovered through either excavation or screening of this site. These include KNM-KP 35840, 35847 and 37523.

This partial crown is made up of four joined fragments that comprise the buccal and most of the distal sides of a mandibular left molar crown, probably M<sub>2</sub>. The Prd is broken through near its tip but the Hyd and Hld are complete, as are the bases of the lingual cusps. The lingual cusps would have been taller than the buccal ones. The Prd is larger than the Hyd. The buccal cusps are lightly worn and polished, and a tiny spot of dentine is exposed on the Prd. A pit-like Fp is present. There is also a pit in which the distobuccal groove terminates. The pronounced mesiobuccal groove intersects the Mlg in the Fc. The mesiobuccal groove continues down the entire preserved buccal face, giving it its bilobate contour. A small protostylid is located about half-way down the Prd from its tip. Small patches of surface enamel on the buccal face are pitted. Perikymata are visible over most of the buccal face.

**KNM-KP 37523: R mandibular M fragment** (not figured). This specimen was recovered in the screening for KNM-KP 34725 and 35839. The occlusal wear indicates that it is unlikely to belong to either one of these specimens and it cannot be associated with any certainty to any of the other specimens recovered through either excavation or screening of this site. These include KNM-KP 35840, 35847 and 37522.

The specimen appears to be the lightly worn lingual half of a R mandibular molar, probably M<sub>2</sub> or M<sub>3</sub>. There is a complete End, a small part of the Med, and what appears to be a C<sub>6</sub>. Some polishing is visible.

**KNM-KP 37524: tooth fragments** (not figured). These are four tooth fragments. They were found with KNM-KP 34725, KNM-KP 37522 and KNM-KP 37523. The first is a partial labial and mesial or lateral face of a mandibular incisor or canine with about 5 of the root. The second is a partial buccal face of a mandibular premolar crown. The third is the inferior half of the mesiolingual corner of a molar crown with 6·3 of adjacent root. The crown bulges out from its root and is vertically convex, and shows faint vertical enamel ridges and perikymata. The last is a fragment of worn molar crown with an IPF partly preserved on one side. Although it is slightly worn, the enamel measures 2 thick near the preserved cusp tip.

#### *Postcranial Fossils*

**KNM-KP 271: L distal humerus** (Figure 13). This fossil was found by the Harvard Expedition of 1965 (Patterson & Howells, 1967) and has been discussed by several researchers (e.g., Day, 1978; Senut, 1980; Senut & Tardieu, 1985; Lague & Jungers, 1996) and has been described and discussed by Hill & Ward (1988). Because of this we are not redescribing it here. Hill & Ward

## KNM-KP 271

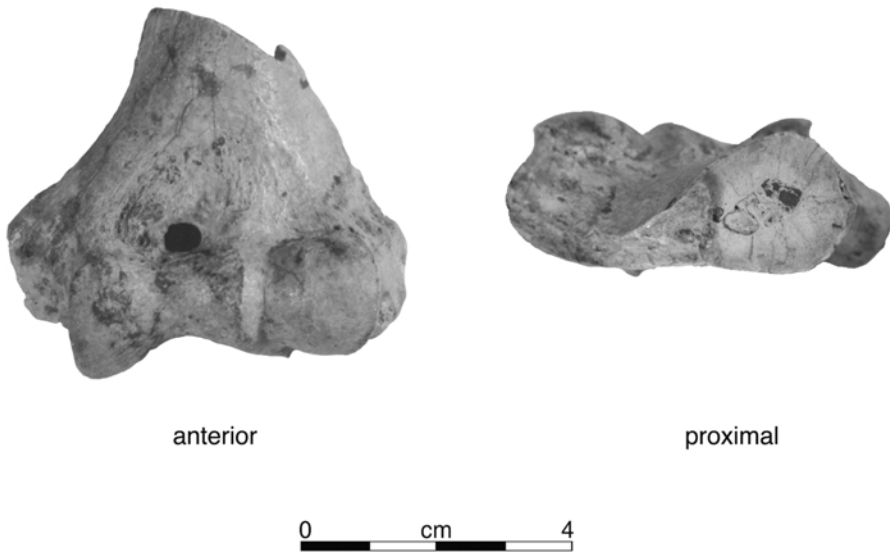


Figure 13. KNM-KP 271 humerus. The distal portion of the lateral trochlear keel is missing. In proximal view, the extremely thick cortical bone is apparent.

(1988) note that “The specimen is cleanly fractured along an oblique plane that begins proximally about 5 cm above the medial epicondyle and terminates about 3 cm above the same point.” This, apparently, was once true, but in its present condition, and as illustrated by Hill & Ward (1988), the clean fracture was clearly made by a rock saw. We have no information about this cut, which was made while the specimen was on loan to Professor Bryan Patterson. It was presumably to take a thin section of the shaft. Casts moulded before this cut was made show a jagged break exposing a roughly cylindrical medullary cavity about 7 in diameter on the diagonal break that is elliptical in cross-section. Several millimeters of bone were cut from the shaft, the greatest loss being on the medial side.

**KNM-KP 29285: R proximal and distal tibia** (Figures 14 and 15). This was a surface find. The proximal fragment was

discovered on the bank of a small channel, whereas the distal fragment had washed into the channel. In spite of extensive screening the middle portion of this tibia was not recovered.

**A: proximal tibia.** This is the proximal portion of a right tibia, probably about a quarter of the total length, measuring 104. It is complete except for some occasional mild abrasion along the margins of the condyles. Little of the medial condyle is missing, and contours are preserved, even in the posterolateral corner where it is most heavily abraded. Laterally, all of the cortex along the anterior, lateral and posterior margins of the subchondral surface are abraded and/or broken away so that the cancellous bone is uniformly exposed, obscuring the original margins of this joint surface. The top of the intercondylar eminence, the anteromedial margin of the lateral condyle, and the posterolateral margin of the medial condyle are also abraded.

KNM-KP 29285A

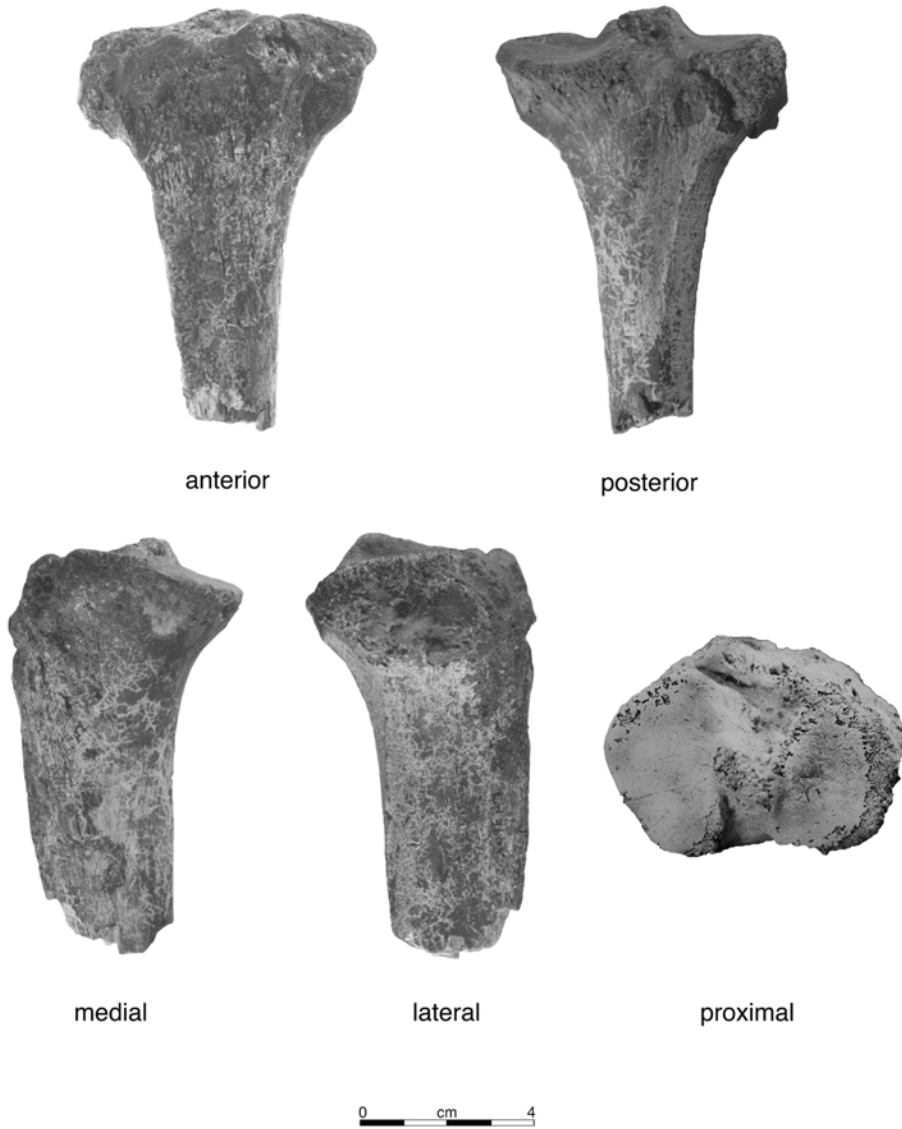


Figure 14. KNM-KP 29285A, right proximal tibia.

There is some irregular bone deposited along the anterior margin of the plateau extending nearly to the fibular facet, which appears pathological in origin. Its extent is primarily along the area for knee joint capsular attachment. This pathology was

apparently not severe, as it has affected no other morphology. The lateral side of the plateau is roughened, but intact. Just distal to it, the bone is abraded in places, and separated from the shaft inferiorly by a large crack up to 3 in diameter, which has

## KNM-KP 29285B

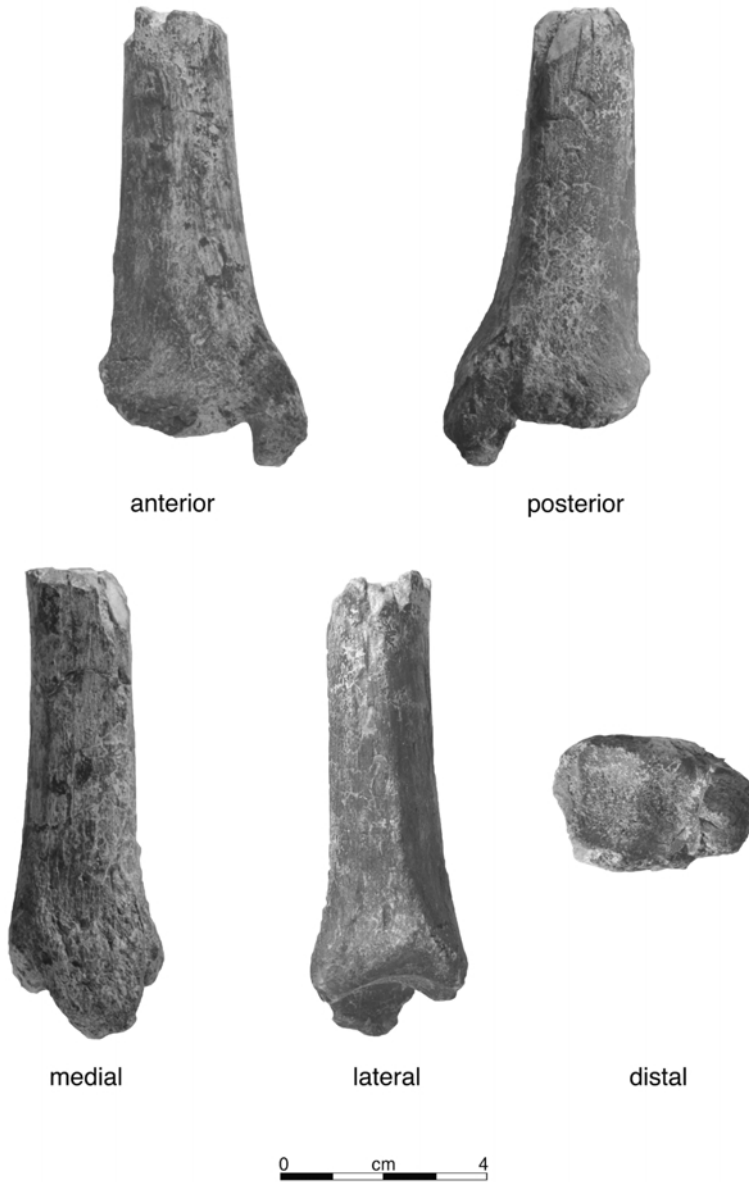


Figure 15. KNM-KP 29285B, right distal tibia.

expanded slightly and is abraded along its edges. This crack was postdepositional, and does not appear to affect the contours of the bone greatly although some slight separation

has occurred. The greatest abrasion occurs posteriorly, so the fibular facet is entirely missing. Still, the fibular facet must not have been very large, because the amount of

bone missing is not extensive. The area of insertion of the iliotibial tract is pronounced, and sits upon a large, raised area with abrasion of only the cortex around its margin.

The cortex of the shaft is weathered but intact. The distal break is nearly transverse, but is slightly lower on the medial side, and about half of the thickness of cortical bone anteriorly is broken off for about 10, tapering toward the break along the medial side. In distal view, the endosteal surfaces are marked by some cancellous bone, but are generally visible so that a reasonable cross-section can be obtained. The bone is radiographically opaque.

Both condyles are concave in most dimensions, but the lateral one becomes AP convex just along its most posterior preserved margin. The relative size of the condylar surfaces cannot be accurately determined due to damage to the lateral one. In proximal view, a distinct line, originating on the anterior-most point of the medial condyle runs laterally and posteriorly to the most anterior points on the lateral condyle and separates the rugose area anterior to it from the gently concave intercondylar area. The anterior attachment for the medial meniscus is a deep groove just posterior to the medial extent of the line demarcating the rugosity. The intercondylar area is peppered with nutrient foramina, and several faint puncture marks. Clear facets demarcating ligamentous and meniscal attachments cannot be detected, but the area for attachment of the anterior cruciate ligament is slightly depressed. The posterior intercondylar area is similarly preserved, but in this case the groove on the posterior margin for attachment of the posterior cruciate ligament is pronounced and clearly visible in proximal and posterior views. There is no apparent notch in the postero-medial margin of the lateral condyle for a posterior attachment of the lateral meniscus. The posterior attachment area for the

medial meniscus is also unclear. The plateau is set at about a 78° angle to the preserved anterior border of the shaft in medial view.

The tibial tuberosity is broad and pronounced but fairly smooth. The rugosity suprajacent to the tibial tuberosity along the anterior margin of the plateau obscures the line demarcating the tendinous and bursal areas of the tuberosity. The rugose area projects anteriorly from the surface of the bone further than the tuberosity. The tuberosity is continuous distally as a sharp and laterally deflected anterior border, with a faint longitudinal ovoid depression flanking it medially for the pes anserinus muscles. The anterolateral surface of the shaft is convex transversely and the medial border is mildly concave. The interosseus attachment forms a large, biconcave, almost triangular depression with a raised rim that is more distinct anteriorly than posteriorly. This facet sits distal to an overhang of the condylar surface that projects about 3·5 medial to the muscle attachment surface.

In posterior (or anterior) view, the metaphyseal region slopes gently from the plateau to the shaft with only a mild concavity. The spiral line is rugose. It runs obliquely across the posterior side of the shaft. It extends distally from a point about 10 mm below the disjunction along the missing portion of subcondylar bone where the fibular facet would have been, running inferiorly to about the center of the shaft at the distal break. Medial to the soleal line near its proximal extent, the bone is gently concave until it meets a mild ridge that extends distal to the posterior cruciate ligament attachment. This ridge meets the spiral line at the distal break. No nutrient foramen is preserved on the shaft.

**B: Distal tibia.** This is the distal portion of the same tibia, probably also about a quarter of the total length. It measures 83 from the center of the talar surface along the keel to the most proximal point preserved,

and 100 in maximum length. It is complete except for some minor spalling along the shaft, abrasion of cortex around the distal end, and some more extensive damage along the inferior and anterior margins of the malleolus, which obscure the original contours. Cortex is missing from the medial side of the malleolus, but the general contours of the bone are discernible. Part of the distal margin of the malleolar articular surface is abraded. Cortical bone is largely intact around the proximal break, except for along the anteromedial corner. Still, a good cross-section can be seen and cortical thicknesses measured accurately.

The shaft is angled  $93^\circ$  medially and  $90^\circ$  posteriorly from the talar articular surface. The metaphysis flares out significantly past the articular margins on all sides. The rounded triangular cross-section measures 20.6 AP by 22.5 ML at the break. The anterolateral and posterolateral sides of the shaft are convex transversely, and the medial side is almost flat. The medial side of the bone is bounded anteriorly and posteriorly by smoothly rounded borders. The interosseus border forms a rounded ridge at the proximal end of the specimen, sharpening to a roughened crest about 36 above the distal end. It is mildly concave anteriorly as it passes from the AP center of the lateral shaft proximally to the top of the synovial fibular facet distally. The widest and most proximal point on the fibular facet is located about two-thirds of the way from the anterior margin of the bone along the interosseus margin. Its dimensions can be estimated to be about 9.4 SI by 17.8 AP. The fibular facet is set at an angle of about  $145^\circ$  to the talar facet.

A flexor hallucis longus groove is preserved along the posterior margin of the malleolus, but its medial margin is abraded for most of its length. The preserved portion of the inferior malleolar margin is concave, and angled from anteroinferior to posterosuperior, and is not articular. As preserved, the

malleolus extends 13.4 from the adjacent talar surface, but this is an underestimate of the original length since the end of the malleolus is missing. As preserved, the malleolus is 21.7 AP by 12.4 ML; probably only a slight underestimate of the original values. The articular surface of the malleolus makes a rounded but distinctly acute angle with the talar surface.

The talar joint surface is almost square, measuring 23.0 AP at its midpoint, with the lateral part widening to 24.1 AP. ML, it is 24.4 at its midpoint, 22.9 posteriorly and 26.7 anteriorly. In distal view, the posterior margin of the facet is straight, and the anterior is mildly bilobate. The medial side is straight and oriented AP, and the lateral side flares anteriorly. There is a distinct keel dividing the joint surface into roughly equal halves. The two halves are gently concave ML. They are more so AP, with the concavity measuring a maximum of 5 deep.

**KNM-KP 30503: Proximal manual phalanx** (Figure 16). This was a surface find and no additional pieces were found in the screening.

The specimen is most of the proximal three-quarters of a manual proximal phalanx that is 32.9 in maximum length. It is preserved distally to an oblique line running just distal to the terminal end of the flexor ridge on the left and about 5 distal to the flexor ridge on the right when viewed palmarly. The cortex is cracked and in several areas small spalls are missing, but it is largely intact except at the distal end where close to the break the dorsal cortex is lost. A large longitudinal crack runs along the palmar surface of the shaft, but does not obscure the dimensions of the bone. More than half of the proximal joint surface is missing, and all its margins are abraded off. Cancellous bone is exposed along the entire proximal dorsal surface and half-way along the right and left sides, as well as in a small area palmarly adjacent to the longitudinal

## KNM-KP 30503



Figure 16. KNM-KP 30503, proximal manual phalanx in dorsal, palmar, side and proximal views.

crack. Most of the palmar tubercle on the right side of the base is preserved, but not on the left.

Based on a comparison with the morphologically similar *A. afarensis* phalanges AL 333-19 and AL 333-63, this phalanx would have been roughly 40–42 long originally. It is not possible to assign it to a particular ray. The palmar aspect of the shaft is ML convex between the flexor ridges proximally, and almost flat near the distal break. Narrow grooves flank the distinct flexor ridges on the palmar side. The flexor ridges are hard to measure precisely since their proximal ends grade into the sides of the shaft, but are about 14 long on the left, and 17 on the right, the right one extending further proximally. In side view, the shaft is markedly convex dorsally, and slightly concave palmarly especially adjacent to the proximal end. In dorsal view, the shaft is slightly ML constricted before the metaphyseal flare. A cross-sectional outline is difficult to estimate due to missing bone externally and an ill-defined endosteal margin. Shaft dimensions at the distalmost point at which cortex is preserved, about 7 from the distalmost point along the break, are 6.2 DP by 9.7 ML. At the center of the flexor ridges, these dimensions are 6.5

by 9.8, and proximally are 7.8 by 9.3. What little that remains of the proximal joint surface suggests that this surface was mildly concave in all dimensions. Maximum ML width of the base can be estimated at about 13 ML, but the dorsopalmar dimension is too damaged to estimate accurately.

**KNM-KP 31724: L capitate** (Figure 17).

This was a surface discovery about 20 m to the west of KNM-KP 30498 and 40 m to the east of the type mandible, KNM-KP 29281 (Wynn, 2000, Figure 2). Screening of this area led to the recovery of additional specimens including KNM-KP 31721 and 31723. None of these can be certainly associated.

This specimen is nearly complete but most of its surface is abraded away, and much of the preserved portion is weathered. The palmar surface of the bone is completely missing, except for a transverse isthmus one-third of the way from the proximal end. Most of the dorsal surface is missing as well. Laterally, the scaphoid facet is preserved except along its dorsal margin which is broken away, and an area along its distopalmar margin. The MC 2 facet is only preserved along its palmar portion to about the dorsopalmar midpoint of the bone, and

## KNM-KP 31724

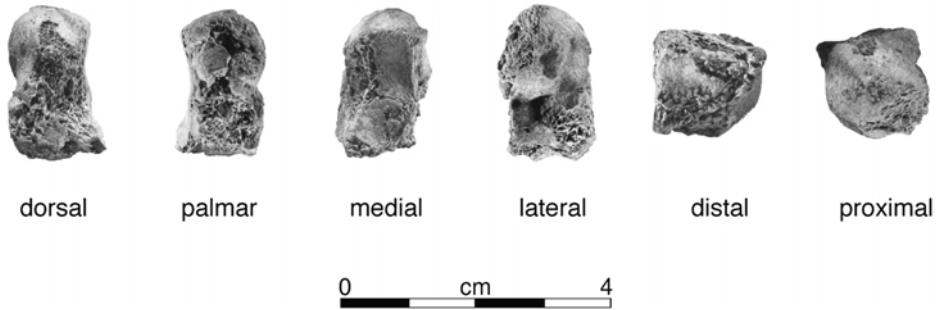


Figure 17. KNM-KP 31724, left capitate.

not quite to the distal edge. Medially, the hamate facet is nearly complete except for abrasion along its dorsal edge that does not affect its original contours, and weathering along its palmar margin that does obscure the margin of the subchondral bone here. Proximally, the head is missing its palmar medial edge, obscuring the palmar margins of the scaphoid and lunate facets. Distally, only the center of the third metacarpal facet is preserved along the dorsal margin to a point about two-thirds palmarwards.

The bone measures 21.6 in proximodistal length. Because of breakage and abrasion, almost no other measurements can be taken reliably (Table 4). The hamate facet is comprised of a single articular surface in two parts. It is about 7 wide.

In medial view, the facet runs straight distally from the margin of the head to a point just more than halfway along the bone, where it curves and runs distally and dorsally to the corner of the bone. The proximal portion is SI flat. There is a slight elevation near the inflection point, where a broad, low, rounded ridge occurs at the dorsal edge of the facet. Distal to this, the facet inclines dorsally and curves medially, most tightly near its distal extent. The palmar surface of the bone is almost completely abraded, and the little cortex

remaining along the distal edge is heavily weathered.

The scaphoid facet occupies about two-thirds of the lateral surface of the bone, and all of the head in palmar view. The scaphoid facet faces mainly dorsally and laterally, and has no proximally directed area on the head. The facet swings laterally along its dorso-distal edge to form a distinct saddle. Palmar to this, a 3-long arm of subchondral bone continues distally and palmarly to the deep intercarpal ligament pit that marks the center of the distal half of this surface. Just distal to the intercarpal ligament pit, most of the palmar half of the second metacarpal facet is preserved, except for the distopalmar corner. This facet is oriented about 90° to the third metacarpal facet, facing directly laterally. In distal view, the preserved part of the second metacarpal facet is only mildly concave. This facet was continuous from palmar to dorsal, with no intervening pit for the intercarpal ligament, which in this specimen is located proximal to the MC 2 facet. The MC 3 facet is concave ML and almost flat dorsopalmarly. Damage obscures the original contours of this surface.

The lunate facet terminates not quite a quarter of the way from the proximal end. The scaphoid facet is also visible in palmar view, owing to its oblique orientation.



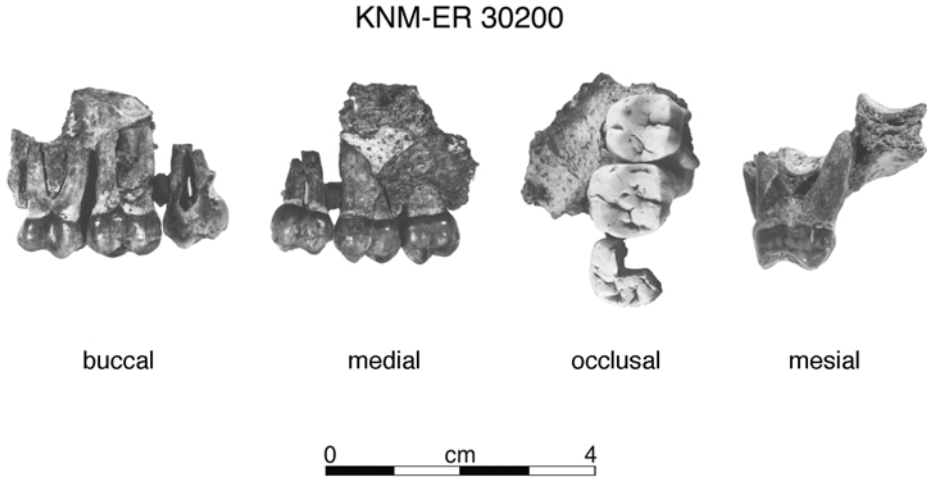


Figure 18. KNM-ER 30200, maxillary fragment with  $M^{1-3}$ .

The lunate facet occupies most of the head. It is tightly curved dorsopalmarly. It extends about 3 distally on the dorsal side, where there is a tiny remnant of a ridge along its presumed palmar margin, but this is difficult to ascertain with certainty due to damage to the specimen. It extends about 6 distally on the medial side. On the head, the junction between scaphoid and lunate facets is mildly crested, and runs from dorsomedial to palmolateral. The lunate facet is narrowest dorsally, measuring an estimated 6.5 ML here, widening palmarly so that it appears roughly triangular in proximal view.

### Allia Bay

#### *Craniodental Fossils*

**KNM-ER 7727:  $LM^2$ .** This was the first fossil to be found in Area 261 at Allia Bay and was described by [Leakey & Walker \(1985\)](#) and [Coffing \*et al.\* \(1994\)](#).

**KNM-ER 20420  $LM^2$ , KNM-ER 20421  $RM^3$ , KNM-ER 20422  $LM_1$ , KNM-ER 20423  $LM_2$ , KNM-ER 20427  $LM^1$ , KNM-ER 20428  $LM_3$ , KNM-ER 20432 L**

**mandibular fragment ( $P_{3-4}$ ), KNM-ER 22683  $LP_4$ , & KNM-ER 24148  $Ldm^2$ .** These specimens were found over several years by surface collecting at the main Allia Bay site in Area 261, East Lake Turkana. They were described and discussed by [Coffing \*et al.\* \(1994\)](#) and are not redescribed here.

**KNM-ER 30200: L maxillary fragment ( $M^{1-2}$ , partial  $M^3$ ) (Figure 18).**

**A: L maxillary fragment ( $M^{1-2}$ ).** This adult specimen preserves part of the alveolar process of the maxilla with  $M^1$  and  $M^2$ . The lateral side of the bone is missing. The palatine process is preserved for about 15 ML and up to 23.8 AP, but it is missing its cortex except for a diamond-shaped area 12 AP and ML that extends from the mesial root of  $M^2$  to the midline. Superiorly, the floor and part of the lateral wall of the maxillary sinus remain, and a ML convex section of the nasal floor is preserved for 13.1 anteroposteriorly by 9.0 ML. A tiny portion of the midline suture remains near the posterior edge of the fragment, at the level of  $M^2$ . The alveolar margins are broken away medially, so that 4.8 of the lingual  $M^1$

root and the entire lingual  $M^2$  root are exposed. The distobuccal  $M^2$  root is broken off. The lingual  $M^2$  root is exposed by the loss of a flake of bone of the sinus wall. The  $M^1$  is complete except for the very tips of the buccal roots. The  $M^2$  is complete except for most of the distobuccal root, the tip of the mesiobuccal root, and some enamel missing adjacent to the distolingual cervix.

The palate arcs up to a depth of about 10 above the cervical margins of the teeth. The palatal process is 8.0 thick at the midline. This was a narrow palate relative to its tooth size. An estimate of the horizontal distance from the lingual cervix of  $M^2$  to the midline is 13. The thin plate of bone that separated the nasal aperture from the maxillary sinus is broken off. Part of the sinus wall remains, narrowing to an isthmus about 7 long AP on its medial wall, and lengthening to about 20 AP along its floor. The exposed sinus floor is relatively smooth and does not invaginate deeply between the molar roots. Anteriorly, parts of the  $P^4$  alveoli are preserved.

The occlusal outline of  $M^1$  is a rounded transverse rectangle. From smallest to largest the cusp areas are: Me, Pr, Hy, Pa. The buccal cusps are higher than the lingual ones and set mesial to them. A broad Co is present. A tiny pit is visible on the mesiolingual corner of the tooth. The tooth is lightly worn across its occlusal surface, with flattening of both lingual cusps, the Pa and the mesial marginal ridge and polishing of additional ridges and crests. Pinpoints of dentine are exposed on the mesial cusps. There is a trace of a slit-like 3 wide Fa remaining. The Fp is in the form of a distinct pit, bounded posteriorly by a thick Dmr marked by a tiny cleft that runs towards the distal IPF. The buccal groove is mesial to the lingual one. It deeply incis the occlusal margin but becomes faint towards the cervix. The lingual groove is milder occlusally and interrupted by an enamel ridge at the occlusal margin, but it is strong on the lingual face. Both lingual and

buccal faces are bilobate. The lingual face has a series of small enamel wrinkles about 2.5 inferiorly from the cervix. The mesial IPF measures 4.7 by 2.4 and incis the occlusal surface. The buccal enamel line arcs up over each root, but the lingual line is fairly straight. The single lingual root displays a longitudinal groove. The vertically implanted buccal roots diverge at an angle of 25°. The roots were not much longer than their preserved lengths of just more than 10.6 for the mesiobuccal one and 11 for the distobuccal one.

The  $M^2$  crown is similar to that of the  $M^1$  except in a few features, and because it is less worn the features are easier to discern. It is more rhomboidal in outline. There is slight flattening of the lingual cusps and all cusps are polished but no dentine is exposed. The slit-like Fa measures 3.9 wide and clearly demarcates the Mmr. The Fp is deeper and BL broader. The lingual and buccal grooves are stronger on the occlusal surface. A small distal IPF measures 2.3 BL by 1.4 SI, and is set lingual to the MD axis of the tooth and does not meet the occlusal plane. The lingual root measures 8.0 MD near the cervix. It is about 15 long, and is marked by a lingual groove. It angles lingually towards its apex. The mesiobuccal root extends directly superiorly.

**B:  $M^3$ .** This tooth is missing its mesio-buccal corner to its center. About 10 of its lingual root remains, but only 4 of its root buccally. Judging by the curvature of the remaining part of the Pr it appears that the tooth had two larger mesial cusps and two smaller distal ones. The distal margin of the tooth is rounded. There is light polishing and some facetting of the cusps and ridges. There is a small pit at the mesiolingual break. The lingual groove terminates in a series of vertical enamel wrinkles midway up the crown. There are fainter wrinkles on the distal face that incis the distal occlusal margin, one of which ends as a small cleft in the margin. The small Me has grooves on

Allia Bay Isolated Teeth

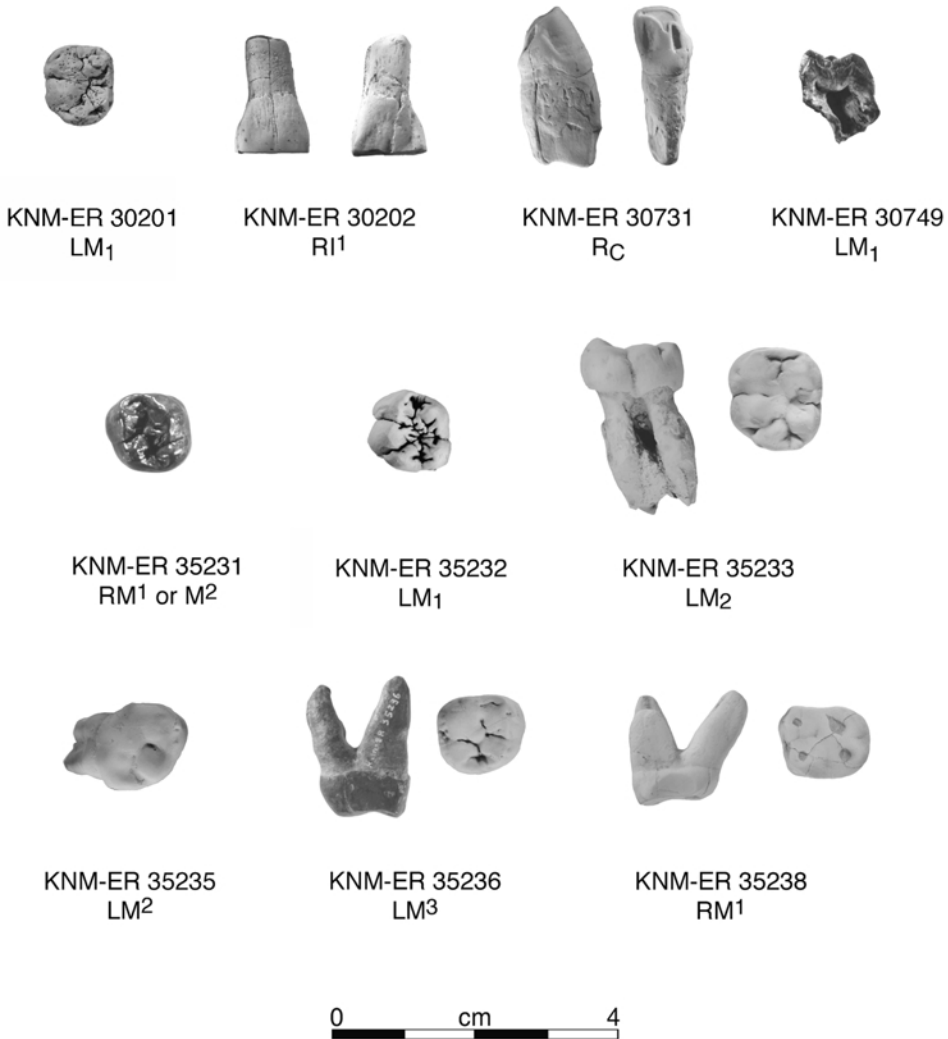


Figure 19. Isolated dental specimens from Allia Bay. KNM-ER 30201 in occlusal view, KNM-ER 30202 in labial and lingual views, KNM-ER 30731 in distal and lingual views, KNM-ER 30749 in buccal view, KNM-ER 35231 and KNM-ER 35232 in occlusal view, KNM-ER 35233 in buccal and occlusal views, KNM-ER 35235 in occlusal view, KNM-ER 35236 in mesial and occlusal views, and KNM-ER 35238 in mesial and occlusal views.

either side and an apex at the edge of the crown. The remaining mesial face of the crown does not extend far enough to see its IPF.

**KNM-ER 30201: LM<sub>1</sub>** (Figure 19). This is a lightly worn and weathered crown preserved almost to the cervical line. It is mildly elongate with 5 cusps. There is light

polishing of the buccal cusps and Hld. The Med is largest, followed by the subequal buccal cusps, and the End and Hld. The foveas are crenulated. The Fa is situated toward the lingual side of the tooth, extending almost to the Med apex. A secondary fissure traverses the mesiobuccal Med face. Another groove swings up the distal side of the Med almost to its apex, and is nearly continuous with the Fa, leaving an almost unbroken rim of enamel around the Med. The Fp is a deep pit. The faint lingual groove is set just distal to the buccal one. Both disappear midcrown on the sides of the tooth, as does the distobuccal groove. The buccal side of the crown is trilobate, deeply incised by the buccal and distobuccal grooves. The lingual side is straighter. A pit is present on the mesiobuccal corner of the tooth.

**KNM-ER 30202: RI<sup>1</sup>** (Figure 19). This crown is complete, with only some slight abrasion of the cervical enamel line lingually, and some hairline cracks which cause no distortion. About 9 of its root is preserved, and shows polish from rolling. The crown is worn occlusally, exposing a strip of dentine 9·0 MD by 1·3 LaL inside a thick enamel rim. The crown widens from 6·8 MD at its base to 10·5 at the occlusal margin, and would probably have been wider before it was worn. The occlusal plane slopes slightly distally and lingually. The lingual face is slightly concave in both directions, with little basal enamel swelling, an indistinct lingual ridge, and faint mesial and distal lingual fossae and ridges. The labial face is smoothly convex in both directions with faint vertical enamel wrinkles. A mesial IPF measures 3·2 LaL by 2·5 SI, extending to the occlusal plane. A distal one does not meet the occlusal plane, and measures 2·1 LaL by 3·4 SI. The root has pronounced mesial and distal grooves, and the pulp cavity is exposed on the broken root.

**KNM-ER 30731: RIC** (Figure 19). This is a complete crown and most of its root, missing only its apex. The crown is rolled and polished, and the root is spalled in many places. Its occlusal outline is a MD compressed oval. The crown is worn at its apex, with the wear surface exposing a tear-dropped area of dentine that slopes distally and cervically from its mesiolabial corner. It flares out from the root more strongly mesially than distally. The Mmr and Dmr are both strong on the lingual face, and merge with the moderately well defined basal tubercle. These ridges, along with a strong lingual ridge, help to demarcate clearly defined mesial and distal lingual fossae. The Mmr extends much further superiorly than does the Dmr, giving the tooth an asymmetrical appearance in lingual and labial views. The labial surface of the tooth is smoothly convex SI, and much more tightly curved transversely. The distolabial groove is deeper than the mesiolabial one, but both extend to the occlusal surface as preserved. They are continuous with one another across the base of the crown, forming a cingulum-like structure. The inferior portion of the labial surface shows transverse grooves that may represent hypoplastic features, and weathering in places has exposed perikymata over parts of the surface. Rolling has obscured any trace of IPFs. The root is compressed MD, measuring 6·6 MD by 10·2 LaL. Its contours are obscured by damage to the specimen. It is broken towards its apex, and a small area of the pulp cavity is exposed.

**KNM-ER 30744: RC/** (not figured). This worn and rolled tooth preserves about 12 of the root, but only 3 of enamel is left buccally, and 2 mesially and lingually. No enamel is left distally where the cervix arches toward the crown. The pulp cavity is exposed and secondary dentine is filling it. The root is hemicylindrical, rounded mesially and grooved distally.

## KNM-ER 30745

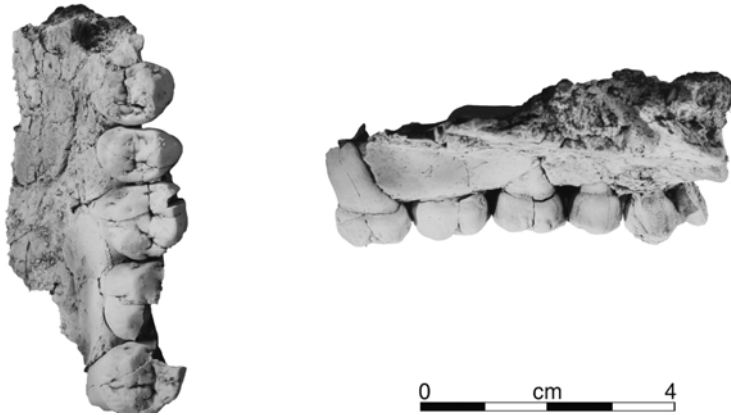


Figure 20. KNM-ER 30745, maxilla, in palatal and medial views.

**KNM-ER 30745: L maxillary fragment (C1, P<sup>3</sup>-M<sup>1</sup>, partial M<sup>2</sup>, M<sup>3</sup>) (Figure 20).**

*Preservation.* This is a left maxilla, preserving the palatine process to the midline, and no maxillary bone on the lateral surface. The buccal tooth roots have been lost to weathering and exposure, but the lingual roots are mostly preserved. The I<sup>1</sup> alveolus is partially preserved, with part of its lingual margin remaining. The interalveolar process between I<sup>1</sup> and I<sup>2</sup> appears complete. The I<sup>2</sup> alveolar margin is preserved mesially and lingually, but distally its dimensions are difficult to estimate due to damage here and around the canine root. The rest of the alveolar margin is abraded throughout most of its extent, and only completely preserved between P<sup>3</sup> and M<sup>1</sup>, and along the distal portion of M<sup>2</sup>. Only the distobuccal corner of the canine and a short segment of adjacent root remain. The premolars are complete. The M<sup>1</sup> is missing a small sliver of bone from the mesiobuccal corner, the M<sup>2</sup> is missing the entire buccal half, and the M<sup>3</sup> is missing the mesiobuccal corner.

*Description.* The bone of the palate is in a friable and delicate state. It is cracked and slightly weathered, but the contours are preserved. The midline suture can be

followed from near alveolare to a position level with M<sup>2</sup>. The incisive canal opens into a smooth incisive fossa so that its distal margin is at the level of the P<sup>3-4</sup> junction. Its aperture was about 5 long AP, and, as far as can be judged, was probably not this wide. The anterior margin of the incisive canal runs up and backwards at an angle of about 42° from the plane of the palate. The thickness of the palatine process cannot be measured.

Palate widths from midline to the teeth are about: at P<sup>3</sup> 14, P<sup>4</sup> 14.5, and M<sup>1</sup> 16. Distances at M<sup>2</sup> and M<sup>3</sup> cannot be measured accurately because of missing bone in this region. The palate is shallow anteriorly, sloping steadily up and backwards until at the level of M<sup>3</sup> it is about 12 deep at the greater palatine groove. Just lateral to the M<sup>3</sup> lingual root, a small, biconcave section of the floor of the maxillary sinus remains, measuring 8.3 by 4.3.

An estimate of the I<sup>1</sup> alveolus diameter near the margin is 7. The distal half of the canine is preserved, but the tip and lingual sides have been broken off. Its LaL diameter is about 11 at the cervix. Enamel on the lingual side is eroded, but enough remains

to show that there was a shallow distal groove ending superiorly in a distal depression. The root adjacent to the distobuccal corner is preserved for about 5.

The P<sup>3</sup> crown is complete, and is slightly expanded by a MD crack running through the groove separating the two cusps. No root remains buccally. Its crown is ovoid in occlusal outline with a flattened, slightly oblique mesial edge. The Pa is the larger of the two cusps, and is more projecting. Wear was slight but cannot be fully assessed due to weathering of the occlusal surface. The Fa is small, and restricted to a small pit immediately mesial to the Pa and bordered mesially by a thin rather slight Mmr. The slit-like Fp is 3.5 wide and is connected to the Fa by an irregular furrow. It is bordered distally by a wide Dmr. One or two small grooves run from each cusp towards the Mlg. The buccal surface slopes markedly upwards and has two shallow grooves demarcating moderate mesial and distal buccal ridges. The buccal enamel line is convex rootward with a strong mesiocervical enamel extension. The lingual surface is only slightly sloping.

The P<sup>4</sup> crown is complete, but its buccal root is also missing. Its occlusal outline is also a MD compressed oval, with an almost pointed apex buccally and a mesial surface flattened at the IPF. Wear was light with polishing across the occlusal surface and some flattening of the lingual cusp. The P<sup>4</sup> crown is less asymmetrical than the P<sup>3</sup> crown, with the two cusps being subequal in size. There is a small pit-like Fa, but the Fp is indistinctly defined. Both the Mmr and Dmr are well developed, the latter the more so. The lingual and buccal slopes are approximately the same. The mesial and distal buccal ridges are weakly developed. Buccal enamel extends rootwards, but not to the extent seen in the P<sup>3</sup>. A single distal lingual groove marks the lingual face. Occlusally, the groove separating the cusps runs from a slit-like curved 2.7-long Fa to

a more irregular but longer Fp. Several accessory cuspules fill the Fp.

The M<sup>1</sup> is a rectangular tooth with a strongly sloping lingual surface. Its occlusal outline is a rectangle slightly compressed MD with a rounded distal margin. All cusps are lightly worn with extensive polishing and flattening of the lingual cusps. The Pr is the largest cusp, with the other three subequal in size. The buccal cusps are taller than the lingual ones. All cusps are worn, but only the Pr has dentine exposed in a small area about 0.4 wide. The tiny, slit-like Fa is only about 1.5 long. The Fp forms a Y-shaped bifurcation of the Mlg that separates the two distal cusps and sets apart a hypoconule. The buccal groove starts in a shallow pit in the Fc, and terminates about half-way up the buccal surface. The lingual groove is faint at the occlusal margin, but is deep and double-furrowed before it terminates half-way up the lingual face. Other, fainter lingual grooves mark the lingual face of the tooth.

Only the Pr and part of the Hy of the M<sup>2</sup> remain. Both are flattened by wear but neither has dentine exposed. Part of a small Fa is apparent at the front of the tooth. A cingular remnant can be seen at the mesiolingual corner and slightly at the termination of the lingual groove about midway up the crown. The lingual groove has two parts on the lingual face. One extends on the occlusal surface to the break, and the other is a short branch swinging mesially, but not reaching the occlusal surface.

The M<sup>3</sup> is missing its mesiobuccal corner. It is a broad oval in occlusal outline, with its long axis running mesiobuccally to distolingually. Its Pr is largest, and the Pa is only slightly smaller. All cusps are lightly worn, the Pr is extensively flattened, the Hy less so, and the lingual cusps are faceted. The distal margin of the tooth is rounded, due to the weak development of the distal cusps that exist primarily as the Dmr. The Fp is large and well developed, and is connected to the

Fc by a groove separating the Me and Hy. The buccal groove extends from the Fc to terminate halfway up the buccal face. The lingual groove terminates in a series of soft, irregular grooves on the lingual face. The distolingual margin of the tooth has irregular vertical ridges running down the enamel. The lingual root of  $M^3$  is completely exposed. It is missing only its tip, and measures 12.7 as preserved. It angles gently distally from the crown.

**KNM-ER 30747: LP<sub>4</sub>** (not figured). This is the distolingual half of a small crown and up to about 4 of the adjacent root only. It is cracked through the Med, and preserves the Fp. The tooth was lightly worn. Radial ridges lead from the Med and Dmr into the basin. Two lingual grooves mark the lingual surface extending to the occlusal rim. A distal IPF measures about 3.4 BL by 2.1 high. The crown does not flare out strongly from the root.

**KNM-ER 30748: L maxillary M fragment** (not figured; see [Figure 31](#)). This is a rolled and lightly worn maxillary molar fragment consisting of the mesiolingual corner of a left molar, and the lingual half of the mesial root. The wear facet cuts into the slit-like Fa, and there is a cingular remnant on the lingual corner. Part of the IPF is visible lingual to the break. The cervical margin is straight in the parts preserved, and the roots diverge strongly toward their apices. This specimen has been sectioned for analysis of enamel structure by M. C. Dean. The section is shown in [Figure 31](#) and discussed in the comparative morphology section below.

**KNM-ER 30749: LM<sub>1</sub>** ([Figure 19](#); see also [Figure 31](#)). This is the distolingual half of a small unworn LM<sub>1</sub>, broken diagonally from mesiolingual to distobuccal, preserving the lingual cusps, the End and the Hld, half of the Med and a sliver of the Hyd. It has up to

6.5 of its root preserved at its distolingual corner, extending into the groove between the roots lingually, and just past a longitudinal depression between the buccal and lingual portions of the distal root. The cusps show light polishing which could be due to wear. The main cusps are demarcated by distinct fissures, with accessory fissures and ridges running from the cusps to the basins. The lingual groove extends from the Fc to terminate about half-way down the side of the crown, as do the two grooves delineating the Hyd. Perikymata are visible on the lingual and distal sides. No IPF is visible. This specimen has been sectioned for analysis of enamel structure by M. C. Dean. The section is shown in [Figure 31](#).

**KNM-ER 30750: R/C** (not figured). This is a R/C crown and about 11 of its root. Its occlusal outline is a MD compressed oval. The crown was worn, with a tip facet set obliquely, running from the mesial side at the apex inferiorly and distally. The enamel on the labial side is about 1 thick. There is a chip of enamel missing from the mesial side of the apex. The buccal surface is cylindrical with only a distal labial groove adjacent to a sharply defined Dmr that has a small tubercle at its base. On the lingual surface, there is a strong distal groove and only a mild, shallow mesial groove. Loss of enamel obscures any Mmr. The crown bulges out only slightly from its root on all sides. The enamel line is fairly straight on three sides, but arches towards the crown mesially. The root is compressed MD, measuring 5.6 MD by 8.3 LaL at the cervix, and curves gently distally towards its apex.

**KNM-ER 35228: RP<sub>4</sub>** ([Figure 21](#)). This is the almost complete slightly rolled crown of a germ, missing a small amount of enamel from the cervical margin on the mesial side. The top of the root was just beginning to form.

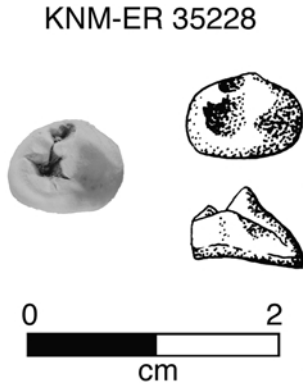


Figure 21. KNM-ER 35228, RP<sub>4</sub>, in occlusal and distal views. Drawings by Susan Alta Martin.

Although this tooth has an ovoid crown outline, it is unlikely to be a P<sub>3</sub> for several reasons. The Med is well developed, and although the Prd is large, its apex is placed mesial to the mesiodistal midpoint of the crown. The Mmr is high, and there is a deep Fa that opens superiorly, rather than mesiolingually. The transverse crest is distinctly notched. The distolabial groove is pronounced, delineating a distal cuspule. There is no mesiolabial groove. Its morphology is described here without reference to it being a P<sub>3</sub> or P<sub>4</sub>.

This is a very small tooth. In occlusal view, the ovoid crown outline has its long axis running mesiobuccally to distolingually, with the distal surface slightly more convex than the mesial one. The Prd is located near the center of the tooth on the BL axis and at about the mesial third on the MD axis. It closely approximates the much smaller Med, which is set almost directly lingual to it. Two distal cuspules representing the Hyd and End, are set farther apart than the main cusps, and sit along the pronounced Dmr separated from the main cusps by small furrows. The End cuspule is slightly lower, and set just mesial to the Hyd one, so that it sits almost on the distal slope of the Med. The Fa is much smaller and set higher than the Fp. The Fp is wider BL than MD. Both

the Fa and Fp are located on the lingual half of the tooth and are separated by a strong, notched transverse crest. The Fa is round in occlusal outline and almost featureless. In mesial or distal view, the buccal surface of the tooth slopes strongly towards the Prd cusp tip. It bulges just above the cervix and again at the cusp apex, and is mildly concave in between. The mesial, lingual and buccal surfaces are all similarly concave SI. The buccal surface is marked by a broad distobuccal groove that meets the occlusal surface but fades out before the cervix.

**KNM-ER 35229: L mandibular M fragment** (not figured). This is the distolingual corner of an M<sub>1</sub> or M<sub>2</sub> germ. It is broken through the End and preserves most of the Hld. There is a tiny cupsule adjacent to the End on the Dmr. The Fp is a pit. Crown formation is incomplete. The dentine–enamel junction is not discernable.

**KNM-ER 35230: M fragment** (not figured). This hexagonal fragment consists of the central portion of an unworn molar crown, probably a lower molar. It is about 6 in diameter, and preserves the Fc, and bases of five cusps. It is not crenulated.

**KNM-ER 35231: RM<sup>1</sup> or M<sup>2</sup>** (Figure 19). This is a slightly worn complete crown with up to 1–2 of root preserved. Areas of enamel are missing around the cervix, so that the crown appears to have more of a basal bulge than it would have had when intact. Its occlusal outline is a rounded trapezoid, with the mesiobuccal corner inflated relative to the other three, so that the crown is broader mesially than distally. From largest to smallest the cusp areas are: Pr, Pa, Me, Hy. The two lingual cusps are more rounded, and set somewhat distally to the buccal ones, but all are roughly equal in height. A tiny spot of dentine is exposed on the Pa tip, but the tip of the Me is broken off, rather than being worn. Facetting is



visible on the occlusal surfaces of both mesial cusps, and just onto the mesial and lingual marginal ridges. The Fa is bounded by a smooth, continuous Mmr. The Fp, which is bounded distally by the strong Dmr, is continuous with the deep Mlg connecting it with the Fa. The Mlg separates the Pr from Me, completely bisecting the weakly developed Co. The foveas are slightly crenulated. The lingual groove is deep, and terminates midway along the lingual face. The buccal groove is similarly developed on the occlusal surface, but less marked on the buccal face. The lingual side of the crown slopes strongly towards the occlusal surface and is convex in mesial and distal view, whereas the buccal surface is flatter and less strongly sloping. The distal side of the crown is rounded in lateral view, while the mesial one flares mesially towards the occlusal surface. An ovoid mesial IPF measuring 1.3 SI by 2.6 BL sits just buccal of the MD axis of the tooth, but none is apparent distally.

**KNM-ER 35232: LM<sub>1</sub>** (Figure 19). This is a slightly worn crown with 2–4 mm of root. Enamel is missing around the entire cervical margin. In occlusal view, the crown is a rounded trapezoid in outline, broader distally than mesially. The buccal cusps and Hld show wear at the tips, but dentine is exposed only on the Prd as a tiny point. The Med is higher and more pointed than the other four cusps, which are roughly equal in height and is also larger in occlusal view. From largest to smallest the cusp areas are Med, End, Hyd, Prd, Hld. The deep Fa is bounded mesially by a strong Mmr and distally by an incised crest connecting the Med and Prd. The Fc is large and traversed by numerous secondary fissures and inflated ridges and cuspules. There is a small, transverse Fp and Dmr marked by two faint transverse grooves. The shallow lingual groove terminates halfway down the lingual surface, whereas the deep mesiobuccal

groove divides the entire buccal side of the crown. A deep distobuccal groove separates the Hyd and Hld on the buccal face just above the break. Each of these grooves originates in the Fc and incises the occlusal margin. The buccal face slopes more strongly than the nearly vertical lingual face. A mesial IPF measuring 1.4 SI by 1.6 BL is visible.

**KNM-ER 35233: LM<sub>2</sub>** (Figure 19). This tooth is nearly complete, but rolled, weathered and polished so that it lacks much surface detail. Its roots are partially invested in bone. Enamel is broken along the cervical margin, and some of the surface of the root abraded off beneath the enamel junction. The occlusal outline is a rounded rectangle with convex distal margin. The five primary cusps are bounded by distinct grooves delineating them in a Y-pattern. C<sub>6</sub> and C<sub>7</sub> are small, but present. A trace of a proto-stylid is visible. The lingual cusps are higher and more pointed than the buccal ones, and were probably only slightly worn. The buccal ones are worn but no dentine is exposed. From largest to smallest, in occlusal view, the cusps are Med, Prd, Hyd, End and Hld. A pronounced Mmr bounds the Fa, which is a transverse slit. The Fc is extensive, but the pit-like Fp is small. It is bounded posteriorly by a Dmr and the C<sub>6</sub>. The lingual groove continues half-way down the lingual face. Another, less extensive vertical furrow runs mesial to C<sub>7</sub>. The mesiobuccal groove extends to the cervix, contributing to the bilobate shape of this face in occlusal view. A distobuccal groove extends a short way onto the buccal face, terminating in a small cingular remnant. The buccal face is more strongly sloping than the lingual one, and is tightly convex in distal view compared with the nearly straight contour of the lingual face. Mesial and distal IPFs are visible but do not reach the occlusal surface. The mesial one measures 3.1 SI by 4.0 BL, and the distal one 2.5 SI and 2.5 BL.

There are distinct mesial and distal roots of approximately the same length. The mesial root is BL broader than the distal one. Each has a mild but distinct longitudinal groove, and each terminates in a pair of apical tips. Their length is difficult to measure accurately because of the missing cervical enamel and weathering, but the mesial one was probably about 18 and the distal one about 16 long. They are mildly inclined buccally, and more so distally.

**KNM-ER 25234: LP<sub>3</sub>** (not figured). This is a badly rolled lower crown missing most of its enamel, and its nearly complete root. Its occlusal outline is a rounded triangle. No observable crown morphology is preserved. This tooth had a single root that is curved slightly distally near its apex.

**KNM-ER 35235: LM<sup>2</sup>** (Figure 19). This is an extremely rolled and polished crown with up to 3 of root preserved distally and 7 lingually. Most of the crown morphology is lost and the occlusal surface has little remaining topography. The occlusal outline is a rounded trapezoid that is broader mesially than distally. Cusps are barely delineated, and from largest to smallest appear to have been: Pa, Pr, Hy and Me. The Mmr and Fa are barely distinguishable. The median longitudinal groove incises the strong Co. There is a strong Dmr bounding a deep Fp. The distobuccal and lingual roots diverge strongly. The lingual root appears as two fused columns, separated by a longitudinal groove.

**KNM-ER 35236: LM<sup>3</sup>** (Figure 19). This slightly weathered tooth is missing only the distobuccal root and a small piece of enamel at the mesiobuccal cervical margin. The crown is a rounded trapezoid in occlusal view tapering distally, and wider BL than MD. Wear has polished the occlusal surface but there is no dentine exposure. From largest to smallest the cusp areas are: Pr, Pa,

Me, Hy. A small, slit-like Fa is positioned buccally. The deeper, elongated pit-like Fp is delineated by a strong Dmr that has a small cuspule situated at its center. The Fc is interrupted by a broad Co, which is incised by a Mlg connecting lingual and buccal grooves. The buccal and lingual grooves originate at mid-crown, but the lingual one is more deeply incised on the side of the tooth where it terminates in a crenulated depression. Faint vertical enamel wrinkles ring the crown along the occlusal surface. Perikymata are occasionally visible on the sides, particularly near the cervical margin, and are especially evident on the distobuccal corner. Slightly deeper and more irregular transverse furrows near the base may be mild hypoplastic features. The buccal face slopes more strongly than the lingual one. A 3·2 SI by 5·0 BL IPF is visible on the straight mesial face. The distal face is convex in lingual view. The roots are angled distally from the cervix, and diverge BL towards their tips. The lingual one is double, incised by a median fissure, and notched at its tip. It is 12·3 long. The mesiobuccal root is 12·6 long. Only 4·1 of the distobuccal root is preserved.

**KNM-ER 35238: RM<sup>1</sup>** (Figure 19). This tooth has the crown and roots preserved, but is weathered and missing most of its detailed morphology. In occlusal outline, it is a rounded, transversely wide rectangle with mesial and distal sides made flatter by a pronounced concave mesial IPF and a smaller distal one. The crown is slightly broader mesially than distally. The Pr is the largest cusp, and the other three appear subequal in area. The tooth is worn, exposing circles of dentine at each cusp tip, about 2 wide on the lingual cusps and 1 wide on the buccal cusps. Evidence of the Fa is obscured by wear, and the Fp and Dmr are barely distinguishable. The crown bulges out slightly from the root on all faces. In distal view, the lingual face is the most convex. The buccal groove terminates half-way up

the crown in a cingular remnant. The lingual groove is faint, and also terminates near the crown midpoint. A 3.5 SI by 6.7 BL IPF has worn away almost the entire mesial margin of the tooth, and can be seen in occlusal view as a large, gentle concavity. A smaller IPF, 2.9 SI by 5.8 BL, flattens the distal margin of the crown. The lingual root is single and grooved along its buccal face. It is angled slightly distally, and diverges markedly lingually while the buccal roots ascend straight up from the crown in distal view. The mesiobuccal root is much shorter than the distobuccal one. The lingual root is 12.4 long, the distobuccal one 11.4 and the mesiobuccal one 9.8 long.

#### *Postcranial Fossils*

#### **KNM-ER 20419: L radius (Figure 22).**

This fossil was recovered from sediments on the northern flanks of Sibilot Hill, about 20 km northeast of the Area 261-1 excavation. It has been described by Heinrich *et al.* (1993), so is not redescribed here.

Subsequent to that publication, however, another small shaft fragment was found that articulates with the proximal portion just distal to the radial tuberosity. This fragment does not join the proximal and middle portions, but suggests that the original length of the bone was closer to the upper end of the 265–275 mm estimate given by Heinrich *et al.* (1993).

#### **Comparative morphology**

The morphology of the Kanapoi and Allia Bay hominin fossils is described here in reference to other relevant early hominins, as well as to other relevant fossil and extant hominoids. In this section, we treat *A. anamensis* as a distinct species that may have been ancestral to *A. afarensis*. The taxonomic assignment is covered further in the discussion section. Although this may eventually be proven incorrect, at present it is a plausible hypothesis that is not falsified

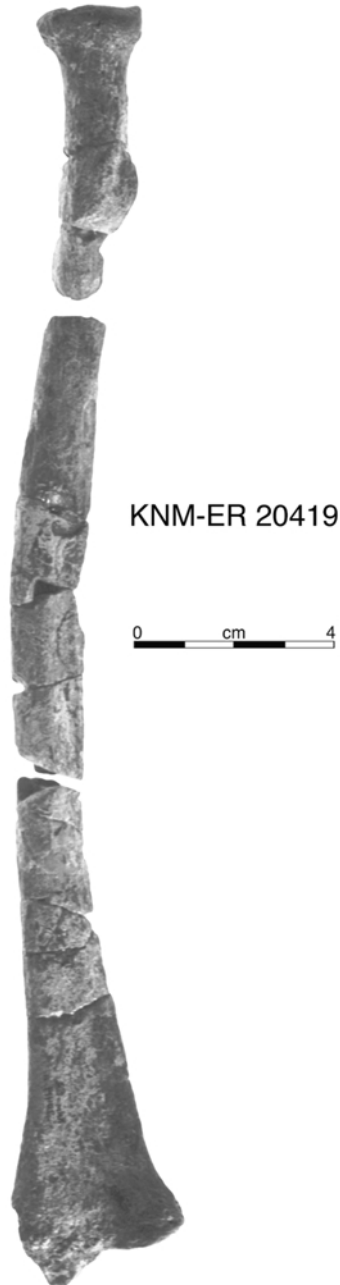


Figure 22. KNM-ER 20419, Sibilot radius showing additional fragment at the distal end of the proximal fragment.

by data, and so provides a useful comparative framework from which to compare the morphology of these taxa.

### Occipital

Although little morphology is preserved on the left occipital squame fragment (KNM-KP 34725U), a large groove for the transverse sinus is apparent. There is no confluens area remaining, so it is not possible to determine the origin of the blood that drained into the transverse sinus. The area where an occipital marginal sinus groove would be is not preserved. The enlarged transverse sinus does not necessarily imply the lack of an enlarged occipital marginal system in this individual, however. Both sinus systems are enlarged in a number of australopithecine specimens (Falk & Conroy, 1983; Falk, 1986, 1988), and at least one *A. boisei* specimen (KNM-ER 23000) has a transverse/sigmoid pattern on one side and an occipital/marginal pattern on the other (Brown *et al.*, 1993). A dominant transverse/sigmoid sinus system is the typical pattern for African apes and humans, and is likely to be the primitive hominin condition (Kimbel, 1984), but the observed variability in *Australopithecus* should underscore the need for caution when using this character for taxonomic purposes.

### Temporal

The small temporal fragment associated with the holotype mandible gives a few clues about the condition of the temporomandibular joint and the external acoustic porus. It shows that the temporal squame was well pneumatized in this adult individual. Placing the specimen in its correct orientation is difficult in the absence of whole crania of the species, but using other *Australopithecus* crania as a guide, we can make some statements with comparative certainty.

The articular eminence of *A. anamensis* is less well developed than in other *Australopithecus* and *Homo* species. In *A. robustus* and *A. boisei* the eminence develops into a strong cylinder anterior to the mandibular fossa. The KNM-KP 29281B eminence is even

less well developed than in the only cranial specimen of *A. aethiopicus*, KNM-WT 17000 (Leakey & Walker, 1988). Eminence development is somewhat variable, however, with the *A. afarensis* specimen A.L. 333-45 being flatter than other *A. afarensis* and later hominins and most closely approaching the condition seen in *A. anamensis*. The preserved portion of the temporomandibular joint represents perhaps half of the original joint surface, although this is extremely difficult to estimate. The preserved surface is situated directly inferior to the temporal squame, rather than further laterally as is seen in most robust australopithecines. It is difficult to measure the angle at which the tympanic plate meets the fossa because of problems with orientation and the fact that neither is perfectly flat. Despite this, the Kanapoi temporal gives the strong impression that the two meet at a very obtuse angle, closer to 180° than in any other hominin.

KNM-KP 29281B has a smaller external acoustic porus than any other hominin, and in this respect is more like that of great apes (Leakey *et al.*, 1995) (Table 5). Thus, *A. anamensis* retains the primitive condition. This preserved diameter of the porus is the true maximum, because the outer edge of two-thirds of the bony porus is preserved. The margin shows the characteristic rugose appearance of the edge that is seen in all complete hominoid temporal bones. The posterior wall of the porus is broken, but a thin sliver of bone remains stuck to the matrix filling the canal, which confirms that the canal itself had a small diameter.

### Maxilla

A difference between *A. anamensis* and *A. afarensis* previously cited (Leakey & Walker, 1997) was that KNM-KP 29283 had a more vertical maxillary canine root than does *A. afarensis*. The robust canine root is indeed more vertical than the majority of *A. afarensis* specimens (Leakey *et al.*, 1995),

Table 5 External auditory porous dimensions

	n	SI height			AP breadth				Area (SI × AP)				
		Mean	S.D.	Min	Max	Mean	S.D.	Min	Max	Mean	S.D.	Min	Max
<i>A. anamensis</i>	1	8.9	—	—	—	5.7	—	—	—	50.7	—	—	—
<i>A. afarensis</i>	4	10.9	1.23	9.5	12.3	10.1	1.73	6.4	11.8	101.6	34.3	60.8	139.2
<i>Pan troglodytes</i>	9	8.1	1.33	5.6	9.8	6.7	1.24	5.2	9	55.1	14.2	29.1	72.0
<i>Gorilla gorilla</i>	9	9.0	0.91	8.1	10.7	8.3	1.54	6.5	10.3	75.3	19.7	53.3	110.2
<i>Pongo pygmaeus</i>	9	7.0	1.03	4.9	8.1	6.2	1.14	4.6	7.5	43.5	10.6	27.4	56.9
<i>Homo sapiens</i>	9	10.6	1.36	7.6	12.5	7.3	0.89	5.6	8.5	77.1	13.7	57.0	89.8

Only adult *A. afarensis* specimens were used. *A. afarensis* data kindly provided by W. H. Kimbel. n=sample size, S.D.=standard deviation, Min=minimum, Max=maximum.

but is close to the orientation seen in AL 333-2, and is now known to match one unpublished specimen (W. H. Kimbel, personal communication). Still, *A. anamensis* differs from the majority of preserved *A. afarensis* maxillae in this feature.

Commensurate with the robust vertical canine roots are the large canine juga of KNM-KP 29283. These juga contribute to the rounded lateral margins of the nasal aperture, which are smooth with no lateral nasal crest (Leakey *et al.*, 1995) (Figure 23). This condition contrasts with all *A. afarensis* specimens (McCollum *et al.*, 1993), except for the single Laetoli specimen from Garusi (Kohl-Larson, 1943; Puech, 1986; Puech *et al.*, 1986; Leakey & Walker, 1995; Senut, 1999). Except for the Garusi specimen, *A. afarensis* has distinct lateral nasal crests that are structurally distinct and situated medial to the canine juga. The Garusi maxilla and *A. anamensis* share a rounded nasal aperture confluent with the canine juga with most African apes. *A. africanus* specimens, with the exception of STS 52, have rounded lateral nasal margins related to the presence of anterior pillars, but these structures are distinct from the canine juga (McCollum *et al.*, 1993). This implies that *A. afarensis* may be derived in its lateral nasal aperture contour relative to the other early australopithecine taxa.

The rest of the subnasal region of KNM-KP 29283 resembles that described

for *A. afarensis* (McCollum *et al.*, 1993), and is also similar to that found in African apes. It has a stepped nasal cavity floor with a broad incisive fossa, but damage along the midline obscures any evidence of an incisive crest on the vomer. The root of the zygomatic is partly broken away, but appears to be adjacent to M<sup>1</sup>, as in *A. afarensis*.

The *A. anamensis* palates (KNM-KP 29283, KNM-ER 30200 and KNM-ER 30745) all preserve at least parts of the midline. The postcanine tooth rows of KNM-KP 29283 were originally reported to converge slightly posteriorly (Ward *et al.*, 1999b). This specimen is weathered, however, and closer inspection reveals that the intermaxillary suture is less complete posteriorly than originally reported. This changes the measurements slightly, so that this specimen can now be reconstructed to have nearly parallel, but very slightly divergent maxillary postcanine tooth rows, falling at the narrow end of the *A. afarensis* distribution (Table 6). Palate length/breadth index (Table 6) shows that the *A. anamensis* palate is similar in length/breadth relations to that of *A. afarensis* and chimpanzees, and very similar to that of gorillas.

KNM-ER 30200 appears particularly narrow (Figure 18). In this respect, it is similar to the Garusi specimen (Puech, 1986; Puech *et al.*, 1986) which is also very narrow (Figure 23). Unfortunately, it is not possible to compare them directly because

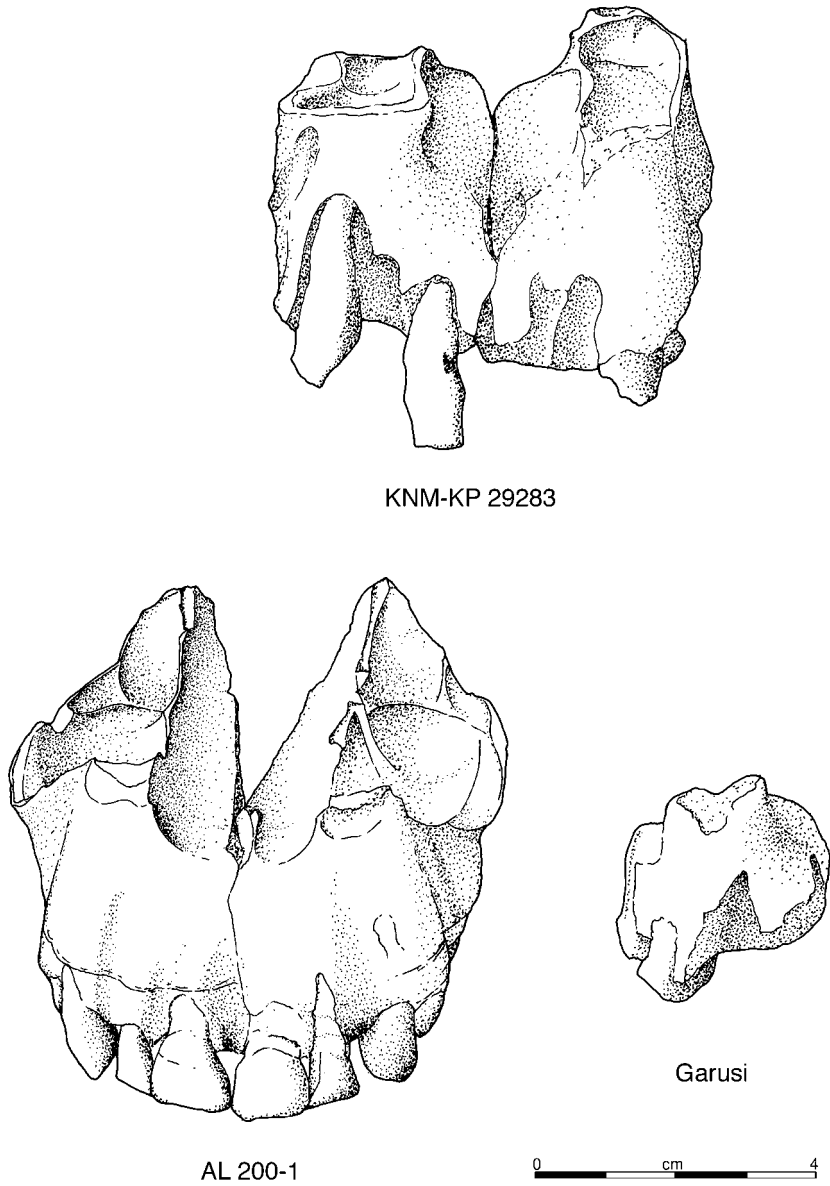


Figure 23. The KNM-KP 29283 *A. anamensis* maxilla compared with the AL 200-1 maxilla from Hadar and the Garusi maxillary fragment from Laetoli, both of which are attributed to *A. afarensis*. Both KNM-KP 29283 and Garusi have rounded lateral nasal apertures lacking crests, unlike the AL 200-1. They also have large canine juga contributing to this margin, whereas the juga are anatomically distinct from it in AL 200-1. The Garusi specimen is the only *A. afarensis* to share these features with *A. anamensis*. Garusi also appears to have very narrowly set postcanine tooth rows, like some *A. anamensis* and few other *A. afarensis* maxillas. Drawn by Susan Alta Martin.

Table 6 Palatal wedging and measurements used in its calculation

n	X: Bi-canine breadth*			Y: Bi-M2 breadth†			AP distance from X to Y lines			Palate length/breadth			XY			Palatal wedging‡												
	Mean	S.D.	Min	Max	Mean	S.D.	Min	Max	Mean	S.D.	Min	Max	Mean	S.D.	Min	Max	Mean	S.D.	Min	Max								
<i>A. anamensis</i>																												
KNM-KP 29283	34.5	—	—	—	33.7	—	—	—	33.2	—	—	—	1.02	—	—	—	1.4	—	—	—								
KNM-ER 30745	33.8	—	—	—	34.0	—	—	—	36.2	—	—	—	0.94	—	—	—	0.3	—	—	—								
<i>A. afarensis</i>	7	27.7	4.03	23.0	35.0	32.0	5.26	24.0	41.0	35.1	3.13	31.0	40.0	0.91	0.11	0.73	1.03	0.87	0.08	0.78	1.04	7.0	4.4	—	1.7	12.9		
<i>P. troglodytes</i>	24	38.1	2.20	34.6	41.8	36.1	2.10	32.8	41.1	36.9	2.60	32.8	42.2	0.98	0.08	0.80	1.12	1.06	0.06	0.94	1.16	—	3.0	3.0	—	8.7	3.8	
<i>G. gorilla</i>	24	41.1	3.57	35.9	50.8	36.0	3.34	30.1	42.9	49.9	4.52	42.6	58.0	0.72	0.09	0.59	0.98	1.15	0.07	1.02	1.31	—	5.9	2.7	—	11.2	—	0.7
<i>H. sapiens</i>	15	23.4	1.38	20.6	25.1	40.2	2.38	35.3	43.6	29.1	1.79	25.1	31.4	1.39	0.11	1.18	1.59	0.58	0.03	0.54	0.63	32.2	3.2	3.2	27.5	38.2		

\*Minimum distance between canine crowns.

†Minimum distance between M<sup>2</sup> crowns.

‡Palatal wedging calculated using formula from DiGiovanni *et al.* (1989).

Data figured in Ward *et al.* (1999b).

*A. afarensis* data kindly provided by W. H. Kimbel.

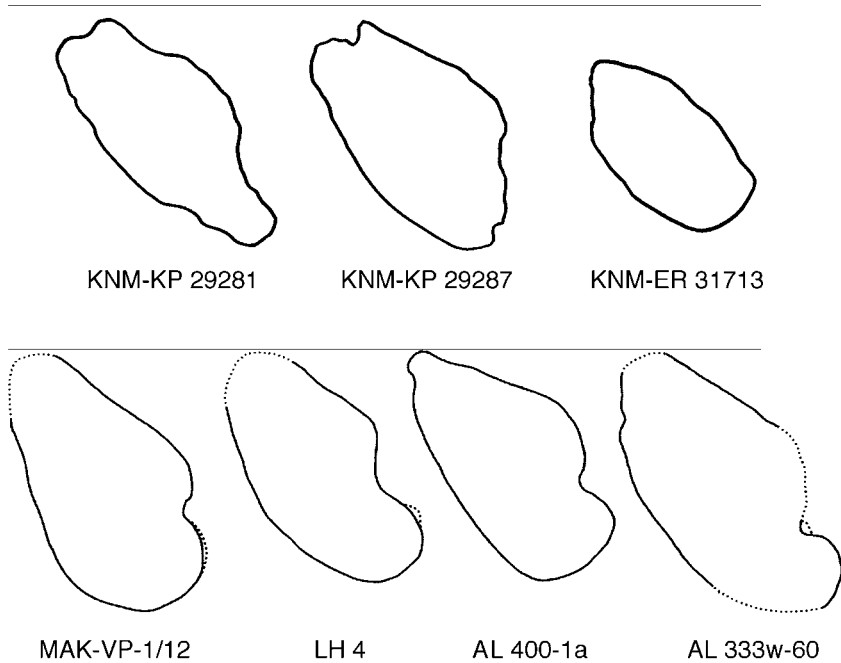


Figure 24. Symphyseal profiles of *A. anamensis* mandibles in top row, compared with those of *A. afarensis* in bottom row. Adapted from White *et al.* (2000). Note the sloping orientation of the *A. anamensis* symphises, especially the external contour basally, and the elongate anteroposterior extent of the symphises relative to their height.

they do not preserve relevant similar parts. Although it is missing anterior to  $M^2$ , KNM-ER 30200 does not appear to have had divergent tooth rows. KNM-ER 30745 is difficult to assess in this respect also because it is missing palatal bone adjacent to  $M^2$  and  $M^3$ . Its reconstruction shows some distortion in tooth orientation. Still, the overall impression it gives is of parallel post-canine tooth rows. *A. anamensis* can still be characterized as having a primitive palate shape with little postcanine tooth row divergence. The closely set, parallel mandibular tooth rows support this interpretation (see below).

#### Mandible

The mandible of *A. anamensis* is distinct from that of other hominin taxa. The mandible attributed to *A. bahrelghazali* (Brunet *et al.*, 1996) is morphologically equivalent to

those of *A. afarensis*, and at present we consider them synonymous.

Most notably, all three sufficiently preserved Kanapoi mandibles (KNM-KP 29281, 29287 and 31713) have strongly sloping symphises with strongly receding symphyseal contours, overlapping with only one other *Australopithecus* specimen, AL 198-1 (Leakey *et al.*, 1995; Ward *et al.*, 1999b) (Figure 24; Table 7). The sloping symphysis is reflected in occlusal view as a long postincisive planum extending further posteriorly than is typical for any other species of *Australopithecus* (Figure 25). The external symphyseal contour is distinctive, being convex throughout its extent. African apes and other hominids tend to become flatter in section basally, with a more abrupt basal margin. *A. anamensis* is unique among extant hominoids and fossil hominins in its smooth convexity across this contour.



**Table 7** Angle of mandibular symphysis relative to tooth row

<i>Australopithecus</i>	Specimen	Angle			
<i>A. anamensis</i>	KNM-KP 29281	141			
	KNM-KP 29287	135			
	KMN-KP 31713*	(142)			
	Mean	139			
<i>A. afarensis</i>	LH 4	107			
	AL 198-1	138			
	AL 266-1	122			
	AL 277-1	121			
	AL 288-1	100			
	AL 333-12	130			
Mean	120				
Extant taxa	Mean	S.D.	Min	Max	<i>n</i>
<i>Pan troglodytes</i>	134	6	123	149	39
<i>Gorilla gorilla</i>	137	7	123	154	37
<i>Pongo pygmaeus</i>	135	7	125	154	51
<i>Homo sapiens</i>	88	14	57	118	46

Midline symphyseal outlines were obtained by molding Coltene President putty around the symphysis. A wooden rod was placed at the alveolar margin of the symphysis and directed lingually to rest upon a second rod spanning the posterior margin of the tooth row. Data from Sherwood *et al.* (in prep).

\*KNM-KP 31713 is edentulous, so the value obtained represents an estimate.

This shape appears to be associated with the narrowly set, parallel postcanine tooth rows (Figure 25; see below). This morphology is typical of ape mandibles, but again is unmatched among other *Australopithecus* or *Homo* species, all of which have tooth rows that diverge posteriorly. This morphology reflects that suggested by the maxillary dental arcades discussed above.

The holotype mandible (KNM-KP 29281) is slightly distorted, so that its incisors and, to a lesser extent, its canines are inclined further anteriorly than they would have been originally. This may give a mistaken impression of more procumbent incisors than is accurate. Figure 26 shows a photo of the KNM-KP 29281 mandible with the incisors replaced closer to their original positions. Incisor orientation in *A. anamensis* does not appear to have differed from that of other early hominins.

The *A. anamensis* mandibles also show the narrow, parallel postcanine tooth rows evidenced in the maxillary dental arcade, which is a major difference between the masticatory apparatus of *A. anamensis* and *A. afarensis* (Figure 25). The larger I<sub>2</sub> and mandibular canine teeth (see below) of *A. anamensis* must contribute to this shape in *A. anamensis* by making the anterior tooth row mesiodistally broad relative to the position of the molar teeth, which are not expanded relative to those of *A. afarensis*.

This morphology is reflected in the external alveolar contour as well, which is distinctive in *A. anamensis* relative to other hominins. In occlusal view, the most laterally projecting portion of the alveolar process is at the canine juga. The bony contour and toothrow itself turns medially anterior to the canines, and posterior to them continues in a roughly straight line posteriorly and slightly laterally (Figure 25). The canine jugae are more laterally projecting than are the P<sub>3</sub> jugae. In contrast, East African *A. afarensis* mandibles and the specimen from Chad (Brunet *et al.*, 1996) have toothrows that turn medially at P<sub>3</sub>, with the corresponding alveolar contour curving medially anterior to the P<sub>3</sub> jugum. So, in contrast to *A. anamensis*, the P<sub>3</sub> jugae are situated lateral to the canine jugae in these other taxa. This disparity is not due simply to expanded canine roots, because even presumed female *A. anamensis* (KNM-KP 29284 and KNM-KP 31713) specimens with relatively small canines display this morphology while large, presumed male, *A. afarensis* mandibles do not.

The narrow jaws of *A. anamensis* may have influenced chewing mechanics and temporomandibular joint form and function. When tooth rows are narrow and parallel there are two main consequences. First, the amount of wishboning due to the lateral pull of the external masticatory muscles (Hylander *et al.*, 2000) is greater than if the tooth rows diverge. This is because the masticatory muscle lever arms

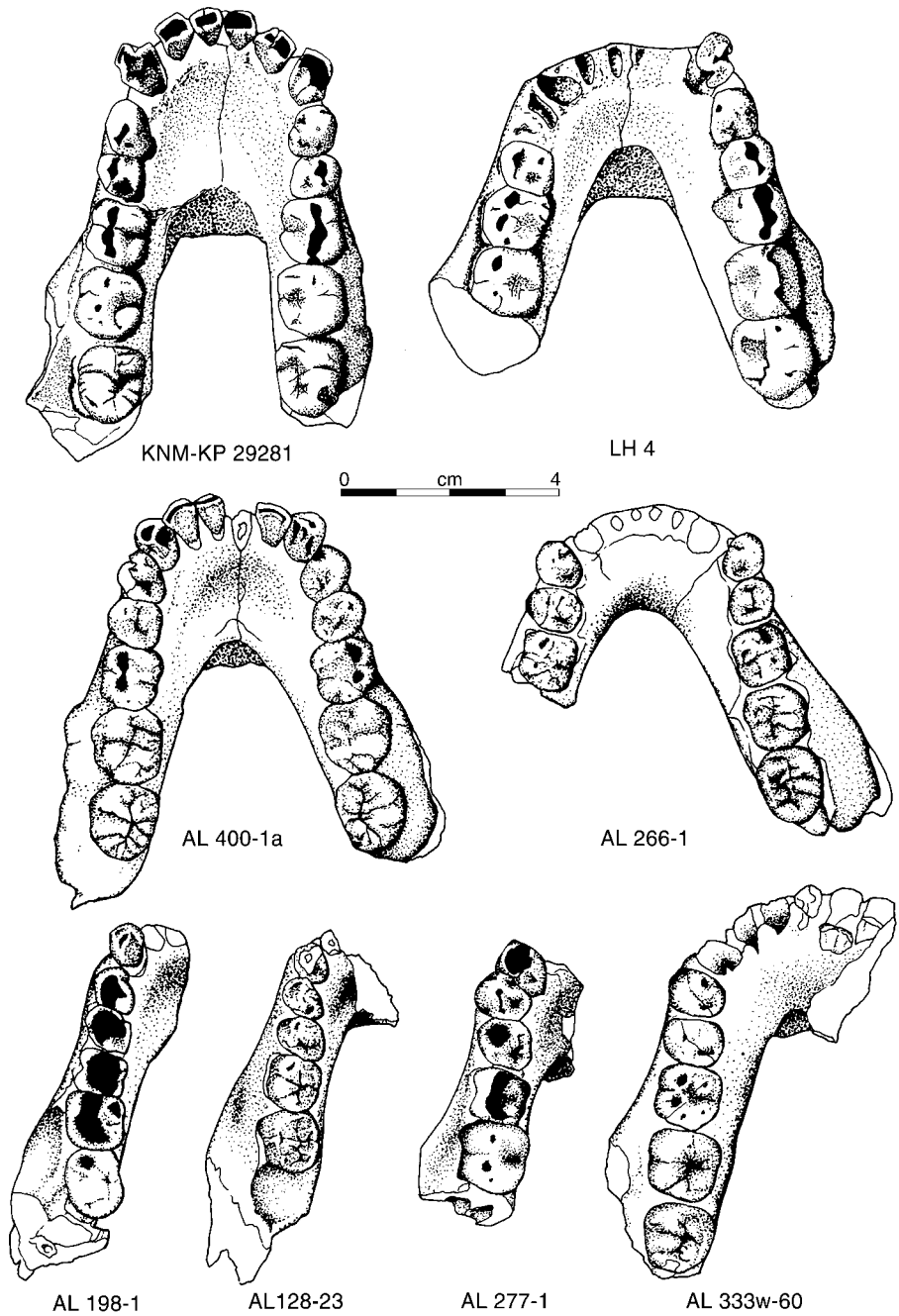


Figure 25. Occlusal views of the *A. anamensis* holotype mandible, KNM-KP 29281A, compared with the *A. afarensis* holotype, LH 4 from Laetoli, and several *A. afarensis* specimens from Hadar. The other two *A. anamensis* mandibles are not figured here because of uncertainty in reconstructing the angle of their postcanine toothrows accurately. Note the narrowly set, parallel postcanine toothrows of KNM-KP 29281 compared with the others. Also apparent in this comparison is that the broadest point across the external alveolar profile anteriorly is at the canine juga in *A. anamensis*, but always posterior to this near P<sub>3</sub> in *A. afarensis*. AL 128-23 appears close, but still does not match *A. anamensis* in this contour. This contour can also be seen in KNM-KP 29287 in Figure 6, and in KNM-KP 31713 in Figure 10. *A. anamensis* and LH4 drawn by Susan Alta Martin, Hadar specimens adapted by her from drawings by Luba Gudz featured in White & Johanson (1982).

KNM-KP 29281  
anterior tooth  
position reconstructed



Figure 26. KNM-KP 29281 with anterior teeth reconstructed in their original position. These teeth are not preserved in their original positions, but have been rotated anteriorly and inferiorly several millimeters.

decrease in length by the value  $x=1(1 - \cos \theta)$ , where  $l$ =mandibular length from center of rotation of symphysis to center of combined wishboning muscle attachment and  $\theta$  is the angle of divergence from the midline. The value  $x$  reaches about a quarter of the original length if the divergence is about  $40^\circ$ . Parallel tooth rows are found in great apes and in *A. anamensis*, and in those species this is accompanied by the addition of bone between the bodies in the form of strong posteriorly developed tori, which can best resist the greater wishboning.

Second, dorsoventral shear forces at the symphysis are due to the different forces of rotation caused by muscles from the balancing or working sides of the mandible (Walker, 1978; Hylander *et al.*, 2000). These forces are more concentrated in the sagittal plane in parallel-sided and close-together tooth rows, as is the case with

scissors. As tooth rows diverge, the shear forces at the symphysis spiral more strongly in opposite directions. The amount of bone needed to resist these forces is also greater in forms with parallel tooth rows. In all cases, however, resisting bone can be in any position away from the center of shear and not necessarily concentrated posteriorly.

The *A. anamensis* mandible is less robust in proportion than that seen in any later hominin on average (Teaford & Ungar, 2000), overlapping the *A. afarensis* and *A. africanus* distribution. This can be quantified by the breadth/height index at the level of  $M_1$ , and is close to the values typical of living and fossil apes (Figure 27; Tables 3 & 8). This may indicate that on average, *A. anamensis* mandibles tended not to be capable of resisting such high levels of transverse bending and torsion as those of later hominins (Daegling & Grine, 1991). This slight difference may be related to a trend in diet to harder or tougher foods in these later hominins than was typical for *A. anamensis* (Teaford & Ungar, 2000).

#### Permanent tooth size

External crown dimensions of *A. anamensis* teeth are generally similar to those of *A. afarensis* (Table 9). *A. anamensis* teeth are generally larger than those presently documented for *Ardipithecus ramidus*, with a few exceptions. The only dental dimensions in which *Ar. ramidus* exceeds *A. anamensis* is the upper canine MD length and BL breadth, and the  $M^2$  BL breadth. The two taxa are equivalent in  $\frac{1}{C}$  BL breadth,  $P_4$  and  $M_2$  dimensions. The greatest difference between *A. anamensis* and *A. afarensis* is that *A. anamensis* has larger lower lateral incisors (Figure 28; Table 9), mainly due to expanded MD dimensions. This almost certainly contributes to its distinctive mandibular shape. In addition, while *A. anamensis*  $P_3$ s overlap the size range of *A. afarensis* values, they are larger on average

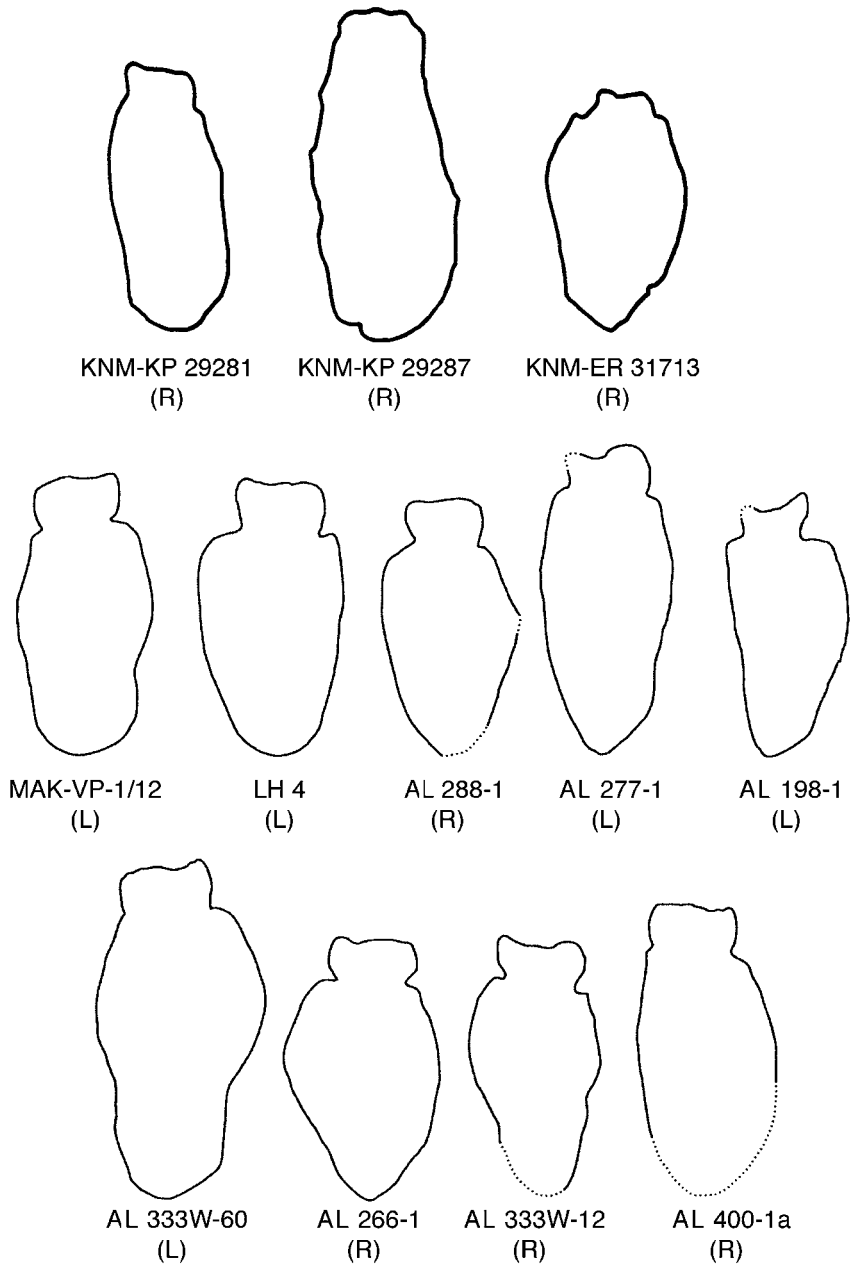


Figure 27. Mandibular corpus cross-sections at the first molar mid-crown perpendicular to the lingual alveolar margin. Adapted from [White \*et al.\* \(2000\)](#). The *A. anamensis* mandibular corpus is generally less robust on average in breadth relative to height than in *A. afarensis*, although there is overlap. Data listed in Table 8.

Table 8 Comparative mandibular corpus size and shape at M<sub>1</sub>

	Transverse breadth			Superoinferior height			Shape [(breadth/height) × 100]					
	<i>n</i>	Mean	S.D.	Max/Min × 100	<i>n</i>	Mean	S.D.	Max/Min × 100	<i>n</i>	Mean	S.D.	Max/Min × 100
<i>A. anamensis</i>	3	18.6	1.0	110.8	3	35.3	6.5	144.1	3	53.6	6.8	129.6
<i>A. afarensis</i>	12	19.0	2.2	149.4	10	32.9	3.4	135.2	10	57.8	6.3	142.4
<i>A. africanus</i>	6	21.5	2.2	125.0	4	36.1	1.7	110.6	4	59.8	5.9	121.8
<i>P. troglodytes</i>	20	14.2	1.3	132.2	20	28.8	2.7	143.8	20	49.5	5.5	158.1
<i>G. gorilla</i>	20	19.3	2.2	155.6	20	38.2	4.6	153.7	20	50.9	4.7	146.2

Comparative data from Daegling & Grine (1991) and Lockwood *et al.* (2000).  
*n* = sample size, S.D. = standard deviation, Min = minimum, Max = maximum.

Table 9 Comparative permanent tooth metrics

	Mesiodistal				Labio/Buccolingual				Crown Area (MD × BL)				Crown Shape (MD/BL)							
	n	Mean	S.D.	Min	Max	n	Mean	S.D.	Min	Max	n	Mean	S.D.	Min	Max					
Maxillary dentition																				
I <sup>1</sup>																				
Kanapoi	2	11.7	—	10.9	12.4	2	8.6	—	8.2	8.9	2	99.9	—	89.4	110.4	2	1.36	—	1.33	1.39
Allia Bay	1	10.5	—	—	—	1	9.3	—	—	—	1	97.7	—	—	—	1	1.13	—	—	—
<i>Ar. ramidus</i>	1	10.0	—	—	—	2	7.8	—	7.5	8.2	1	75.0	—	—	—	1	1.25	—	—	—
<i>A. afarensis</i>	6	10.6	0.91	9.0	11.8	8	8.4	0.71	7.1	9.7	6	89.7	13.5	63.9	101.9	6	1.26	1.10	10.80	1.40
C/																				
Kanapoi	2	11.2	—	10.6	11.7	2	10.7	—	10.2	11.2	2	119.6	—	108.1	131.0	2	1.04	—	1.04	1.04
Allia Bay	0	—	—	—	—	1	11.0	—	—	—	0	—	—	—	—	0	—	—	—	—
<i>Ar. ramidus</i>	2	11.4	—	11.2	11.5	2	11.4	—	11.1	11.7	2	129.4	—	124.3	134.5	2	1.00	—	1.01	0.98
<i>A. afarensis</i>	13	10.0	0.68	8.9	11.6	13	10.9	1.02	9.3	12.5	13	108.9	16.7	82.8	145.0	13	0.92	0.55	0.81	1.01
P <sup>3</sup>																				
Kanapoi	3	9.9	1.64	8.7	11.8	2	12.7	—	12.1	13.2	2	113.7	—	112.5	114.8	2	0.71	—	0.66	0.77
Allia Bay	1	9.9	—	—	—	1	13.0	—	—	—	1	128.7	—	—	—	1	0.76	—	—	—
<i>Ar. ramidus</i>	1	7.7	—	—	—	1	12.5	—	—	—	1	96.3	—	—	—	1	0.62	—	—	—
<i>A. afarensis</i>	9	8.7	0.53	7.5	9.3	9	12.4	0.63	11.3	13.4	9	108.1	11.2	84.8	120.9	9	0.71	0.025	0.66	0.74
P <sup>4</sup>																				
Kanapoi	3	7.7	0.46	7.2	8.1	0	—	—	—	—	0	—	—	—	—	0	—	—	—	—
Allia Bay	1	8.8	—	—	—	1	13.9	—	—	—	1	122.3	—	—	—	1	0.63	—	—	—
<i>Ar. ramidus</i>	1	8.4	—	—	—	1	11.3	—	—	—	1	94.9	—	—	—	1	0.74	—	—	—
<i>A. afarensis</i>	17	9.1	0.70	7.6	10.8	11	12.4	0.84	11.1	14.5	11	112.2	17.9	84.4	156.6	11	0.73	0.04	0.66	0.81
M <sup>1</sup>																				
Kanapoi	3	11.7	0.17	11.6	11.9	3	13.3	0.56	12.8	13.9	2	159.2	—	157.1	161.2	2	0.87	0.047	0.83	0.90
Allia Bay	5	11.4	1.24	10.0	12.9	5	12.7	0.90	11.7	14.1	4	149.0	21.8	120.5	172.0	4	0.93	0.087	0.87	1.06
<i>Ar. ramidus</i>	0	—	—	—	—	0	—	—	—	—	0	—	—	—	—	0	—	—	—	—
<i>A. afarensis</i>	15	12.1	1.03	10.5	13.8	12	13.4	0.92	12.0	15.0	11	167.8	22.4	129.6	202.5	11	0.92	0.58	0.85	1.04

Table 9 Continued

	Mesiodistal				Labio/Buccolingual				Crown Area (MD × BL)				Crown Shape (MD/BL)							
	n	Mean	S.D.	Min	Max	n	Mean	S.D.	Min	Max	n	Mean	S.D.	Min	Max					
Maxillary dentition <i>continued</i>																				
M <sup>2</sup>																				
Kanapoi	1	14.2	—	—	—	2	14.9	—	14.8	14.9	3	198.9	11.4	189.6	211.6	3	0.10	0.040	0.88	0.95
Allia Bay	4	12.9	1.45	11.4	14.8	4	13.5	0.80	12.9	14.7	3	176.0	23.5	150.5	196.8	3	0.94	0.15	0.84	1.11
<i>Ar. ramidus</i>	2	11.8	—	11.8	11.8	2	14.6	—	14.1	15.0	2	171.7	—	166.4	177.0	2	0.81	—	0.84	0.79
<i>A. afarensis</i>	10	13.0	0.62	12.1	14.1	11	14.7	0.64	13.4	15.8	10	191.0	17.0	162.1	222.8	10	0.88	0.025	0.84	0.91
M <sup>3</sup>																				
Kanapoi	5	12.0	0.82	11.1	13.0	4	14.6	0.81	13.8	15.7	3	185.0	18.3	164.5	199.4	3	0.83	0.045	0.80	0.88
Allia Bay	3	11.8	0.79	11.2	12.7	3	13.7	0.75	13.0	14.5	3	162.4	19.0	149.5	184.2	3	0.86	0.036	0.82	0.88
<i>Ar. ramidus</i>	1	10.2	—	—	—	1	12.3	—	—	—	1	125.5	—	—	—	1	0.83	—	—	—
<i>A. afarensis</i>	11	12.5	1.36	10.9	14.8	11	14.3	1.13	13.0	16.3	11	179.9	33.7	141.7	241.2	11	0.88	0.038	0.81	0.95
Mandibular dentition																				
I <sub>1</sub>																				
Kanapoi	4	6.9	0.29	6.6	7.3	3	7.8	0.64	7.3	8.5	3	54.0	7.0	49.5	62.1	0	0.90	0.045	0.86	0.95
Allia Bay	0	—	—	—	—	0	—	—	—	—	0	—	—	—	—	0	—	—	—	—
<i>Ar. ramidus</i>	1	6.0	—	—	—	0	—	—	—	—	0	—	—	—	—	0	—	—	—	—
<i>A. afarensis</i>	6	6.5	0.93	5.6	8.0	6	7.4	0.29	6.9	7.7	5	48.1	8.9	38.6	61.6	5	0.88	0.13	0.75	1.04
I <sub>2</sub>																				
Kanapoi	6	7.9	0.78	6.6	8.7	5	8.3	0.37	7.8	8.6	4	68.1	3.6	64.5	73.1	4	0.98	0.11	0.87	1.12
Allia Bay	0	—	—	—	—	0	—	—	—	—	0	—	—	—	—	0	—	—	—	—
<i>Ar. ramidus</i>	0	—	—	—	—	0	—	—	—	—	0	—	—	—	—	0	—	—	—	—
<i>A. afarensis</i>	7	6.3	0.82	5.0	7.2	7	8.0	0.72	6.7	8.8	6	49.7	7.8	41.5	59	6	0.82	0.14	0.57	0.93
C/																				
Kanapoi	6	9.8	0.92	8.7	11.0	5	10.3	0.92	9.4	11.4	5	100.9	16.3	81.8	115.4	5	0.94	0.086	0.83	1.09
Allia Bay	2	7.5	—	6.6	8.3	2	9.9	—	9.2	10.6	2	74.4	—	60.7	88.0	2	0.75	0.046	0.72	0.78
<i>Ar. ramidus</i>	0	—	—	—	—	1	10.0	—	—	—	0	—	—	—	—	0	—	—	—	—
<i>A. afarensis</i>	12	9.0	1.14	7.5	11.7	14	10.5	1.15	8.8	12.4	9	95.5	19.5	66.8	121.7	9	0.89	0.16	0.77	1.13

Table 9 Continued

	Mesiodistal					Labio/Buccolingual					Crown Area (MD × BL)					Crown Shape (MD/BL)				
	n	Mean	S.D.	Min	Max	n	Mean	S.D.	Min	Max	n	Mean	S.D.	Min	Max	n	Mean	S.D.	Min	Max
	Mandibular dentition <i>continued</i>																			
P <sub>3</sub>	7	12.1	0.70	11.3	13.4	6	8.9	0.34	8.5	9.4	6	107.4	9.7	97.2	119.3	6	1.36	0.073	1.31	1.51
	1	8.6	—	—	—	1	12.0	—	—	—	1	103.2	—	—	—	1	1.40	—	—	—
	2	7.9	—	7.5	8.2	2	10.7	—	9.9	11.5	2	84.3	—	74.2	94.3	2	0.74	—	0.76	0.71
	25	9.5	1.04	7.9	12.6	25	10.5	0.87	8.9	12.6	25	100.3	14.6	70.3	133.6	25	0.91	0.107	0.71	1.19
P <sub>4</sub>	5	9.1	0.73	8.2	9.8	7	10.7	0.76	9.8	11.7	5	99.4	14.9	80.4	111.7	5	0.83	0.020	0.81	0.86
	4	8.5	1.10	7.4	9.7	4	10.2	1.26	9.0	11.9	4	88.1	21.7	70.2	115.4	4	0.83	0.052	0.77	0.88
	2	8.2	—	7.5	8.9	2	10.7	—	9.9	11.5	2	78.8	—	71.2	86.3	2	0.85	—	0.79	0.92
	23	9.8	1.03	7.7	11.4	20	11.0	0.77	9.8	12.8	20	107.6	16.7	77.0	134.5	20	0.89	0.076	0.74	1.01
M <sub>1</sub>	10	12.8	0.78	11.5	13.8	10	12.0	0.98	10.5	13.5	10	152.7	24.1	105.0	180.8	10	1.06	0.046	0.99	1.15
	2	11.8	—	11.6	11.9	2	10.6	—	10.2	10.9	1	129.7	—	—	—	1	1.09	—	—	—
	2	11.1	—	11.0	11.1	2	10.3	—	10.2	10.3	2	113.3	—	113.2	113.3	2	1.08	—	1.08	1.08
	27	13.0	0.96	10.1	14.8	21	12.3	0.77	11.0	14.8	21	165.7	18.5	124.3	197.1	21	1.05	0.042	0.97	1.13
M <sub>2</sub>	8	14.3	10.40	13.0	15.9	9	13.7	0.86	12.6	15.1	6	200.8	29.4	12.6	238.6	6	1.05	0.063	0.93	1.10
	1	11.6	—	—	—	2	11.3	—	10.2	12.3	1	118.3	—	—	—	1	1.14	—	—	—
	1	13.0	—	—	—	1	11.9	—	—	—	1	154.7	—	—	—	1	1.09	—	—	—
	30	14.3	1.23	12.1	16.5	26	13.4	1.00	11.1	15.2	26	190.0	27.1	137.6	234.1	26	1.06	0.062	0.93	1.18
M <sub>3</sub>	6	14.6	1.19	13.7	17.0	6	12.8	0.66	11.9	13.4	7	182.1	26.6	153.2	227.8	7	1.1	0.15	0.80	1.27
	1	15.7	—	—	—	1	13.7	—	—	—	1	215.1	—	—	—	1	1.15	—	—	—
	1	12.7	—	—	—	1	11.0	—	—	—	1	139.7	—	—	—	1	1.15	—	—	—
	22	15.1	1.18	13.4	17.4	19	13.4	0.99	11.3	15.3	18	199.0	27.0	151.4	266.2	18	1.13	0.062	0.99	1.21



Lower lateral incisor dimensions

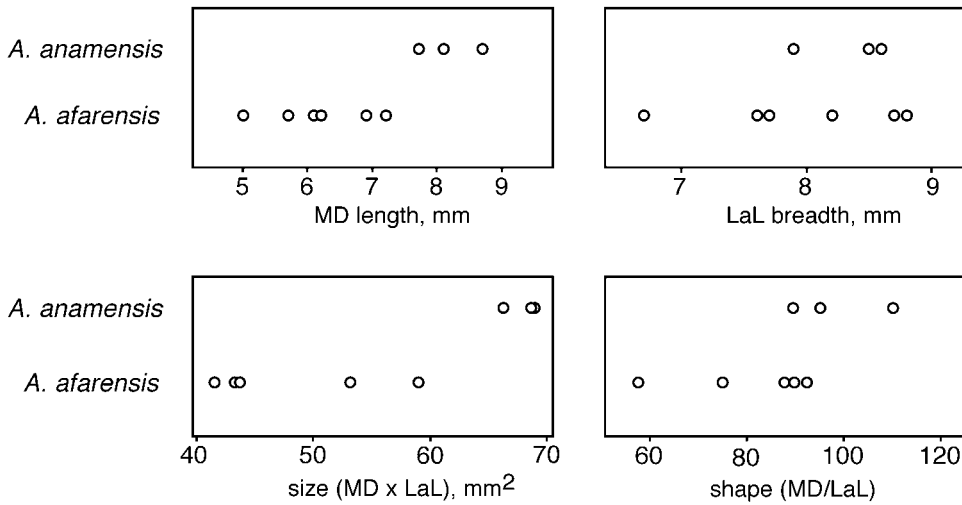


Figure 28. Category scatterplots of lower lateral incisor dimensions in *A. anamensis* and *A. afarensis*. Points represent individual specimens. Data listed in Table 9. *A. anamensis* LI<sub>2</sub>s are broader mesiodistally, although they overlap in labiolingual thickness. This makes them more elongate in occlusal profile than those of *A. afarensis*. It also makes them larger on average in occlusal area, although the distributions overlap in this dimension.

than those of *A. afarensis*. This is mainly because they are more MD elongate. Finally, *A. anamensis* has a more mesio-distally elongate C/ crown than does *A. afarensis*.

The preserved *A. anamensis* canine crowns and roots are similar in absolute size to those in the *A. afarensis* sample, with similar size ranges represented (Table 9; Ward *et al.*, 1999b). These tooth crown and root data seem to suggest that there was a similar amount of canine size dimorphism in *A. anamensis* and *A. afarensis*. The large canine alveolus of KNM-KP 29286, however, exceeds the size that would fit even the largest preserved *A. anamensis* canine root (Ward *et al.*, 1999b). Because in extant African apes and humans canine root dimensions are tightly correlated with crown dimensions (Pearson's  $r^2=0.9931$ ,  $P<0.001$ ,  $n=60$ ), it is reasonable to assume that lower canine crown size dimorphism

exceeded anything we are able to measure directly in *A. anamensis*.

Although they are broadly similar in absolute size of preserved canine crowns and roots, when canine size is considered relative to the size of the postcanine dentition within individuals, it is apparent that *A. anamensis* has relatively larger canines than does *A. afarensis* (Ward *et al.*, 1999b; Table 10). This seems to be supported by KNM-KP 31713, the edentulous mandible. Even though it appears to have been from a female, this specimen also has a large partial canine root preserved (Figure 10). It does not appear larger in dimensions than that of KNM-KP 29281, however, so apparently would not affect estimates of overall canine size range in *A. anamensis*. The presence of relatively larger canine teeth in *A. anamensis*, and perhaps a greater degree of canine size dimorphism, is more primitive than found in later hominins.

**Table 10** Mandibular canine crown area relative to crown areas of associated postcanine teeth

Taxon	Specimen no.	C/P <sub>3</sub>	C/P <sub>4</sub>	C/M <sub>1</sub>	C/M <sub>2</sub>	C/M <sub>3</sub>
<i>A. anamensis</i>	KNM-KP 29281	0.82	1.00	0.55	0.48	0.48
	KNM-KP 29284	1.08	—	—	—	—
	KNM-KP 29286	0.99	1.04	0.79	0.57	0.61
	Mean	0.96	1.02	0.67	0.53	0.55
<i>A. afarensis</i>	AL 128-23	0.85	0.87	0.54	0.44	—
	AL 198-1	0.88	0.90	—	0.51	0.44
	AL 333w-58	1.20	—	—	—	—
	AL 400-1a	0.70	0.68	0.46	0.36	0.37
	LH 3	0.71	0.74	0.67	—	—
	LH 14	0.85	0.75	—	—	—
	Mean	0.87	0.79	0.56	0.44	0.41

Ratios are of crown areas calculated as MD × BL.

Measurements represent average of right and left sides when both were available.

*A. afarensis* data kindly provided by W. H. Kimbel.

Data figured in Ward *et al.* (1999b).

#### *Deciduous dentition*

The deciduous teeth of *A. anamensis* are also similar in size to those of *A. afarensis* (Table 11). The most notable feature of the *A. anamensis* deciduous dentition is the narrow dm<sub>1</sub> (KNM-KP 34725). The specimen is worn, but displays a poorly differentiated Fp (Leakey *et al.*, 1998). This tooth is more similar in shape to that of *Ar. ramidus* and the African apes, lacking the BL expansion typical of all other hominins. It is almost as long MD as the longest *A. afarensis* tooth, but narrower BL than the smallest. The KNM-KP 34725 dm<sub>1</sub> is more similar to those of *A. afarensis* in overall size, however (Table 12).

#### *Crown heights*

Crown heights of the incisors and canines appear equivalent in *A. anamensis* and *A. afarensis*, although this is difficult to quantify due to wear on most specimens. In contrast, *A. anamensis* molars are lower-crowned than those of *A. afarensis* (Leakey *et al.*, 1995; Hlusko, 1998). Their mandibular molars have more sloping lingual faces and the maxillary molars more sloping buccal faces (Leakey *et al.*, 1995). This

appears to be due to a superobuccal expansion of the protoconid on the *A. anamensis* mandibular molars (Hlusko, 1998), and presumably a complementary apical expansion of the maxillary molars. The resulting differences in crown height may have functional implications, supporting interpretations of selection for altered tooth use, and presumably diet, in *A. afarensis* as compared with *A. anamensis*.

The discrepancy between incisor and molar tooth crown heights, combined with what appear to be slightly larger canine teeth on average in *A. anamensis*, suggest that the discrepancy between the level of the incisal and postcanine occlusal wear planes may have been slightly greater in *A. anamensis* than *A. afarensis*.

#### *Canine/premolar complex*

The maxillary canine of *A. anamensis* is unique in form, with strong basal tubercles found both mesially and distally. KNM-KP 35839, the only unworn upper canine of *A. anamensis*, has its mesial and distal basal tubercles at nearly the same distance from crown tip, sitting immediately adjacent to the cervical margin. Both *A. afarensis* and

Table 11 Comparative deciduous tooth metrics

	Mesiodistal				Labio/buccolingual				Crown size (MD × BL)				Crown shape (MD/BL)			
	n	Mean	Min	Max	n	Mean	Min	Max	n	Mean	Min	Max	n	Mean	Min	Max
di <sup>2</sup>																
<i>A. anamensis</i>	1	4.5	—	—	1	4.0	—	—	1	18.0	—	—	1	1.1	—	—
<i>A. afarensis</i>	—	—	—	—	—	—	—	—	—	—	—	—	—	—	—	—
d <sub>c</sub>																
<i>A. anamensis</i>	2	6.8	6.7	6.8	2	5.6	5.5	5.6	2	37.5	36.9	38.1	2	1.22	1.22	1.21
<i>A. afarensis</i>	2	6.6	6.5	6.6	2	5.8	5.8	5.8	2	38.0	37.7	38.3	2	1.13	1.12	1.14
dm <sub>1</sub>																
<i>A. anamensis</i>	1	9.3	—	—	1	6.7	—	—	1	62.3	—	—	1	1.39	—	—
<i>A. afarensis</i>	3	9.1	8.5	9.5	3	7.9	7.7	8.0	3	71.8	68.0	75.1	3	1.16	1.06	1.22
dm <sub>2</sub>																
<i>A. anamensis</i>	2	9.9	9.7	10.0	2	7.9	7.9	7.9	2	77.8	76.6	79.0	2	1.25	1.23	1.27
<i>A. afarensis</i>	2	11.7	11.6	11.7	2	9.6	9.4	9.7	2	111.3	109.0	113.5	2	1.22	1.23	1.21

n=sample size, Min=minimum, Max=maximum.

Table 12 Lower first deciduous molar metrics

	<i>n</i>	Mesiodistal length				Buccolingual breadth				Crown area (MD × BL)				Crown shape (MD/BL)			
		Mean	S.D.	Min	Max	Mean	S.D.	Min	Max	Mean	S.D.	Min	Max	Mean	S.D.	Min	Max
<i>A. anamensis</i>	1	9.3	—	—	—	6.7	—	—	—	62.3	—	—	—	1.39	—	—	—
KNM-KP 34725	1	7.3	—	—	—	4.9	—	—	—	35.8	—	—	—	1.49	—	—	—
<i>A. ramidus</i>																	
ARA-VP-1/129																	
<i>A. afarensis</i>	4	9.2	0.50	8.5	10	7.9	0.40	7.6	8.4	72.5	5.70	68.0	80.6	1.16	0.07	1.06	1.22
<i>A. africanus</i>	5-7	8.8	0.20	8.4	9	7.6	0.40	7.1	8.1	66.6	5.50	59.6	73.7	1.16	0.02	1.12	1.18
<i>P. paniscus</i>	21	7.4	0.56	6.3	9	5.1	0.31	4.4	5.5	37.6	4.74	27.7	48.4	1.46	0.08	1.35	1.60
<i>P. troglodytes</i>	29	8.1	0.57	7.0	9	5.2	0.35	4.6	5.8	42.2	5.19	32.9	54.5	1.58	0.10	1.42	1.83
<i>G. gorilla</i>	20	11.0	0.69	9.8	12	7.5	0.55	6.7	8.9	82.3	10.71	71.4	108.6	1.48	0.08	1.32	1.63
<i>P. pygmaeus</i>	6	9.2	0.67	8.4	10	7.1	0.61	6.4	8.1	66.2	10.31	53.8	82.6	1.30	0.04	1.24	1.36
<i>H. sapiens</i>	21	8.4	0.47	7.4	9	7.2	0.41	6.4	8.1	60.4	6.09	47.4	69.9	1.18	0.06	1.06	1.30

Comparative data kindly provided by T. D. White.

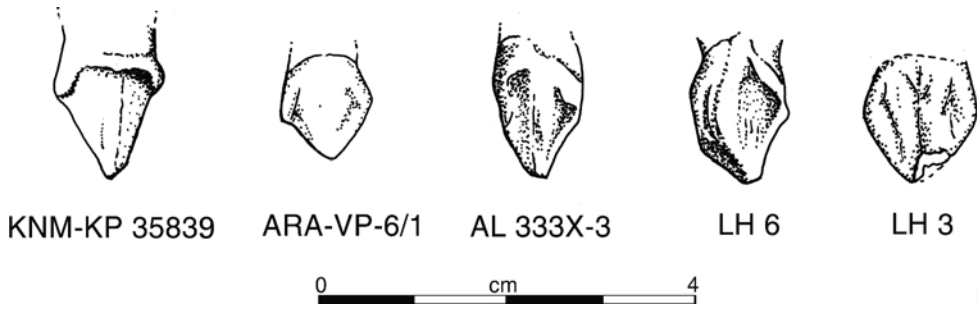


Figure 29. Upper canines of *A. anamensis* (KNM-KP 35839), *A. ramidus* (ARA-VP-6/1) and *A. afarensis* (AL 333x-3, LH 6 and LH 3) compared in lingual view. *A. anamensis* is unique in having two low but strong lingual and distal basal tubercles, and a symmetrical profile. Adapted from White *et al.* (1994) by Susan Alta Martin.

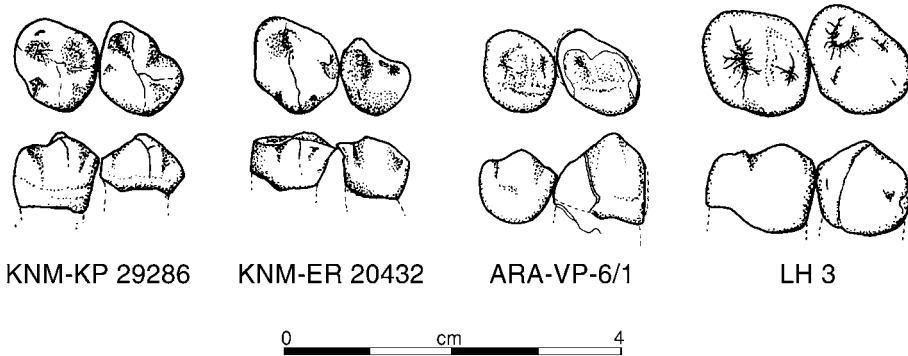


Figure 30. Lower  $P_3$  and  $P_4$  of *A. anamensis* (KNM-KP 29286 and KNM-ER 20432), compared with those of *A. ramidus* (ARA-VP-6/1) and *A. afarensis* (LH 3). *A. anamensis* resembles *A. ramidus* in having unicuspid  $P_3$ s and  $P_4$ s with less expanded talonids than *A. afarensis*. Adapted from White *et al.* (1994) by Susan Alta Martin.

*Ar. ramidus* (White *et al.*, 1994) tend to have crown shoulders that are placed further apically, and that are not in the form of distinct tubercles (Figure 29). KNM-KP 35839 also has less distinct apical crests than does *Ar. ramidus*, especially mesially. It is more symmetrical in lingual or labial view than the Hadar canines, and matched most closely by the mostly unworn canines LH 3 and 6 in symmetry. At Hadar, the mesial tubercle and marginal ridge are further inferiorly along the crown towards the apex than are the distal ones. LH 3 and 6 are similarly symmetrical, however no published *A. afarensis* specimen displays the strong basal tubercles seen in KNM-KP 35839

(White *et al.*, 1994), nor as distinct a basal tubercle or ridge lingually. Metrically, the maxillary canine tooth of *A. anamensis* is MD elongated relative to those of *A. afarensis* (Table 9), perhaps reflecting the pronounced basal tubercles (Figure 29).

Mandibular canines of *A. anamensis* are similar to those of other early hominins in form, but are MD narrower and more blade-like in shape. Their distal slope is concave in lingual or labial view, terminating in a strong basal tubercle (Ward *et al.*, 1999b). The most similar *A. afarensis* specimens are LH 2 and 3, but even these have distal slopes that are convex towards the cusp apex

Table 13 Nonmetric crown features (following Wood &amp; Abbot, 1983, and Wood, 1991)

Specimen	Maxillary dentition			Mandibular dentition			C7	Protostylid
	Caribelli	crista obliqua	Specimen	Fissure pattern	C6	C7		
M <sup>1</sup>								
KNM-ER 20427	1	2	M <sub>1</sub>	+	0	0	0	2,3,4
KNM-ER 30200	1	2	KNM-ER 20422	Y	0	0	0	4
KNM-ER 30745	1,2	2	KNM-ER 35232	Worn	Worn	Worn	Worn	
KNM-ER 35238	2,3 (Worn)	—	KNM-KP 29281	Worn	0	0	0	2
KNM-KP 30498R	2	2	KNM-KP 29286L	Y	0	0	0	2
			KNM-KP 29286R	Worn	1	0	0	2
M <sup>2</sup>			KNM-KP 29287L	—	1	—	—	1
KNM-ER 7727	?0	1 (Worn)	KNM-KP 29287R	Worn	—	0	0	3
KNM-ER 20420	Worn	Worn	KNM-KP 30500L	Worn	—	0	0	3
KNM-ER 30200	1	2	KNM-KP 30500R	Worn	—	0	0	3
KNM-ER 30745	1,2	—	KNM-KP 31712L	Too wrinkled	0	0	0	3
KNM-ER 35235	Worn	Worn	KNM-KP 31712R	Too wrinkled	0	0	0	3
KNM-KP 34725	2,3	Too wrinkled	KNM-KP 31728	Y	0	0	0	—
M <sup>1</sup> or M <sup>2</sup>			KNM-KP 34725	Y	0	0	0	3
KNM-ER 35231	1	3	KNM-KP 37522	2	Broken			
KNM-KP 35842	1,2	2	M <sub>2</sub>					
M <sup>3</sup>			KNM-ER 20423	Y	(1)	0	0	3
KNM-ER 20421	0	0	KNM-ER 35233	Y	1	1	1	4
KNM-ER 30200	2	2	KNM-KP 29281L	—	1	0	0	0
KNM-ER 30745	1,2	2	KNM-KP 29281R	—	1	0	0	3
KNM-ER 35236	2,3	2	KNM-KP 29286L	Y	1	0	0	3
KNM-KP 30498R	2	Too wrinkled	KNM-KP 29286R	X	(1)	0	0	2
KNM-KP 31717	2	Too wrinkled	KNM-KP 29287L	Y	1	0	0	2
KNM-KP 35840	2	2	KNM-KP 29287R	Y	1	0	0	3

Table 13 Continued

Specimen	Maxillary dentition		Specimen	Mandibular dentition				Protostylid
	Caribelli	crista obliqua		Fissure pattern	C6	C7	C7	
?M KNM-ER 20748			KNM-KP 30500L	Too wrinkled	0	0	0	3
			KNM-KP 30500R	Too wrinkled	0	0	0	3
			KNM-KP 34725	Too wrinkled	1	0	0	3,4
			KNM-KP 35847	Y	—	—	—	—
			M <sub>1</sub> or M <sub>2</sub>					
			KNM-KP 29282	Worn	Worn	Worn	Worn	
			M <sub>3</sub>					
			KNM-ER 20428	X	1 (worn)	0	0	1,4
			KNM-KP 29281L	X	1	0	0	4
			KNM-KP 29281R	X	1	0	0	3
			KNM-KP 29286L	Y	1	0	0	3
			KNM-KP 29286R	Y	1	0	0	3
			KNM-KP 29287L	—	Too wrinkled	—	—	3
			KNM-KP 29287R	Too wrinkled	Damaged	0	0	2
		KNM-KP 30500L	Too wrinkled	0	0	0	3	
		KNM-KP 30500R	Too wrinkled	0	0	0	3	
		KNM-KP 30502L	Y	1	1	1	3	
		KNM-KP 30502R	Y	0	0	1	3	
		KNM-KP 31717	Too wrinkled	Worn	Broken	Broken	2	
		KNM-KP 35838	Broken	0	Broken	Broken	Broken	

All occlusal nonmetric scoring system described by Wood & Abbot (1983) and Wood (1991).  
 Caribelli scoring system: 0=absent; 1=pit or groove at mesiolingual corner; 2=grooves or ridges running from lingual groove to mesiolingual corner; 3=definite shelf of enamel related to protocone.

Crista obliqua scoring system: 1=present and continuous; 2=present but interrupted; 3=absent.

C6 & C7 scoring system: 0=absent; 1=present.

Protostylid scoring system: 0=absent; 1=shape and branching pattern of the mesiobuccal groove suggestive of protostylid formation; 2=small shelf of enamel below a distinct branch off the mesiobuccal groove; 3=long and well-developed enamel shelf; 4=vertical grooves and ridges on the mesiobuccal surface of the protoconid.

with broader crowns superior to the basal tubercles.

The premolars reflect this difference in canine/premolar complex development (Ward *et al.*, 1999b) (Figure 30). The *A. anamensis* third premolars all are more unicuspid than that of any *A. afarensis*, with the metaconid existing only as a tiny tubercle on the transverse crest. The protoconid sits in the middle of the occlusal surface and is high and sharp. In all *A. afarensis* P<sub>3</sub>s, the metaconid is relatively more developed in height where preserved and in occlusal area. The *A. anamensis* P<sub>3</sub> anterior fovea opens lingually, as the thin mesial marginal ridge tends to have a notch along the mesiolingual edge of the tooth. This morphology, seen at both at Kanapoi and Allia Bay, is most closely matched in ways by AL 128-23 and LH 3, but even these specimens are not as unicuspid as the *A. anamensis* P<sub>3</sub>s.

The P<sub>4</sub>s of *A. anamensis* tend to have less expanded posterior foveas than do those of *A. afarensis*, although there is more overlap in these teeth than in the P<sub>3</sub>s. The Chad specimen (Brunet *et al.*, 1995, 1996) has much more expanded premolar posterior foveae than does *A. anamensis* and even many *A. afarensis* specimens.

The maxillary premolars of *A. anamensis* are similar in morphology to those of *A. afarensis*. The P<sub>3</sub>s exhibit a similarly distinctive mesiocervical enamel extension on the buccal face of the crown, which appears to be plesiomorphic for hominins.

#### *Occlusal molar morphology*

*Australopithecus anamensis* specimens have a similar pattern of molar cusp size as seen in *A. afarensis* specimens. The protocone tends to be the largest cusp on the upper molars, and either the protoconid or metaconid on the lower ones. There is variation in fissure patterns (Table 13) within the *A. anamensis* sample for two reasons. First, most unworn molars show extensive secondary fissures, obscuring interpretation of cusp margins

and primary groove patterns. Second, cusp contact is generally fairly close, so although that X, Y and + patterns (Wood, 1991) are seen, many teeth coded as X or Y are, in fact, very close to the + pattern. Variability in fissure pattern reinforces the need to be cautious when using such features for taxonomic purposes, at least for this taxon.

#### *Protostylid/Carabelli's features*

All but one of the 25 sufficiently well-preserved *A. anamensis* individuals display some form of cingular remnant features on their molars, visible as Carabelli's features on the maxillary teeth and protostylid complexes on the mandibular ones (Table 13) (see also Hlusko & Mahaney, 2000). These features are usually in the form of ridges, although they generally do not reach the level of the occlusal surfaces. Almost all mandibular molars and the Kanapoi maxillary molars have a cuspule or ridge. There is no clear distinction between the Kanapoi and Allia Bay samples in cusp detail, but in general the Allia Bay teeth show less pronounced features, with KNM-ER 30200, 30745 and 35231 showing only pits on the sides of the teeth. The only individual in the *A. anamensis* sample that lacks any evidence of a cingular feature is KNM-ER 20421, an isolated M<sup>3</sup>. The significance of the latter for appreciating the near ubiquity of at least some types of these features is lessened by the fact that third molars are variable, and in two associated dentitions from Kanapoi when features are present on M<sup>1</sup> or M<sup>2</sup>, they are missing on M<sup>3</sup> (KNM-KP 29283 and 30498).

The presence of Carabelli's and protostylid features is common in *A. afarensis*, but is found only on about half of the molars, and then rarely expressed as more than pits or mild ridges (White *et al.*, 1981). *A. africanus* teeth from Sterkfontein and particularly Makapansgat have particularly large cingular features (White *et al.*, 1981),



often larger than those typical for *A. anamensis*. White *et al.* (1981) suggested that the cingular remnants in *A. africanus* may not be primitive, but instead may be a by-product of crown expansion. The near ubiquity of cingular features in *A. anamensis* teeth suggests that if these features have any phylogenetic signal, *A. afarensis* represents a more derived condition. Extra enamel on the lingual sides of mandibular, and buccal sides of maxillary, molars may slightly slow wear on these low-crowned teeth when much of the enamel is gone.

#### *Tooth wear*

*Australopithecus anamensis* teeth exhibit a distinctive pattern of wear. Evident in older individuals, the anterior teeth are worn very heavily, much more so than the molars and premolars. The KNM-KP 29281 anterior teeth are heavily worn, with nearly half of the incisor and canine crowns obliterated but only about 1 mm-wide area of dentine exposed on  $M_2$  and none on  $M_3$ . A similar pattern is also seen on the KNM-KP 29283 maxilla, which has the crowns almost completely obliterated on the incisors and canine, but more than half of the occlusal enamel remains on  $M^2$  and  $M^3$ . The other two mandibles and the associated dentitions do not show much tooth wear at all, and so were presumably from much younger individuals. Where significant amounts of dentine are exposed on the postcanine teeth, they tend to be deeply hollowed, suggesting fairly intense molar tooth use.

All worn canines display apical wear combined with wear along their distal slopes. This is similar to the condition found in *A. afarensis* (White *et al.*, 1981), although the canine is slightly larger on average in *A. anamensis*. Although no mandible preserves these relationships well, the morphology of KNM-KP 28291 suggests that the canine tip was approximately level with or slightly above the incisor occlusal margins, and so was a continuation of this

functional wear surface as in *A. afarensis* (White *et al.*, 2000).

The *A. anamensis* molars also show a strong buccal/lingual wear discrepancy, also found in *A. afarensis* and other hominins (White *et al.*, 1981). On the mandibular molars, the buccal cusps both expose dentine before the lingual ones, and the reverse on maxillary molars. The uneven wear does not seem to be due to unequal molar cusp height, because on unworn specimens the lingual and buccal cusps are subequal in height. This wear discrepancy is also seen on *A. anamensis* premolars, especially on KNM-KP 29283 which has the  $P^3$  worn almost to its root lingually, but preserves almost 6 mm of enamel from the cervical margin buccally. The  $P^4$  is also worn unevenly.

The only worn upper lateral incisors are associated with the maxilla KNM-KP 29283. These crowns are heavily worn with worn faces oriented labially and distally, presumably from contact with the lower canine. Although these teeth have unusually mesiodistally narrow roots, their wear pattern demonstrates that they are, indeed, maxillary incisors. This pattern is accentuated by the very worn state of the entire dentition. This pattern is not evident on any *A. afarensis* incisors.

#### *Enamel thickness*

M. C. Dean is currently investigating enamel thickness and structure in *A. anamensis*. The following discussion and micrographs were kindly provided by him (Figure 31).

Enamel thickness is notoriously difficult to quantify. Enamel thickness increases distally through the tooth row and also varies among the cusps of molars. Beynon & Wood (1986) and Grine & Martin (1988) have previously published both linear measurements of enamel thickness, as well as relative or average values of enamel thickness, where there has been an attempt to

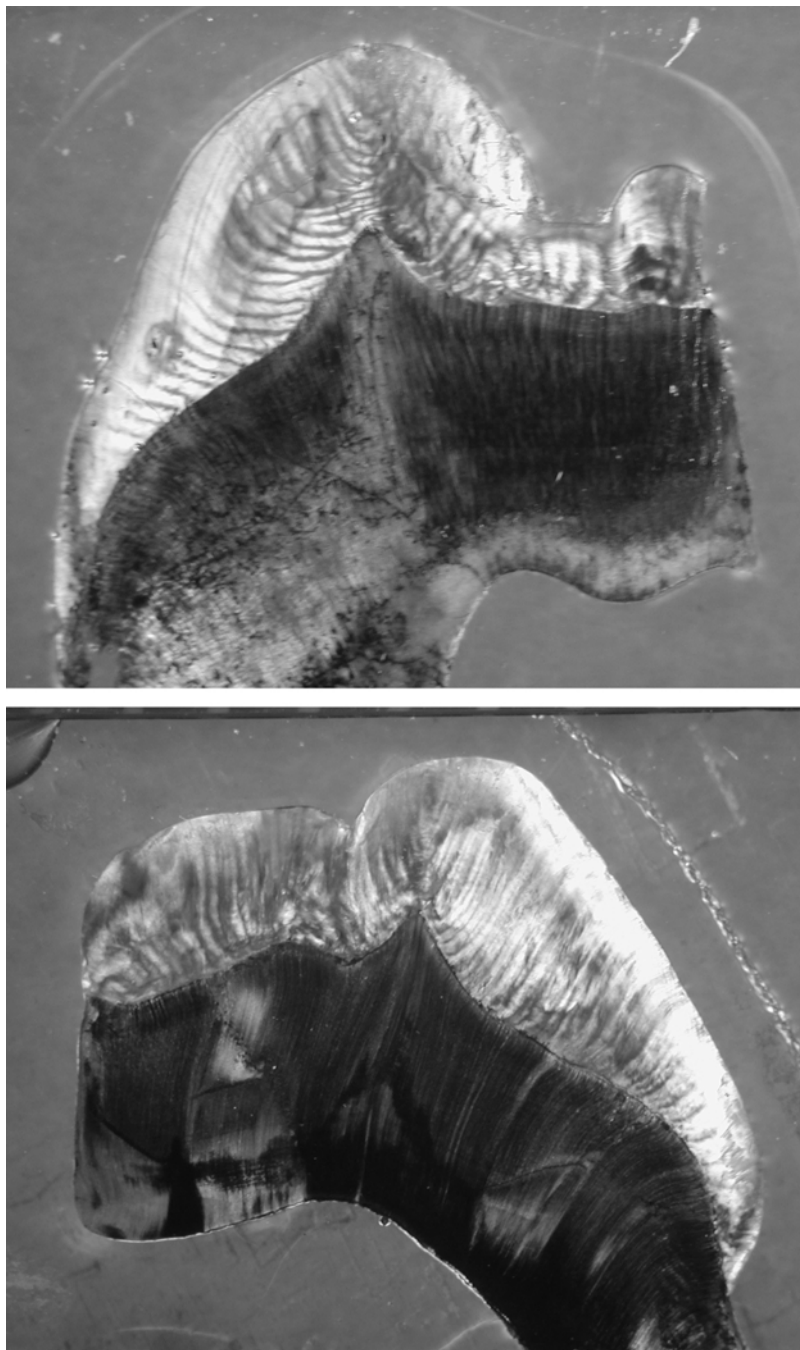


Figure 31. KNM-ER 30748 above and KNM-ER 30749 below, sectioned through the protocone and hypoconid respectively. Both display relatively thick enamel. Metric data are given in text. Photographs kindly provided by M. C. Dean, who is undertaking a more complete study of enamel structure in *A. anamensis*.

scale for tooth size, in certain fossil hominin and modern hominid molar teeth. More recently, Schwartz (2000) has also published a comprehensive data set of linear measurements of enamel thickness made from sections through the mesial cusps of modern human and great ape molar teeth. These measurements were also scaled using the linear distance between the BL cemento-enamel junctions (CEJ). Unfortunately, it is difficult to scale enamel thickness measurements on tooth fragments where neither the complete dentine cap nor the BL CEJ diameter is preserved. Quantifying enamel thickness in the *A. anamensis* sample is difficult, as many specimens with breaks exposing enamel sections are in non-standard orientations and not through cusp tips, or are worn, obscuring accurate measurements of enamel thickness.

Enamel structure of two *A. anamensis* molar tooth fragments naturally fractured close to the axial plane of one cusp were examined by M. C. Dean (Figure 31). KNM-ER 30748 is a maxillary molar fractured through the axial Pr, and KNM-ER 30749 is a mandibular molar, fractured through the Hyd. As part of a more extensive study on the microstructure of fossil hominin enamel, each fractured surface was polished until the dentine horn lay in the surface plane and a 100  $\mu\text{m}$ -thick section cut from the face. Linear measurements that correspond to those defined by Beynon & Wood (1986) and Schwartz (2000) were made to the nearest 0.1 from photomontages of the thin sections with spreading calipers.

For the Pr, linear measurements “lingual occlusal basin” (LOB)=1.9, “linear cusp tip” (LCT)=1.9, and “lingual cervical wall” (LCW)=2.1. For the Hyd, linear measurements equivalent to “buccal occlusal basin” (BOB)=1.6, “buccal cusp tip” (BCT)=1.0 and “buccal cervical wall” (BCW)=1.8. (The measurement LCT of the Pr includes 0.1 to compensate for estimated wear of this

cusps.) These linear measurements of enamel thickness are, on average, less than those reported for robust *Australopithecus* by Grine & Martin (1988, Table 1.15, p. 30). Their measurements ranged broadly between 2.0 and 3.5. The closest match of measurements made on the *A. anamensis* fragments is with those made by Grine & Martin on Stw 402, attributed to *A. africanus*. It seems clear that molar enamel was thick in *A. anamensis*, but not absolutely as thick as in robust *Australopithecus*.

Much has been made of the proportions of cuspal and lateral molar enamel in *Australopithecus*. In the *A. anamensis* Pr there were approximately 400 daily enamel cross striations between the dentine horn and the surface. The lateral enamel contained 61 striae with a periodicity of 7 days each. Thus, the time to form lateral and cuspal enamel was almost equal in this cusp. Likewise in the Hyd, there were approximately 400 days of cuspal enamel formation and 84 striae with a periodicity of 7 days (588 days) in the lateral enamel. Neither of these molar cusps is likely to have included both the start and end of enamel formation but total enamel formation times were 2.28 years in the Pr and 2.72 years in the Hyd. The greater time for cusp formation in the KNM-KP 30749 Hyd than the KNM-KP 30748 Pr suggests that this specimen belongs more distal in the tooth row than does KNM-KP 30748. The near equal division of lateral and cuspal enamel formation times contrasts that described for robust *Australopithecus*, where there is a dominance of cuspal enamel and fewer striae (that are more obliquely aligned to the enamel dentine junction) in the lateral enamel (Beynon & Wood 1987; Grine & Martin 1988).

#### *Humerus*

The *A. anamensis* humerus, KNM-KP 271 (Figure 13), has been included in numerous studies of distal humeral morphology. Some

**Table 14** Percent cortical area at break of KNM-KP 271 and at 20% humeral location in extant hominoids

Taxon	<i>n</i>	% CA mean	S.D.	Min	Max
KNM-KP 271*	1	86.5	—	—	—
<i>Pan troglodytes</i>	20	70.0	9.8	51.5	87.7
<i>Gorilla gorilla</i>	20	69.4	7.9	51.0	86.7
<i>Pongo pygmaeus</i>	20	82.8	7.0	68.0	96.1
<i>Homo sapiens</i>	40	65.2	7.6	47.5	82.9

Comparative data kindly provided by C. B. Ruff.

*H. sapiens* sample from Pecos Pueblo, all individuals <40 years old.

\*Note that KNM-KP 271 is broken distal to what probably would have been 20%, and so probably represents a minimum comparative value.

*n*=sample size, S.D.=standard deviation, Min=minimum, Max=maximum.

have found this specimen more similar to *Homo* than *Australopithecus* or African apes (Senut & Tardieu, 1985; Baker *et al.*, 1998; Senut, 1999). More thorough studies, however, have determined that KNM-KP 271 cannot be distinguished from those attributed to *A. afarensis*, and is indeed most similar to that taxon than any other (Feldesman, 1982; Hill & Ward, 1988; Lague & Jungers, 1996). The anterior margin of the lateral trochlear keel is slightly abraded almost to its distalmost extent, making this ridge appear less pronounced than it would have been (Figure 13). This may have contributed to the impression that this bone appears more like *Homo*. Discrepancies among these studies are also due to the fact that human and ape humeri are broadly similar while at the same time being quite variable, so that in most details the ranges of variation overlap, obscuring apparent morphological distinctions.

One way in which hominin humeri consistently differ from those of African apes is in the lack of trochlear joint surface extension along the lateral margin of the olecranon fossa, a feature typical of African apes. This may be due to resisting loads incurred during hyperextension of the elbow during quadrupedalism. It is occasionally found to a certain extent in some *Pongo* individuals, however. Not surprisingly, this

extension is absent in KNM-KP 271. KNM-KP 271 also lacks an elongate, superoposteriorly extended lateral humeral epicondyle which is noted for *Ar. ramidus* (White *et al.*, 1994), resembling *A. afarensis* in this feature.

One feature of KNM-KP 271 not previously noted is the extraordinarily thick cortical bone visible at the proximal break. Although it is broken slightly distal to what would have been 20% of its original length, it can be compared at least roughly to African apes and humans. KNM-KP 271 has a percent cortical area of about 86%, almost the maximum of the observed range of African apes and humans (Table 14), but typical for *Pongo*. Because it is broken slightly distal to where the cortical area was measured for the extant specimens, its relative value might be slightly inflated. Still, it was unlikely that the cortical bone would be thicker here than at the true 80% location, if that was further proximal to the break. KNM-KP 271 is clearly a robust bone. The functional or behavioral significance of this extraordinary cortical thickness is difficult to interpret in such a small fragment. While a robust humeral shaft might appear to suggest forelimb-dominated arboreality, it should be noted that the humeri of African apes are not as robust but these apes certainly climb trees. Without bone length,

diaphyseal morphology is difficult to interpret with respect to bending rigidity and any behavioral conclusion is difficult to make without detailed further research into the significance of cortical thickness in such a small fragment of humerus.

#### *Radius*

KNM-ER 20419 is a long radius. If, for instance, the individual to which it belonged had body proportions like those of modern *Homo*, the estimated stature from regression data is as follows;  $182.96 \pm 4.32$  cm for white males,  $175.61 \pm 0.43$  cm for black males (regression equations from Trotter & Gleser, 1952). These estimates are high and well above the stature means (132–151 cm) generated by McHenry (1992) from data for presumed males of four *Australopithecus* species including *A. afarensis*. Rather than suggest that these hominins were tall with modern human proportions, we believe instead that they were shorter in stature with relatively long forearms, based on inference from all other hominins prior to 2 Ma. This appears to be similar to the condition in *A. afarensis*, which also appears to have had relatively long forearms (Kimbel *et al.* 1994).

The radius is similar in morphology to other *Australopithecus* radii and is distinguished from great apes by having a thick neck relative to the shaft and a distal shaft that is semilunar in cross-section. It differs from African apes and humans in particular in the relative proportions of the articular surface areas for the lunate and scaphoid (Heinrich *et al.*, 1993). Only *Australopithecus* has a lunate contact facet that is larger than that of the scaphoid. Richmond & Strait (2000) recently used a cast of KNM-ER 20419 in a multivariate analysis of distal radial morphology. They claim that this bone retains morphological evidence of knuckle-walking. They did not, unfortunately, correct for the missing styloid process, which could affect their angular and

breadth measurements and, thus, the outcome of their analysis. Even if they had done this, the significance of the dorsal ridge limiting extension in knuckle-walkers has yet to be demonstrated, so their results should remain tentative. The uniquely broad lunate facet of *Australopithecus* must also be taken into account in any functional analysis of the radiocarpal joint.

#### *Capitate*

Abrasion of most of the cortex of the capitate (KNM-KP 31724) obscures much of its morphology. This bone was large, though, being similar in overall length to that of a chimpanzee or female gorilla. It appears to have had a large head, although it cannot be measured due to damage. What is preserved of the head shows that almost all of its proximally-facing surface was comprised by the lunate facet, as in other *Australopithecus* specimens (Ward *et al.*, 1999a). In contrast, extant great apes and humans have more extensive scaphoid facets here. This morphology may be related to a relatively large area of contact between the lunate and radius, found in *Australopithecus*, but not in extant African apes and humans.

Enough of the specimen is intact to indicate that the MC 3 surface probably had less topographic relief than that typical of African apes. Enough of the second metacarpal surface is preserved to show that this facet was not complete dorsopalmarly as it is in later hominins, but instead there was a ligamentous attachment area in the dorsopalmar center of the distal end of the bone separating two MC 2 facets (Leakey *et al.*, 1998).

One feature that is clear is that the MC 2 facet was set at about a 90° angle to the MC 3 facet (Leakey *et al.*, 1998). This condition is typical for African apes but not humans, who have their MC 2 facet set at a 112–155° angle to the MC 3 facet (Table 15; Figure 32). This obliquity, combined with a dorsopalmarly continuous MC 2 facet,

Table 15 Comparative metrics of the capitae

<i>n</i>	MC 2/MC 3 facet angle, °			Dorsopalmar diameter of head, mm			Proximodistal length of bone, mm		
	Mean	S.D.	Min Max	Mean	S.D.	Min Max	Mean	S.D.	Min Max
<i>A. anamensis</i>	90	—	—	14.8	—	—	21.8	—	—
<i>A. afarensis</i>	120	—	120	12.2	—	10.8	18.1	—	16.2
cf. <i>A. afarensis</i>	115	—	—	15.0	—	—	20.8	—	—
<i>Pan troglodytes</i>	86	7.2	71	33.3	2.3	29.2	22.9	1.6	19.3
<i>Gorilla gorilla</i>	85	6.7	73	45.5	6.1	36.0	26.4	3.2	22.1
<i>Homo sapiens</i>	134	10.9	112	44.5	3.4	39.5	21.8	1.9	17.7

MC 2/MC 3 facet angle measured from tangents of palmar aspects of these joint surfaces.  
cf. *A. afarensis* data is from the Turkwel hominid, KNM-WT 22944 (Ward *et al.*, 1999b).

Orientation of 2nd metacarpal facet on capitate

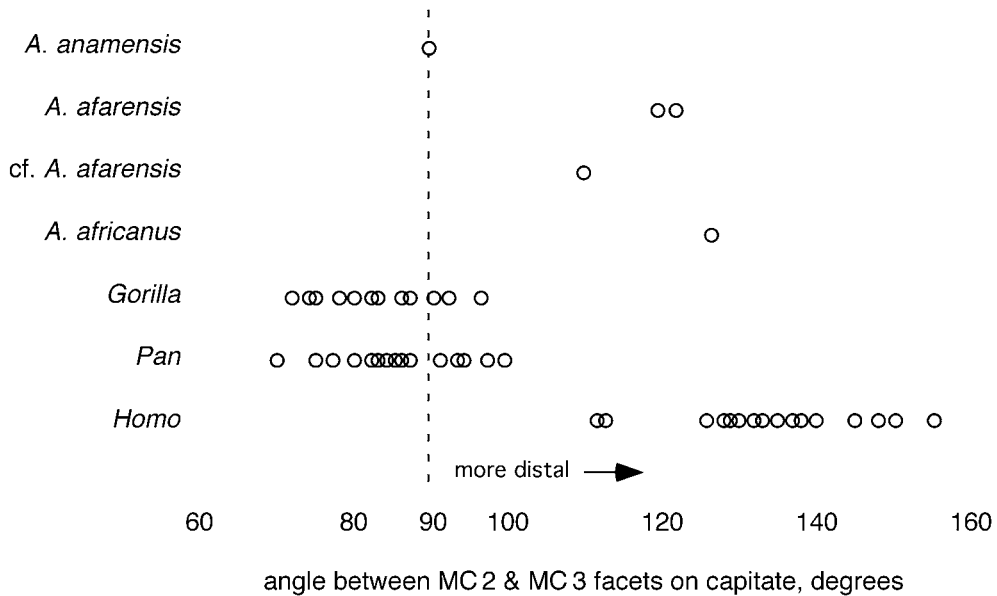


Figure 32. Orientation of second metacarpal facet on capitate. Measurement taken between MC 2 facet and palmar portion of MC 3 facet. Points represent individual specimens. Data listed in Table 15. *A. anamensis* is the only hominin specimen to have a laterally-facing MC 2 facet. All others overlap modern humans in having a distolaterally inclined facet. In these later hominin specimens, the MC 2 facet is mildly concave and uninterrupted by an intercarpal ligament. In humans, this contributes to up to 20° of rotation at the second carpometacarpal joint, contributing to cupping of the palm. Although the facet is damaged obscuring potential evidence of an intercarpal ligament, the orientation and flat preserved contour of the MC 2 subchondral surface suggests that this motion was not possible in *A. anamensis*.

allows rotation at this joint (Lewis, 1977; Dubosset, 1981; Marzke, 1983, 1997; Marzke & Shackley, 1986). Such movement would not have been possible for the KNM-KP 31724 individual (Leakey et al., 1998; Ward et al., 1999a). Other australopithecine specimens are intermediate in orientation, with human-like continuous facets (Broom & Schepers, 1946; Le Gros Clark, 1947; Lewis, 1973; McHenry, 1983; Marzke, 1983, 1997; Ward et al., 1999a). In this respect, KNM-KP 31724 is more great ape-like than any known *Australopithecus* or *Homo* specimens.

*Phalanx*

The manual phalanx, KNM-KP 30503, is very similar to those of *A. afarensis* from

Hadar in size and morphology (Johanson et al., 1982; Bush et al., 1982). The specimen exhibits a gentle palmar concavity and clear flexor ridges along the central portion of its shaft. It shows no appreciable differences in form compared to those of *A. afarensis*. This morphological similarity suggests functional and developmental history similarity, but whether this implies arboreality or not remains a matter of debate (summarized in Stern, 2000).

*Tibia*

The KNM-KP 29285 tibia is similar to those described for *A. afarensis* from Hadar (Lovejoy et al., 1982). The tibia gives clear signs of being adapted for bipedal locomotion, particularly in the vertical

orientation of the shaft relative to the talar facet (Latimer *et al.*, 1987; Ward *et al.*, 1999b). Apes all have an obliquely oriented tibial diaphysis. KNM-KP 29285 is slightly larger than the largest tibia recovered so far from Hadar, AL 333-42 (Lovejoy *et al.*, 1982). Using McHenry's (1992) regression equation based on humans, KNM-KP 29285 came from a 47–55 kg individual.

KNM-KP 29285 resembles *A. afarensis* tibias in several other features including a rectangular proximal epiphysis, concave condyles that are roughly equal in area, a marked depression anteriorly for the pes anserinus muscles, a straight shaft, and a semilunar articular facet for the distal fibula. It also has swollen metaphyses that are expanded in all dimensions past the subchondral bone. This latter feature can be functionally linked to bipedality as a mechanism for expanding cancellous bone as a shock-absorbing mechanism to dissipate high peak loads incurred during heel strike in bipedal gait (Kunos & Latimer, 2000).

The superior fibular facet is abraded, but cannot have been very big. Together with the small semilunar facet for the inferior fibular articulation, this is evidence that the fibula may have been relatively small. Great apes have a large fibula for attachment of the large flexor hallucis longus muscle associated with a divergent hallux. A marked anterior depression for the pes anserinus insertion (mistakenly described in Johanson *et al.* (1982) for the tibialis anterior insertion) is a common feature of great apes, and is found in all *Australopithecus* individuals in which it can be seen. The functional significance of this feature is under investigation by one of us (A.W.).

## Discussion

### *Taxonomy and evolutionary implications*

The Allia Bay hominids have been considered part of the *A. anamensis* hypodigm and the sample includes paratypes for this

species (Leakey *et al.*, 1995, 1998; Ward *et al.*, 1999b). The holotype of *A. anamensis* is from Kanapoi, where all of the features described as diagnostic are found. The Allia Bay sample is less complete than that from Kanapoi, with fewer fossils. It is not that the Allia Bay fossils lack diagnostic features, it is rather that the body parts and characters necessary to make a conclusive species attribution are not preserved at this site. Sizes of the preserved teeth from both sites overlap, as they do in all observable aspects of morphology. Given the present samples, the Allia Bay fossils preserve no morphology indicating that they should not belong to *A. anamensis*.

Several Allia Bay specimens have possible taxonomic implications. At first glance, it might appear that the mandible KNM-ER 20432 (Coffing *et al.*, 1994) does not have a sloping symphysis. This specimen is fragmentary, however, and preserved only as far anteriorly as P<sub>3</sub>, so is missing enough bone to make it unclear what the symphyseal contour would have looked like. When casts of the more complete Kanapoi specimens are broken at the same points as KNM-ER 30745, they too lose all evidence of their characteristic symphyseal morphology. Thus, symphyseal morphology cannot be reconstructed accurately based on KNM-ER 20432.

This mandible does appear to be morphologically more similar to *A. anamensis* mandibles than *A. afarensis* ones in preserved morphology, however. The alveolar contour of this specimen is similar to the Kanapoi mandibles. Although the canine jugum is partly missing, it is clear that it would have flared laterally at least as far as does the P<sub>3</sub> jugum, a feature found only among *A. anamensis* mandibles within hominins.

The P<sub>3</sub> of KNM-ER 20432 is quite similar to all Kanapoi P<sub>3</sub>s (Coffing *et al.*, 1994, Figure 30). These teeth have only a dominant, centrally placed protoconid,



with the metaconid present as only a small tubercle along the marginal ridge, and strongly demarcated cusp ridges. All of these teeth are very similar. This morphology is not matched by any *A. afarensis* specimen, despite the great variability in  $P_3$  morphology in that species. This specimen, then, suggests that the Allia Bay hominids should remain with *A. anamensis*.

KNM-ER 20432 also preserves the broken root of a very large canine, another *A. anamensis* feature. Because of the difficulty in quantifying broken canine root dimensions, it is difficult to compare metrically. *Australopithecus anamensis* does, however, appear to have had slightly larger canine teeth than did *A. afarensis*, so this character also would appear to link Allia Bay with Kanapoi.

Another premolar with potential taxonomic implications is KNM-ER 35228, a premolar germ that we argue is  $P_4$ , but has some unusual morphology (Figure 21). It is similar in some ways to *A. afarensis*  $P_{3s}$ , which could lead some to doubt its assignation as a  $P_4$ . The somewhat unusual nature of KNM-ER 35228 is worth noting because if this tooth were a  $P_3$ , it would suggest that the Allia Bay sample was aligned morphologically more closely with *A. afarensis*.

Compared with other *A. anamensis* and *A. afarensis*  $P_{4s}$ , KNM-ER 35228 has a more ovoid occlusal outline with reduced mesiolingual corner, a more sloping buccal face and relatively large protoconid with smaller lingual cusps than found in most *A. anamensis* or *A. afarensis*  $P_{4s}$ . Among the *A. afarensis*  $P_{4s}$ , it is most similar to the specimen AL 288-23, but still differs from it.

Although KNM-ER 35228 somewhat resembles some Hadar  $P_{3s}$  in overall form, it has a notched lingual cusp ridge with the anterior fovea opening lingually, a large distal cuspule with a distinct distobuccal groove and no mesio Buccal groove, and a relatively short mesial cusp ridge. These

features are found together only on *A. afarensis* or *A. anamensis*  $P_{4s}$ . The greater weight of the anatomical evidence suggests that this tooth is, indeed, a  $P_4$ . We recognize that KNM-ER 35228 differs from other *A. anamensis*  $P_{4s}$ , however, in occlusal outline and cusp structure.

Until more fossils are found with which to test the hypothesis of conspecificity of the Allia Bay and Kanapoi hominins, it seems most reasonable to retain the Allia Bay hominins in *A. anamensis*.

As noted by Leakey *et al.* (1995, 1998) the fossils attributed to *A. anamensis* display a suite of characters which differentiate them from all previously described species, including *A. afarensis* (contra Senut, 1996, 1999; Wolpoff, 1999). This justified the naming of the new species.

It is worthwhile to note that with the possible exception of the strong basal tubercles on the male upper canine (Figure 29), and perhaps the basal convexity of the external mandibular symphyseal contour, there are no apomorphies of *A. anamensis* that are not present in *A. afarensis*. On cladistic grounds, then, some might be tempted to argue that the *A. anamensis* samples should be referred to *A. afarensis* (e.g. Wolpoff, 1999) or *Praeanthropus africanus* (e.g. Senut, 1996, 1999). We argue that there is biological merit in distinguishing *A. anamensis* as a separate species. Combining these samples in one taxon does not preclude the distinct possibility that they do not have an ancestor-descendent relationship, much less an exclusive one which would make it appropriate to combine them. Given the many similarities between these two taxa, and the fact that most of the ways that *A. anamensis* differs from *A. afarensis* appear to be in the retention of primitive traits, a reasonable working hypothesis is that *A. anamensis* was ancestral to *A. afarensis*. Until future discoveries of fossils are made which disprove this hypothesis, it provides a useful scientific framework with

which to explore ideas about the early evolution of *Australopithecus*.

This hypothesis that *A. anamensis* may be ancestral to *A. afarensis* is consistent with the phylogeny recently published by Strait & Grine (1999) that placed *A. anamensis* as a sister taxon to *A. afarensis* and other hominins. Traits from their list that can be assessed in *A. anamensis* are, by number (Strait *et al.*, 1997): 4, anterior pillars—absent; 5, nasoalveolar clivus contour in coronal plane—convex; 6, protrusion of incisor alveoli behind bicanine line (basal view)—yes; 7, nasal cavity entrance—stepped; 8, palate thickness—thin; 12, anterior palatal depth—shallow; 32, relative depth of mandibular fossa—shallow; 34, configuration of tympanic—tubular; 44, mandibular cross section at  $M_1$ —small; 45, orientation of mandibular symphysis—very receding; 46, direction of mental foramen opening—anterior/superior; 47, hollowing above and behind mental foramen—present; 49, mandibular deciduous canine shape—apex central, mesial convexity, low; 50, incisal reduction—moderate; 51, canines reduced—somewhat/slightly less than in *A. afarensis*; 53/54, premolar/molar crown area—like *A. afarensis*; 56, dmr of  $M_2$ —low; 57, separation of molar and premolar cusp apices—wide; 58, frequency of well developed  $P_3$  metaconid—absent; 59, relative enamel thickness—thick. This list does not summarize all characters visible in *A. anamensis*, however, not mentioning the small external auditory porus, rounded lateral nasal margins, rounded external inferior mandibular symphysis contour, mandibular alveolar contour not curving medially until /C, slightly larger canine teeth with robust roots, narrow  $dm_1$ , large C/ basal tubercles, low-crowned molars with sloping sides, thick humeral cortex, laterally-oriented MC 2 facet on the capitata, for example. All of these but the mandibular symphyseal shape and C/ form are primitive for hominins excluding *Ar. ramidus*, so no

further characters presented here would likely alter the hypothesis supported by their results. A trait list that would enable one to more thoroughly assess the phylogenetic position of *A. anamensis* relative to *Orrorin* and *Ardipithecus* would have to include other characters, and must wait until these latter fossils have been further analyzed and published.

Senut has argued that the *A. anamensis* sample be combined with the Garusi (*A. afarensis*) specimen in what would now be referred to as *Praeanthropus afarensis* (Senut, 1999) based on similarities between the Garusi maxilla and KNM-KP 29283. It is true that these fossils share robust canine juga contributing to a rounded lateral nasal margin, features not seen in other *A. afarensis* specimens (Figure 23). *A. anamensis* overlaps morphologically with other *A. afarensis* specimens in other features, however, including in the maxilla. This could be attributable to a close phylogenetic or even ancestor-descendent relationship. The process of population differentiation and speciation involves shifting frequencies of traits that vary within populations, so finding some traits which overlap should neither preclude taxonomic separation or require grouping of samples which are otherwise distinct. At the present time, we recognize these similarities between *A. anamensis* and the Garusi maxilla, but prefer that no taxonomic reallocation be given until more is known about patterns of variation in these morphologies within and among extant and fossil hominoid taxa.

Some additional Ethiopian fossil samples are broadly contemporaneous with *A. anamensis*. One is the collection of heavily worn teeth from Fejej (Fleagle *et al.*, 1991) that were initially attributed to *A. afarensis*. The taxonomic affinity of this highly fragmentary material is indeterminate, however, and this specimen may as well belong to *A. anamensis*, which was unknown at the time

of their publication (Ward *et al.*, 1999b). Other contemporaneous fossils are the Belohdelie frontal, dated to 3.9 Ma (Asfaw, 1987), and the Maka femur, dated to 3.5–4.0 Ma (Clark *et al.*, 1984), but because no frontals or femora are known for *A. anamensis*, direct comparisons cannot be made to assess possible taxonomic affinities among these samples.

### Diet

Dietary implications of the Kanapoi and Allia Bay fossils are summarized by Teaford & Ungar (2000). The thick enamel of *A. anamensis* teeth compared with the thin enamel of *Ar. ramidus* and African apes suggests a shift in emphasis towards eating harder or more abrasive foods, while retaining an ability to process softer fruits. This is also supported by the apparently reduced levels of anterior tooth wear, slight reduction in anterior teeth, flat molars and slightly thicker mandibular corpora than found in apes. Later australopithecines appear to have continued trends toward harder object feeding. Thus, selection for the ability to process harder food objects seems to be a trend that began in the ancestors of *A. anamensis* and continued in later *Australopithecus*. *A. anamensis* then, would perhaps have been able to process foods with a more variable set of material properties than can African apes, perhaps widening the dietary niches and microhabitats that they were capable of exploiting.

The dietary shift suggested by the *A. anamensis* dentognathic morphology may be related to environmental shifts occurring at the time. Evidence for dietary driven adaptive radiations at this time is not limited to *A. anamensis* or even to fossil hominins. Faunal accumulations from East Africa document a major turnover in the late Miocene. Fauna characteristic of the Miocene was replaced by new taxa of modern aspect, incorporating the last occurrence of archaic Miocene taxa with ancestors of

the extant biota including hippos, giant pigs, grazing antelopes, true giraffes and elephants (Leakey & Harris, 2001). This faunal change appears to be directly related to changing habitats resulting from the expansion of C<sub>4</sub> grasses (Cerling *et al.*, 1997a). Evidence for changing paleoecology has been indicated through analyses of stable carbon isotopes in pedogenic carbonates and in tooth enamel of herbivorous mammals. Both approaches indicate a global event, marking the expansion of C<sub>4</sub> plants (Quade *et al.*, 1992; Cerling *et al.*, 1997a, 1998). This is believed to be the result of decreasing CO<sub>2</sub> levels reaching a threshold that favors C<sub>4</sub> photosynthesis (Ehleringer *et al.*, 1997; Cerling *et al.*, 1998). Stable isotope studies of paleoecosystems have shown that few C<sub>4</sub> plants were present in significant abundance anywhere prior to about 8 mya (Morgan *et al.*, 1994; Cerling *et al.* 1997b). After this time, however, mixed C<sub>3</sub>/C<sub>4</sub> habitats with a significant C<sub>4</sub> component became widespread (Quade *et al.*, 1992; Cerling *et al.*, 1997a).

Although the fossil record provides little evidence of increased diversity in non-mammalian species, evidence for faunal change and dietary-driven adaptive radiations among mammals in the late Miocene and Pliocene has been well demonstrated in sites as widely separated geographically as the Siwaliks, North America and Africa (Quade *et al.*, 1989, 1992; Morgan *et al.*, 1994; Cerling *et al.*, 1997a). The earliest African mammalian assemblages to exploit C<sub>4</sub> plants are found in the Lothagam sediments and Samburu Hills succession (Cerling *et al.*, 2001). Lothagam sediments range in age from greater than 7.4 Ma at the base of the lower Nawata Formation to 4.2 Ma at the top of the Apak Member of the Nachukui Formation (McDougall & Feibel, 1999). Samburu Hills overlaps in age with the earliest Lothagam sediments. Several lineages of herbivores including proboscideans, equids, rhinos and suids

show a change from C<sub>3</sub> to C<sub>4</sub> dominated diets (Cerling *et al.*, 2001). In contrast, analyses of pedogenic carbonates and mammalian tooth enamel from earlier sediments at Nakali (Cerling *et al.*, 2001), Ngorora (Morgan *et al.*, 1994), and Fort Ternan (Cerling *et al.*, 1997b) that predate Lothagam, show little evidence of C<sub>4</sub> photosynthesizing plants (Cerling *et al.*, 2001). The emergence of hominins in the late Miocene or early Pliocene may be part of this global phenomenon in which changing ecosystems prompted a radiation of species using the newly available habitats and food resources.

#### *Locomotion*

The Kanapoi tibia clearly demonstrates that *A. anamensis* was adapted for habitual bipedality (Leakey *et al.*, 1995; Leakey *et al.*, 1998; Ward *et al.*, 1999b). This tibia is the earliest conclusive postcranial evidence of hominin bipedality documented so far, showing that habitual terrestrial bipedal locomotion was selectively advantageous for hominins prior to 4.2 Ma. This adaptation may be older, as *Ar. ramidus* is alleged to have been bipedal at 4.4 Ma based on the position of its foramen magnum (White *et al.*, 1994), and analysis of its postcranial anatomy currently underway will reveal the extent of its bipedal adaptation.

The apparently long radius and mildly curved manual phalanx represent primitive characters retained in the skeleton. The significance of these features for interpreting behavior and adaptive history is complicated, however. There are two major questions commonly asked about locomotion in *Australopithecus*. First, what type of locomotion had been selected for in a particular species, and second, what were those animals capable of doing and/or spent time doing. These are fundamentally different questions requiring different types of evidence to address. The adaptive significance

of primitive retentions is not readily testable, as it is difficult to refute either the hypothesis that plesiomorphic characters were retained by stabilizing selection or that they merely had not been selected against. This is particularly difficult in *Australopithecus* in light of the clear and strong directional signal towards bipedality and away from arboreality. Because the ape-like characters of the *A. anamensis* skeleton are primitive, it is not possible to say conclusively whether or not they indicate that arboreality was an adaptively significant component of the *A. anamensis* behavioral repertoire at this point. It will always be difficult to say, even if *A. anamensis* climbed trees, whether this behavior enhanced their survival and reproductive success, or whether they were selectively neutral because of their primitive nature, especially given the overwhelming shift towards terrestrial bipedality evident in the skeleton.

The second question is slightly easier, but still requires more comparative morphological data. Finding characters with a strong epigenetic component, and thus influenced by an individual's actual activity patterns over its lifetime, could possibly demonstrate that an animal may have engaged in a particular behavior. Recently, possible ontogenetic influences of climbing behavior on phalangeal curvature have been suggested (Paciulli 1995; Richmond, 1997, 1999) but have yet to be supported convincingly by data in the literature. If these data are supported, phalangeal curvature could indicate occasional climbing in *A. anamensis*, although still we could not be sure that behavior influenced the individual's fitness. Some have argued, in fact, that not only were they not selected to do so, *Australopithecus* (*A. afarensis* and the other more recent species, at least) could not have climbed trees regularly (summarized by Latimer, 1991).

Clearly, bipedality had been selected for and positively affected individual

survival and reproduction in the immediate ancestors of *A. anamensis*. There is no conclusive evidence to suggest that arboreality was practiced and/or remained selectively advantageous for *A. anamensis*, although the possibility cannot be ruled out at present.

#### *Body mass and sexual dimorphism*

The apparently large body size range in the *A. anamensis* sample is analogous to that found in *A. afarensis*, which has roughly 2:1 body mass sexual dimorphism (e.g. McHenry, 1992) comparable to the levels typical of *Gorilla gorilla* and *Pongo pygmaeus* (Plavcan & Van Schaik, 1997; Smith & Jungers, 1997). This far exceeds body mass dimorphism levels found in *Homo* and *Pan*, suggesting that reduced body mass dimorphism represents homoplasy in these lineages (Lockwood *et al.*, 1996). These data contradict hypotheses positing that humans and *Pan troglodytes* (e.g., Wrangham, 1999) or *Pan paniscus* (e.g., Zihlman *et al.*, 1978) share extensive aspects of their sociality as an evolutionary heritage.

Canine dimorphism in *A. anamensis* was certainly reduced compared with extant apes and even *Ar. ramidus*, revealing a history of continued selection against large canine size in males early in the hominin lineage. As canines are primarily important for intra-specific displays and combat among males in extant primates, it is reasonable to assume that canine teeth were less valuable as instruments in male–male combat. This trend continued in *A. afarensis* and later hominins.

The fact that body mass dimorphism remained high until the appearance of *Homo*, however, suggests that large male body size (and/or small female size) had not been selected against for all known *Australopithecus* species, and may still have conferred a reproductive advantage, although, similar to interpretations of locomotor morphology, this plesiomorphic character is complicated

to assess. The presence of high levels of body mass dimorphism is associated with polygynous social systems in all anthropoids (see Plavcan, 2000), and would seem to contradict the hypothesis that these early hominins had a pair-bonded social system (Lovejoy, 1981), even in light of reduced canine dimorphism (Plavcan, 2000). Large body size appears to have retained an advantage for males while canine size did not, suggesting an altered emphasis on strategies of male–male combat rather than an elimination of such competition.

It is interesting to note that all five of the known postcranial elements of *A. anamensis* are from large, presumably male, individuals. They all compare in size with the largest known specimens of *A. afarensis* from Hadar. Any comparisons made between *A. anamensis* postcrania and those of other taxa must take body mass into account when making functional interpretations based on this apparently biased small sample.

### Summary and conclusions

*Australopithecus anamensis* predates all other taxa that have been assigned to *Australopithecus*, and in most ways it appears to be more primitive than any other. Although it is readily distinguishable from *A. afarensis*, this is because *A. anamensis* is generally more primitive in all except its uniquely large maxillary canine basal tubercles and rounded inferior contour of the external surface of its mandibular symphysis. The possibility that *A. anamensis* represents an ancestor of *A. afarensis* is not precluded by the evidence available to date.

Because the Allia Bay sample is more poorly represented than the Kanapoi sample, it preserves few diagnostic characters for *A. anamensis*. However, because it is most similar to the Kanapoi hominids morphologically, and is close to it geographically, we recommend it be retained, at least for the moment, in *A. anamensis*.

*Australopithecus anamensis* was a habitual biped that retained some primitive characters in its upper limb. It has thick enamel, with anterior teeth considerably reduced from the putative primitive condition. The lower lateral incisors are relatively larger than those of *Australopithecus afarensis*, and the canine/premolar complex is more primitive with apparently slightly larger canines relative to the postcanine teeth and more unicuspid lower third premolars. The mandibular canines are narrower and more asymmetrical in form, and the maxillary canine displays a unique morphology with subequal mesial and distal basal cuspules.

*Australopithecus anamensis* jaws are narrower than those of other *Australopithecus*, with more parallel postcanine tooth rows. Mandibular robusticity is slightly less than in *A. afarensis*. The *A. anamensis* mandibles also differ from those of later hominins in that the lateral alveolar contour swings mesially only anterior to the canine juga, not at the P<sub>3</sub> juga. The lateral nasal aperture is rounded and is smoothly continuous with the robust maxillary canine juga, while that of *A. afarensis* is separate and there is a prominent lateral nasal crest. The only exception to this in *A. afarensis* is the Garusi specimen from Laetoli, which more closely resembles *A. anamensis* in nasal contour form.

While its thick enamel and reduced anterior dentition suggest a dietary shift towards tougher foods from a primitive, ape-like condition, *A. anamensis* retains a fairly ape-like structure to its jaws with narrowly set parallel postcanine tooth rows, a flat temporomandibular joint and heavy anterior tooth wear. Whatever dietary change corresponded with the appearance of *Australopithecus*, dietary adaptation continued to change with *A. afarensis*, causing the development of a more parabolic dental arcade, less flat glenoid fossa and associated morphology. This dietary change may reflect a long term environmental trend

occurring at the time from closed to more open environments. The reduced canine sexual dimorphism combined with apparently high levels of body mass dimorphism suggests a unique social system characterized by high levels of male–male competition that did not involve use of the canine teeth. Thus, data from *A. anamensis* support hypotheses suggesting that the evolution of hominid bipedality may have been correlated both with changes in diet and/or social behavior.

### Acknowledgements

The authors would like to thank the following people and institutions for their advice and/or support. The Government of Kenya gave us permission to carry out this research and the National Museums of Kenya gave logistical support. We thank the director and staff of the National Museums of Kenya, the staff of the National Museum of Ethiopia and Ethiopian Ministry of Information and Culture, and the curators and staff of the Cleveland Museum of Natural History. We also thank Frank Brown, Deborah Cunningham, Chris Dean, Holly Dunsworth, Victoria Emsch, Craig Feibel, Leslea Hlusko, Bill Kimbel, Francis Kirera, Charlie Kunos, Bruce Latimer, Charlie Lockwood, Ian MacDougall, Lyman Jellema, Donald Johanson, Richard Leakey, Emma Mbua, Anne Mwai, Thierra Nalley, Erica Phillips, Richard Sherwood, Fred Spoor, Gen Suwa, Peter Ungar, and Tim White for help. Members of the field expeditions to Kanapoi (1994–1997) and Allia Bay (1995–1997) included the following: Kiptalam Cheboi, Sila Dominic, Justus Edung, Gabriel Ekalalei, John Ekamais, Christopher Epat, Nicolas Ewalan, Craig Feibel, Patrick Gathogo, Sabine Hagemann, Leslea Hlusko, John Kaatho, Peter Kapoko, Christopher Kiarie, Musa Kieva, Kamoya Kimeu, Katey Coffing, Simon Komolo, Benson Kyongo, Louise Leakey, William

Lokipi, Daniel Lokitar, Robert Lokure, Robert Lorinyok, Eluid Losike, Ninian Lowis, Simon Makathimo, Mathew Eragae, Boniface Malika, Wambua Mangao, Ian McDougall, Simon Milledge, Gertrude Mugaisi, Stephen Muge, Joseph Mutaba, Mwangela Muoka, Daniel Mutinda, Nzube Mutwiwa, Wycliffe Mutwiwa, Njeroge Njigi, Samuel Nguu, Blasto Onyango, Fred Spoor, Kathlyn Stewart and Jonathan Wynn. Input by Charlie Lockwood, Bill Kimbel, an anonymous reviewer and Terry Harrison greatly improved this manuscript. The National Geographic Society and National Science Foundation (NSF SBR 9601025) funded the fieldwork. Caltex (Kenya) provided fuel and Richard and Jonathan Leakey each allowed us the use of their aeroplanes. This research was also supported by NSF BNS 94-04813. Susan Alta Martin did the illustrations.

## References

- Asfaw, B. (1987). The Belohdelie frontal: new evidence of early hominid cranial morphology from the Afar of Ethiopia. *J. hum. Evol.* **16**, 611–624.
- Baker, E. W., Malyango, A. A. & Harrison, T. (1998). Phylogenetic relationships and functional morphology of the distal humerus from Kanapoi, Kenya. *Am. J. phys. Anthrop.* **26** (Suppl.), 66.
- Beynon, A. D. & Wood, B. A. (1986). Variation in enamel thickness and structure in East African hominids. *Am. J. phys. Anthrop.* **70**, 177–193.
- Beynon, A. D. & Wood, B. A. (1987). Patterns and rates of enamel growth in the molar teeth of early hominids. *Nature* **326**, 493–496.
- Broom, R. & Schepers, G. W. H. (1946). *The South African Ape-Men: the Australopithecinae*. Pretoria: Transvaal Museum Memoirs No. 2.
- Brown, B., Walker, A., Ward, C. V. & Leakey, R. E. (1993). New *Australopithecus boisei* calvaria from East Lake Turkana, Kenya. *Am. J. phys. Anthrop.* **91**, 137–159.
- Brunet, M., Beauvilain, A., Coppens, Y., Heintz, E., Moutaye, A. H. E. & Pilbeam, D. (1995). The first australopithecine 2,500 kilometres west of the Rift Valley (Chad). *Nature* **378**, 273–275.
- Brunet, M., Beauvilain, A., Coppens, Y., Heintz, E., Moutaye, A. H. E. & Pilbeam, D. (1996). *Australopithecus bahrelghazali*, une nouvelle espèce d'Hominidé ancien de la région de Koro Toro (Tchad). *C. r. Acad. Sci., Paris.* **322**, 907–913.
- Bush, M. E., Lovejoy, C. O., Johanson, D. C. & Coppens, Y. (1982). Hominid carpal, metacarpal and phalangeal bones recovered from the Hadar Formation: 1974–1977 collections. *Am. J. phys. Anthrop.* **57**, 651–678.
- Cerling, T. E., Harris, J. M., MacFadden, B. J., Leakey, M. G., Quade, J., Eisenmann, V. & Ehleringer, J. R. (1997a). Pattern and significance of global ecologic change in the late Neogene. *Nature* **389**, 153–158.
- Cerling, T. E., Harris, J. M., Ambrose, S. H., Leakey, M. G. & Solounias, N. (1997b). Dietary and environmental reconstruction with stable isotope analysis of herbivore tooth enamel from the Miocene locality of Fort Ternan, Kenya. *J. hum. Evol.* **33**, 635–650.
- Cerling, T. E., Ehleringer, J. R. & Harris, J. M. (1998). Carbon dioxide starvation, the development of C<sub>4</sub> ecosystems, and mammalian evolution. *Phil. Trans. R. Soc. Lond. B.* **353**, 159–171.
- Cerling, T. E., Harris, J. M. & Leakey, M. G. (2001). Isotope paleoecology of the Nawata and Nachukui Formations at Lothagam, Turkana Basin, Kenya. In (M. G. Leakey & J. M. Harris, Eds) *Lothagam the Dawn of Humanity*. New York: Columbia University Press.
- Clark, J. D., Asfaw, B., Assefa, G., Harris, J. W. K., Kurashina, H., Walter, R. C., White, T. D. & Williams, M. A. J. (1984). Palaeoanthropological discoveries in the Middle Awash Valley, Ethiopia. *Nature* **307**, 423–428.
- Coffing, K., Feibel, C., Leakey, M. & Walker, A. (1994). Four-million year old hominids from East Lake Turkana, Kenya. *Am. J. phys. Anthrop.* **93**, 55–65.
- Daegling, D. J. & Grine, F. E. (1991). Compact bone distribution and biomechanics of early hominid mandibles. *Am. J. phys. Anthrop.* **86**, 321–340.
- Day, M. H. (1978). Functional interpretations of the morphology of postcranial remains of early African hominids. In (C. Jolly, Ed.) *Early Hominids of Africa*, pp. 311–345. New York: St. Martin's.
- DiGiovanni, B. F., Scoles, P. V. & Latimer, B. M. (1989). Anterior extension of the thoracic vertebral bodies in Scheuermann's kyphosis: An anatomic study. *Spine* **14**, 712–716.
- Dubosset, J. F. (1981). Finger rotation during prehension. In (R. Tubiana, Ed.) *The Hand*, pp. 202–206. Philadelphia: W.B. Saunders.
- Ehleringer, J. R., Cerling, T. E. & Helliker, B. R. (1997). C<sub>4</sub> photosynthesis, atmospheric CO<sub>2</sub> and climate. *Oecologia* **112**, 285–299.
- Falk, D. (1986). Evolution of cranial blood drainage in hominids: Enlarged occipital/marginal sinuses and emissary foramina. *Am. J. phys. Anthrop.* **70**, 311–324.
- Falk, D. (1988). Enlarged occipital/marginal sinuses and emissary foramina: Their significance in hominid evolution. In (F. E. Grine, Ed.) *Evolutionary History of the "Robust" Australopithecines*, pp. 85–96. New York: Aldine de Gruyter.

- Falk, D. & Conroy, G. C. (1983). The cranial venous sinus system in *Australopithecus afarensis*. *Nature* **306**, 779–781.
- Feldesman, M. R. (1982). Morphometric analysis of the distal humerus of some Cenozoic catarrhines: the Late Divergence hypothesis revisited. *Am. J. phys. Anthrop.* **59**, 73–95.
- Fleagle, J. G., Rasmussen, D. T., Yirga, S., Bown, T. M. & Grine, F. E. (1991). New hominid fossils from Fejej, Southern Ethiopia. *J. hum. Evol.* **21**, 145–152.
- Grine, F. E. & Martin, L. B. (1988). Enamel thickness and development in *Australopithecus* and *Paranthropus*. In (F. E. Grine, Ed.) *Evolutionary History of the "Robust" Australopithecines*, pp. 3–42. New York: Aldine de Gruyter.
- Harris, J. M. (1987). Summary. In (M. D. Leakey & J. M. Harris, Eds) *Laetoli: a Pliocene Site in Northern Tanzania*, pp. 524–531. Oxford: Oxford University Press.
- Heinrich, R. E., Rose, M. D., Leakey, R. E. & Walker, A. (1993). Hominid radius from the middle Pliocene of Lake Turkana, Kenya. *Am. J. phys. Anthrop.* **92**, 139–148.
- Hill, A. & Ward, S. (1988). Origin of the Hominidae: the record of African large hominoid evolution between 14 My and 4 My. *Yearb. phys. Anthrop.* **31**, 49–83.
- Hlusko, L. J. (1998). Euclidean distance matrix analysis of *Australopithecus* molars. M.A. Thesis, Pennsylvania State University, University Park.
- Hlusko, L. J. & Mahaney, M. C. (2000). The genetics of expression of two dental traits in baboons. *Am. J. phys. Anthrop.* **30** (Suppl.), 180.
- Hylander, W. L., Ravosa, M. J., Ross, C. F., Wall, C. E. & Johnson, K. R. (2000). Symphyseal fusion and jaw-adductor muscle force: an EMG study. *Am. J. phys. Anthrop.* **112**, 469–492.
- Johanson, D. C., Lovejoy, C. O., Kimbel, W. H., White, T. D. & Ward, S. C. (1982). Morphology of the Pliocene partial hominid skeleton (A. L. 288-1) from the Hadar formation, Ethiopia. *Am. J. phys. Anthrop.* **57**, 403–452.
- Kimbel, W. H. (1984). Variation in the pattern of cranial venous sinuses and hominid phylogeny. *Am. J. phys. Anthrop.* **63**, 243–263.
- Kimbel, W. H., Johanson, D. C. & Rak, Y. (1994). The first skull and other new discoveries of *Australopithecus afarensis* at Hadar, Ethiopia. *Nature* **368**, 449–451.
- Kohl-Larsen, L. (1943). *Auf den Spuren des Vormenschen; Forschungen Fahrten und Erlebnisse in Deutsch-Ostafrika*. Stuttgart: Strecker & Schroder.
- Kunos, C. A. & Latimer, B. (2000). Cross-sectional geometric properties of the distal tibial metaphysis in humans and apes. *Am. J. phys. Anthrop.* **30** (Suppl.), 202–203.
- Lague, M. R. & Jungers, W. L. (1996). Morphometric variation in Plio-Pleistocene hominid distal humeri. *Am. J. phys. Anthrop.* **101**, 401–427.
- Latimer, B. (1991). Locomotor adaptations in *Australopithecus afarensis*: the issue of arboreality. In (Y. Coppens & B. Senut, Eds) *Origine(s) de la Bipédie chez les Hominidés*, pp. 169–176. Paris: Centre National de la Recherche Scientifique.
- Latimer, B., Ohman, J. C. & Lovejoy, C. O. (1987). Talocrural joint in African hominoids: implications for *Australopithecus afarensis*. *Am. J. phys. Anthrop.* **74**, 155–175.
- Le Gros Clark, W. E. (1947). Observations on the anatomy of the fossil Australopithecinae. *J. Anat.* **81**, 300–333.
- Leakey, M. G. & Harris, J. M. (2001). *Lothagam: The Dawn of Humanity*. New York: Columbia University Press.
- Leakey, M. G. & Walker, A. (1997). Early hominid fossils from Africa. *Sci. Am.* **276**, 74–79.
- Leakey, M. G., Feibel, C. S., McDougall, I. & Walker, A. (1995). New four-million-year-old hominid species from Kanapoi and Allia Bay, Kenya. *Nature* **376**, 565–571.
- Leakey, M. G., Feibel, C. S., McDougall, I., Ward, C. V. & Walker, A. (1998). New specimens and confirmation of an early age for *Australopithecus anamensis*. *Nature* **363**, 62–66.
- Leakey, R. E. F. & Walker, A. (1985). Further hominids from the Plio-Pleistocene of Koobi Fora, Kenya. *Am. J. phys. Anthrop.* **67**, 135–63.
- Leakey, R. E. F. & Walker, A. (1988). New *Australopithecus boisei* specimens from East and West Lake Turkana, Kenya. *Am. J. phys. Anthrop.* **76**, 1–24.
- Lewis, O. (1973). The hominoid os capitatum, with special reference to the fossil bones from Sterkfontein and Olduvai Gorge. *J. hum. Evol.* **2**, 1–12.
- Lewis, O. J. (1977). Joint remodelling and the evolution of the human hand. *J. Anat.* **123**, 157–201.
- Lockwood, C. A., Richmond, B. G., Jungers, W. L. & Kimbel, W. H. (1996). Randomization procedures and sexual dimorphism in *Australopithecus afarensis*. *J. hum. Evol.* **31**, 537–548.
- Lockwood, C. A., Kimbel, W. H. & Johanson, D. C. (2000). Temporal trends and metric variation in the mandibles and dentition of *Australopithecus afarensis*. *J. hum. Evol.* **39**, 23–55.
- Lovejoy, C. O. (1981). The origin of man. *Science* **211**, 341–350.
- Lovejoy, C. O., Johanson, D. C. & Coppens, Y. (1982). Hominid lower limb bones recovered from the Hadar Formation: 1974–1977 collections. *Am. J. phys. Anthrop.* **57**, 679–700.
- MacFadden, B. J., Solounias, N. & Cerling, T. E. (1999). Ancient diets ecology and extinction of 5 million year old horses from Florida. *Science* **283**, 824–827.
- Marzke, M. W. (1983). Joint functions and grips of the *Australopithecus afarensis* hand, with special reference to the region of the capitate. *J. hum. Evol.* **12**, 197–211.
- Marzke, M. W. (1997). Precision grips, hand morphology, and tools. *Am. J. phys. Anthrop.* **102**, 91–110.
- Marzke, M. W. & Shackley, M. S. (1986). Hominid hand use in the Pliocene and Pleistocene: evidence from experimental archeology and comparative morphology. *J. hum. Evol.* **15**, 439–460.



- McCollum, M. A., Grine, F. E., Ward, S. C. & Kimbel, W. H. (1993). Subnasal morphological variation in extant hominoids and fossil hominids. *J. hum. Evol.* **24**, 87–111.
- McDougall, I. & Feibel, C. S. (1999). Numerical age control for the Miocene-Pliocene succession at Lothagam, a hominoid-bearing sequence in the northern Kenya Rift. *J. Geol. Soc.* **156**, 731–745.
- McHenry, H. M. (1983). The capitate of *Australopithecus afarensis* and *A. africanus*. *Am. J. phys. Anthrop.* **62**, 187–198.
- McHenry, H. M. (1992). Body size and proportions in early hominids. *Am. J. phys. Anthrop.* **87**, 407–431.
- Morgan, M. E., Kingston, J. D. & Marino, B. D. (1994). Carbon isotopic evidence for the emergence of C<sub>4</sub> plants in the Neogene from Pakistan and Kenya. *Nature* **367**, 162–165.
- Paciulli, L. M. (1995). Ontogeny of phalangeal curvature and positional behavior in chimpanzees. *Am. J. phys. Anthropol. Suppl.* **20**, 165.
- Patterson, B. & Howells, W. W. (1967). Hominid humeral fragment from early Pleistocene of North-western Kenya. *Science* **156**, 64–66.
- Plavcan, J. M. (2000). Inferring social behavior from sexual dimorphism in the fossil record. *J. hum. Evol.* **39**, 327–344.
- Plavcan, J. M. & Van Schaik, D. P. (1997). Interpreting hominid behavior on the basis of sexual dimorphism. *J. hum. Evol.* **32**, 345–374.
- Puech, P.-F. (1986). *Australopithecus afarensis* Garusi 1, diversité et spécialisation des premiers Hominidés d'après les caractères maxillo-dentaires. *C. r. Acad. Sci., Paris* **303**, 1819–23.
- Puech, P.-F., Cianfarani, F. & Roth, H. (1986). Reconstruction of the maxillary dental arcade of Garusi Hominid 1. *J. hum. Evol.* **15**, 325–32.
- Quade, J., Cerling, T. E. & Bowman, J. R. (1989). Development of Asian monsoon revealed by marked ecological shift during the latest Miocene in northern Pakistan. *Nature* **342**, 163–166.
- Quade, J., Cerling, T. E., Morgan, M. M., Pilbeam, D. R., Barry, J., Chivas, A. R., Lee-Thorp, J. A. & van der Merwe, N. J. (1992). A 16 million year record of paleodiet using carbon and oxygen isotopes in fossil teeth from Pakistan. *Chem. Geol. (Isotope Geoscience Section)* **94**, 183–192.
- Reed, K. (1997). Early hominid evolution and ecological change through the African Plio-Pleistocene. *J. hum. Evol.* **32**, 289–322.
- Richmond, B. G. (1997). Ontogeny of phalangeal curvature and locomotor behavior in lar gibbons. *Am. J. phys. Anthropol. Suppl.* **24**, 197.
- Richmond, B. G. (1999). Reconstructing locomotor behavior in early hominids: evidence from primate development. *J. hum. Evol.* **36**, A20.
- Richmond, B. G. & Strait, D. S. (2000). Evidence that humans evolved from a knuckle-walking ancestor. *Nature* **404**, 382–5.
- Schwartz, G. T. (2000). Taxonomic and functional aspects of the patterning of enamel thickness distribution in extant large-bodied hominoids. *Am. J. phys. Anthrop.* **111**, 221–244.
- Senut, B. (1980). New data on the humerus and its joints in Plio-Pleistocene hominids. *Coll. Anthrop.* **1**, 87–93.
- Senut, B. (1996). Pliocene hominid systematics and phylogeny. *S. Afr. J. Sci.* **92**, 165–166.
- Senut, B. (1999). Les humains les plus anciens. *Les Origines de l'Humanité, Dossier Hors-série Janvier*, 66–69.
- Senut, B. & Tardieu, C. (1985). Functional aspects of Plio-Pleistocene hominid limb bones: implications for taxonomy and phylogeny. In (E. Delson, Ed.) *Ancestors: The Hard Evidence*, pp. 193–201. New York: Alan R. Liss.
- Smith, R. J. & Jungers, W. L. (1997). Body mass in comparative primatology. *J. hum. Evol.* **32**, 523–559.
- Stern, J. T. (2000). Climbing to the top: A personal memoir of *Australopithecus afarensis*. *Evol. Anthrop.* **9**, 113–133.
- Strait, D. S. & Grine, F. E. (1999). Cladistics and early hominid phylogeny. *Science* **285**, 1210–1211.
- Strait, D. S., Grine, F. E. & Moniz, M. A. (1997). A reappraisal of early hominid phylogeny. *J. hum. Evol.* **32**, 17–82.
- Teaford, M. F. & Ungar, P. S. (2000). Diet and the evolution of the earliest human ancestors. *Proc. natl. Acad. Sci.* **97**, 13506–13511.
- Trotter, M. & Gleser, G. C. (1952). Estimates of stature from long bones of American Whites and Negroes. *Am. J. phys. Anthrop.* **10**, 463–514.
- Walker, A. (1978). Functional anatomy of oral tissues: mastication and deglutition. In (J. H. Shaw, E. A. Sweeney, C. C. Cappucino & S. M. Meller, Eds) *Textbook of Oral Biology*, pp. 227–296. Philadelphia: W. B. Saunders.
- Ward, C. V., Leakey, M. G., Brown, B., Brown, F., Harris, J. & Walker, A. (1999a). South Turkwel: A new Pliocene hominid site in Kenya. *J. hum. Evol.* **36**, 69–95.
- Ward, C. V., Walker, A. & Leakey, M. G. (1999b). The new hominid species *Australopithecus anamensis*. *Evol. Anthrop.* **7**, 197–205.
- White, T. D. (1977). New fossil hominids from Laetolil, Tanzania. *Am. J. phys. Anthrop.* **46**, 197–230.
- White, T. D. & Johanson, D. C. (1982). Pliocene hominid mandibles from the Hadar Formation, Ethiopia: 1974–1977. *Am. J. phys. Anthropol.* **57**, 501–544.
- White, T. D., Johanson, D. C. & Kimbel, W. H. (1981). *Australopithecus africanus*: Phyletic position reconsidered. *S. Afr. J. Sci.* **77**, 445–470.
- White, T. D., Suwa, G., Hart, W. K., Walter, R. C. & WoldeGabriel, G. (1993). New discoveries of *Australopithecus* at Maka in Ethiopia. *Nature* **366**, 261–265.
- White, T. D., Suwa, G. & Asfaw, B. (1994). *Australopithecus ramidus*, a new species of early hominid from Aramis, Ethiopia. *Nature* **371**, 306–312.
- White, T. D., Suwa, G., Simpson, S. & Asfaw, B. (2000). Jaws and teeth of *Australopithecus afarensis* from Maka, Middle Awash, Ethiopia. *Am. J. phys. Anthrop.* **111**, 45–68.

- WoldeGabriel, G., White, T. D., Suwa, G., Renne, P. & de Heinzelin, J. (1994). Ecological and temporal placement of early Pliocene hominids at Aramis, Ethiopia. *Nature* **371**, 330–333.
- Wolpoff, M. H. (1999). *Paleoanthropology*, 2nd Edition. Boston: McGraw-Hill.
- Wood, B. (1991). *Koobi Fora Research Project Volume 4: Hominid Cranial Remains*. Oxford: Clarendon Press.
- Wood, B. & Abbott, S. A. (1983). Analysis of the dental morphology of Plio-Pleistocene hominids. I. Mandibular molars—crown area measurements and morphological traits. *J. Anat.* **161**, 1–35.
- Wrangham, R. W. (1999). Evolution of coalitionary killing. *Yearb. phys. Anthrop.* **42**, 1–30.
- Wynn, J. G. (2000). Paleosols, stable carbon isotopes, and paleoenvironmental interpretation of Kanapoi, northern Kenya. *J. hum. Evol.* **39**, 411–432.
- Zihlman, A., Cronin, J., Cramer, D. & Sarich, V. M. (1978). Pygmy chimpanzee as a possible prototype for the common ancestor of humans, chimpanzees and gorillas. *Nature* **275**, 744–746.